Characterization of the novel 4-chloro-1-piperidin-1ylmethyl-1H-indole-2,3-dione compound (Raja 42) for its antibacterial activity against Escherichia coli, Clostridium difficile, Staphylococcus aureus and Helicobacter pylori

by

Alexis Fong

A thesis submitted in partial fulfillment
of the requirements for the degree of
Doctor of Philosophy (PhD) in Biomolecular Sciences

The Faculty of Graduate Studies
Laurentian University
Sudbury, Ontario, Canada

THESIS DEFENCE COMMITTEE/COMITÉ DE SOUTENANCE DE THÈSE
Laurentian Université/Université Laurentienne
Faculty of Graduate Studies/Faculté des études supérieures

Title of Thesis Titre de la thèse	Characterization of the novel 4-chloro-1-piperidin-1ylmethyl-1H-indole-2,3-dione compound (Raja 42) for its antibacterial activity against Escherichia coli, Clostridium difficile, Staphylococcus aureus and Helicobacter pylori
Name of Candidate Nom du candidat	Fong, Alexis Danielle
Degree Diplôme	Doctor of Philosophy
Department/Program Département/Programme	Biomolecular Sciences
Date of Defence Date de la soutenance	November 18, 2020

APPROVED/APPROUVÉ

Thesis Examiners/Examinateurs de thèse:

Dr. Hoyun Lee
(Supervisor/Directeur de thèse)

Dr. Mazen Saleh
(Committee member/Membre du comité)

Dr. Reza Nokhbeh
(Committee member/Membre du comité)

Dr. Kim Tilbe
(Committee member/Membre du comité)

Dr. Alain Stintzi
(External Examiner/Examinateur externe)

Dr. Mery Martinez
(Internal Examiner/Examinateur interne)

Approved for the Faculty of Graduate Studies
Approuvé pour la Faculté des études supérieures
Dr. Lace Marie Brogden
Madame Lace Marie Brogden
Acting Dean, Faculty of Graduate Studies
Doyen Intérimaire, Faculté des études supérieures

ACCESSIBILITY CLAUSE AND PERMISSION TO USE

I, **Alexis Danielle Fong**, hereby grant to Laurentian University and/or its agents the non-exclusive license to archive and make accessible my thesis, dissertation, or project report in whole or in part in all forms of media, now or for the duration of my copyright ownership. I retain all other ownership rights to the copyright of the thesis, dissertation or project report. I also reserve the right to use in future works (such as articles or books) all or part of this thesis, dissertation, or project report. I further agree that permission for copying of this thesis in any manner, in whole or in part, for scholarly purposes may be granted by the professor or professors who supervised my thesis work or, in their absence, by the Head of the Department in which my thesis work was done. It is understood that any copying or publication or use of this thesis or parts thereof for financial gain shall not be allowed without my written permission. It is also understood that this copy is being made available in this form by the authority of the copyright owner solely for the purpose of private study and research and may not be copied or reproduced except as permitted by the copyright laws without written authority from the copyright owner.

Abstract

According to the World Health Organization (WHO), drug-resistant bacteria are prevalent in 83.3% of the regions where WHO conducts surveillance. Furthermore, the number of antibiotic resistant bacterial strains increases every year, necessitating the development of new classes of antibacterial agents. Toward developing a novel class of antibacterial agents, we have created a chemical library using chloroquine as the basic scaffold. We screened our chemical library of 211 compounds to identify antibacterial activity. Twenty-seven were effective on drug-sensitive *E. coli* strains as well as on those resistant to ampicillin, kanamycin or NDM-1. In addition, they were also effective against *Staphylococcus aureus* and methicillin-resistant *S. aureus*. Since all of them contain an isatin moiety, they are classified as the γ-lactam class of antibiotics. Although similarities can be seen in the spectrum of activities of γ-lactam-based and β-lactam-based antibiotics, there are marked differences in the activity against antibiotic resistant bacterial strains. One of the new compounds, Raja 42 (4-chloro-1-piperidin-1ylmethyl-1H-indole-2,3-dione), displayed a lowered MIC value and, therefore, was chosen for further studies. In addition to its excellent activity against *E. coli*, Raja 42 is also notably effective against *Helicobacter pylori* and *Clostridium difficile* isolates from patients.

I set out to unravel the molecular mechanism by which Raja 42 exhibits its antibacterial effects. Data from cellular and fluorescent microscopic assays showed that bacteria were killed rapidly in the presence of Raja 42. A time-kill and membrane depolarization assays confirmed the rapid cell killing by Raja 42, suggesting that the mode of killing by the compound is likely due to the

disruption of bacterial cell membrane. To further investigate this possibility, I carried out protein 2-D gel electrophoresis in an attempt to identify proteins involved in the Raja 42-mediated cell killing. In the process, those proteins differentially expressed in response to Raja 42 were isolated and their identities were determined by peptide fingerprinting using mass spectrometry. The resultant data revealed that several proteins involved in the reactive oxygen species (ROS) pathway are upregulated in the Raja 42-treated samples. In parallel, ten clones resistant to Raja 42 were generated, and their nucleotide sequences were determined. A 27 bp deletion upstream of the promoter region of *ghrA*, a necessary catalytic converter of glyoxylate to glycolate in the glyoxylate shunt pathway, was found to be present in all of the Raja 42-resistant clones. This data suggests that the ablation of ghrA is directly related to the Raja 42 resistant phenotype.

To determine the quantitative gene expression of bacteria in response to Raja 42 treatment, QPCR analysis was carried out. To solidify the mechanism of Raja 42 further, rescue experiments were performed to determine the importance of *ghrA.* Taken all the data together, Raja 42 appears to kill bacteria by upregulating the level of cellular ROS through rapidly redirecting the metabolic pathways.

Keywords

Novel drug discovery, antibiotic resistance, *Escherichia coli*, γ-lactam antibiotics, reactive oxygen species, bacterial genomics, metabolism, *Clostridium difficile*

List of Abbreviations

AhpC	Alkyl Hydroperoxide reductase subunit C
BBA	Brucella Blood Agar
BHI	Brain Heart Infusion
C.diff	*Clostridium difficile*
CDI	*Clostridium difficile* infection
CDT	*Clostridium difficile* (Binary) toxin
CLSI	Clinical Laboratory Safety Institute
CFU	Colony forming units
CNS	Central nervous system
DBS	Double strand breaks
DMSO	Dimethyl sulfoxide
DPA	Dipicolonic acid
ELISA	Enzyme-linked immunosorbent assay
EUCAST	European Committee on Antimicrobial Susceptibility Testing
ESBL	Extended spectrum β-lactamases
E-test	Epsilometer test
ETC	Electron transport chain
E.coli	*Escherichia coli*
ECDC	European Center for Disease Control
ESCMID	European Society of Clinical Microbiology and Infectious Disease
ghrA	Glyoxylate hydroxypyruvate reductase

GSPG4	Chondroitin Sulfate Proteoglycan 4
HAI	Hospital acquired infection
IDSA	Infectious Disease Society of America
H.pylori	*Helicobacter pylori*
LB	Lysogeny broth
LEE	Locus of enterocyte effacement
lpf	Long polar fimbriae
LCT	Large clostridial toxins
LTCF	Long-term care facilities
MH	Muller-Hinton
MIC	Minimum inhibitory concentration
MRSA	Methicillin resistant *Staphylococcus aureus*
NDM-1	New-Delhi metallo β-lactamase 1
OD	Optical density
OM	Outer membrane
PaLoc	Pathogenicity locus
PBP	Penicillin Binding protein
PBS	Phosphate buffer saline
PCR	Polymerase Chain reaction
PKN	Protein kinase N
Prxs	Perodoxins
MOA	Mechanism of action

ROS	Reactive oxygen species
RT	Room temperature
STEC	Shiga-toxin *E.coli*
SCFAs	Short Chain Fatty Acids
SSTIs	Soft tissue infection
SNP	Single nucleotide polymorphism
SOD	Superoxide dismutase
S.aureus	*Staphylococcus aureus*
STSS	Steptococcal toxic shock syndrome
TCA	Citric Acid Cycle
TcdA	*C. difficile* toxin A
TcdB	*C. difficile* toxin B
Tir	Translocated intimin receptor
VRSA	Vancomycin resistant Staphylococcus aureus
WHO	World Health Organization

Acknowledgments

I would first and foremost like to thank my supervisor, Dr. Hoyun Lee, for the opportunities he has given me throughout my time with his group. His encouragement, support and wisdom have greatly contributed to the progression of my thesis. Having started this project as an undergraduate student and having transferred from the M.Sc program to the Ph.D program, I am immensely grateful for the ongoing encouragement provided by Dr. Lee.

I would also like to take this opportunity to thank my mentors and friends Alison Douglas and James Knockleby, for helping me immensely over the course of my thesis. Through their expertise and knowledge in various molecular biology aspects, I have gained experimental and technical insight, allowing me to better progress my thesis.

A special thanks is to Dr. Reza Nokhbeh, Dr. Gustavo Ybazeta and Megan Ross, without whom I would have been a lost student! I thank them for adopting me in their lab group and sharing their extensive knowledge on microbiology. Their continuous guidance and encouragement have allowed me to better my techniques, critical thinking and understanding of microbiology. Their extreme generosity and their research morals have been a constant source of inspiration for me throughout my studies.

I would like to extend my gratitude to Dr. Mazen Saleh and Dr. Tilbe, whom alongside Dr. Nokhbeh and Dr. Lee have served as my internal committee members. Through their guidance and support, they have helped me progress smoothly through the progression of my thesis. Their encouragement and excitement towards my work has helped foster and develop my passion for scientific research.

I also thank Amanda Durkin and Nya Fraleigh in keeping me grounded and keeping my outlook positive. Whether it was through cupcake dates or Japanese stationery orders, my time in the lab would not have been the same without you!

I would also like to extend my sincerest gratitude to Dr. Mery Martinez. Having been a Teaching Assistant for Dr. Martinez' Anatomy and Physiology course, I have grown to confide and develop an important friendship with her. As one of my role models for women in science, Dr. Martinez has given me tremendous support and insight throughout my thesis. She has provided me with the opportunity to grow and develop as a young professional, and for that I am exceptionally grateful.

Finally, I would like to extend the most important gratitude to my family and partner, Kyle for their continuous support. To my parents, Byron and Lise, I am forever grateful for the opportunities you have provided me and for your ongoing support. You have motivated me and encouraged me to always do my best! To my brother Nathan, thank you for your support and

patience throughout my thesis! To my partner Kyle, thank you for helping me practice and go over my presentations when I'm nervous, thank you for being someone I confide in when my spirits were low, but most importantly, thank you for continuously supporting me and being by my side. Last but not least, I would like to thank my fur-baby Nala for alleviating and sometimes inducing my stress. Your mischievous behaviour has helped me stay grounded during the final year of my thesis!

Table of Contents

List of Figures

List of Tables

1.0 Introduction

1.1 Persistent infections and the scarcity of new antibiotics

1.1.1 *The "Golden Era" and the current lack of novel antibiotics in the pipeline*

Prior to the discovery of Penicillin by Alexander Flemming in the early 20th century, infectious diseases were of a significant prevalence and often attributed to death at an early age [1]. Smallpox, cholera and typhoid fever, to name a few of the frequently encountered pathogens at that time, were causative agents for high morbidity and mortality rates worldwide [1].The work accomplished by Flemming led to the "Golden Era" of antibiotics, which expands from 1940 to 1960 [2]. During this time, many novel classes of antibiotics were discovered, including β-lactams, aminoglycosides, sulfonamides, macrolides and tetracyclines (

Figure 1). These discoveries contributed greatly to the extended life expectancy in North America to 80 years of age at present day, from a mere 56.4 years during the 1920's [3,4]. Over time, with overuse and misuse of antibiotics, bacterial resistance has grown common, spurring the use of the term 'superbugs' for multiresistant bacterial organisms [4]. It was once enough a first line antibacterial agent alone; however, it now often requires the use of second generation antibiotics and combinational therapies to kill antibiotic-resistant microbes [5]. Thus, new classes of antibiotics are needed to thwart the ever evolving bacteria [6]. The World Health Organization (WHO) reiterates the importance of novel antibacterial pipelines needing to be developed as there is currently a lack of promising new effective antibiotics [7]. With only 51 new antibiotics currently in development against infectious agents, the WHO has placed tremendous value and

merit towards the development of novel alternative therapies [7]. The ability of bacteria to circumvent

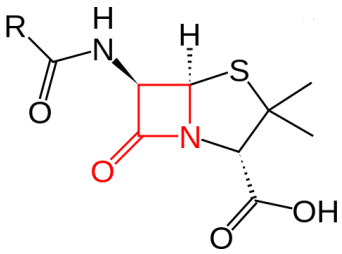

β-lactam

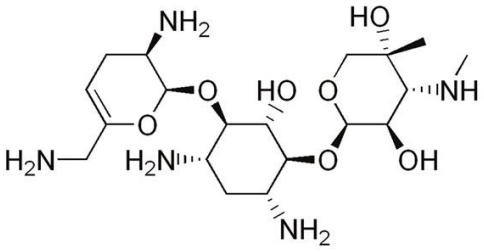

Aminoglycoside

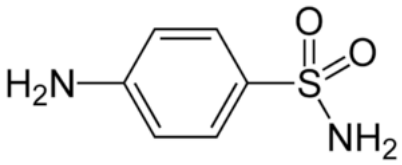

Sulfonomide

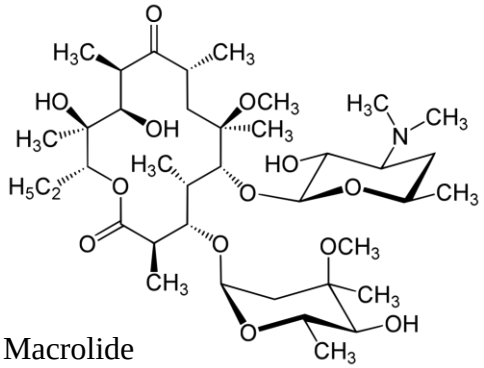

Macrolide

Tetracycline

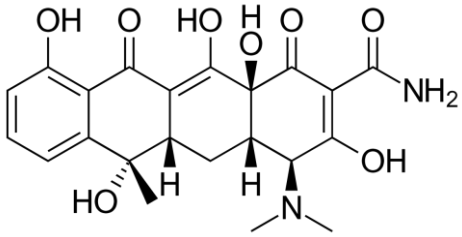

Figure 1: Structures of different classes of commonly used antibiotics

Many antibacterial compounds had been identified during the ``Golden Era``. These antibiotics are classified according to their chemical structures, each exhibiting different properties and spectrum of activities. The chemical backbone of the 5 predominant antibacterial classes, listed above, provides an overview of the modifiable sites in the generation of specific antibacterial compounds.

current antibiotic treatment has led to the reemergence of, otherwise eradicated, infectious diseases [8]. Many incidences of *Staphylococcus, Salmonella, Ysernia and Clostridioides* are being reported in hospital settings, often associated with severe illness and potentially fatal outcomes.

1.1.2 *Prevalence of Nosocomial Infections*

Nosocomial infections, often termed Hospital/Healthcare Acquired Infections (HAI), are a significant cause of morbidity and mortality within communities worldwide, including highly developed countries [9]. Much like in North America, data collected by the European Center for Disease Control (ECDC) in various surveys concluded that the probability of patients acquiring a nosocomial infection during the course of their stay was 6%, with a 95% confidence interval [10]. This statistic supports the notion that 1⁄7 patients from developed countries or 1⁄10 patients from developing countries will acquire a nosocomial infection, as investigated in a community public health assessment [10,11]. With a portion of community members requiring prolonged hospital stay due to the acquisition of an infection, this can have a large financial impact on the healthcare industry. The calculated cost attributed to HAI in the United States alone was estimated to be between US$28 billion-US$45 billion annually [12]. While very few cost assessments have been conducted in the Canadian Health Care system, Methicillin-resistant *Staphylococcus aureus* (MRSA) attributed HAI's alone caused a financial burden of CAD$54 million-CAD$110 million annually, estimating that the average cost per patient is CAD$12,216 per year [13]. Nosocomial infections, which cause a great financial burden to the Canadian health care system, may be acquired from various treatment procedures or physical areas in the hospital. The three most frequent types of nosocomial infections include but are not limited to; catheter-associated urinary tract infections, central line-associated bloodstream infections and surgical site infections [14]. From a global standpoint, catheter-associated infections are the most prevalent cause and account for 12% of reported hospital-mediated infections according to the Center for Disease Control and Prevention (CDC) [14,15]. With the insertion of a catheter in a bacterial bearing orifice and the

imperfect drainage mechanism of the instrument, this creates the perfect environment for bacterial replication to occur rapidly. Central line-associated bloodstream infections represent a noteworthy cause of mortality amongst nosocomial infections, often leading to sepsis-mediated mortality. The mortality rate is 12-15% amongst patients with catheter-associated infections, with the majority of reported incidents occurring in the intensive care unit (ICU) [16]. Surgical sites are also an important source of nosocomial infections with 2-5% of surgical patients contracting an infection [17]. While nosocomial infections have high incidence rates, these infections can be attributed to a few predominant species including *Escherichia coli, Staphylococcus aureus* and its resistant form *Methicillin Resistant Staphylococcus aureus*, as well as *Clostridioides difficile*.

1.2 Overview of Bacterial species studied

1.2.1 *Escherichia coli*

E. coli, undoubtedly the most well-characterized bacterial species in microbiology, is a gram-negative, rod-shaped, flagellated, motile bacterium species which measures 0.35 µm in size [18]. Discovered in 1885 by German scientist Theodor Escherich, *E. coli* is a member of the Enterobacteriaceae family, which notably includes other pathogenic species such as *Salmonella enteria, Yersinia pestis* and *Klebsiella sp.* [19,20]. *E. coli* motility is made possible by the presence of a long flagella and the presence of tiny pili on the surface of its outer membrane [20]. Physiologically, *E. coli*, is a facultative aerobe but cannot grow at extreme temperatures or pH ranges [20]. On the surface of nutrient agar, their colonies appear semi-raised with round uniform edges, which are convex and may be ranged in shades of pale beige to a milky white. Colonies will

typically range from 2-4 mm in diameter and this may depend on agar type and nutrient composition. Predominantly found in the gut microbiome as a commensal, *E. coli* thrives in a nutrient rich environment typically in the digestive tract of humans [21]. *E. coli* metabolism primarily relies on a select few pathways such as the Embden-Myerhoff-Parnas (EMP) glycolytic pathway, the pentose-phosphate (PP) pathway and the Entner-Doudoroff (ED) pathway; thus, allowing it to grow best on simple sugars such as mono and di-saccharides [21]. To the contrary, *E. coli* does not grow well on complex sugars since it lacks the necessary enzymes for its breakdown [21]. Being a gram-negative species, *E. coli* has an outer membrane (OM) composed of a lipid-protein bilayer which is used to separate the external environment from the periplasm (Figure 2). The fluid outer membrane of *E. coli* acts as a selective barrier allowing the transport of specific nutrients while restricting the passage of toxins [22]. The unique β-barrel structure of the outer membrane allows for the dispersal of chaperone proteins including porins which allow the hydrophobic substrates to enter the periplasm of the cell. A unique characteristic of the OM is the uneven distribution of lipids on the outer and inner face, with the outer face containing the vast majority of the bacterium's lipopolysaccharide (LPS). These hydrophobic substrates often find their way to the periplasm, a space interconnecting the OM and the cytoplasm [23]. The periplasm is composed of a gel-like matrix which harbours the necessary binding proteins for amino acids, sugars and ions; thus also acting as a reservoir for specific surface-attachment proteins (S-layer proteins, virulence factors and pili) [24]. Roughly 13-35 nm in width, the periplasm occupies roughly 8-16% of *E. coli's* total volume (Figure 2) [25]. The periplasm is delineated by the inner membrane, helping to separate the internal organelles which perform a variety of different processes. Many of the proteins necessary for energy production, lipid biosynthesis, protein

secretion and transport are localized in the inner membrane. The inner membrane is composed of a phospholipid bilayer with the primary phospholipid groups being phosphatidyl ethanolamine and phosphatidyl glycerol (Figure 2) [26]. In addition, *E. coli* harbours an appendage at its cell surface, allowing its motility.

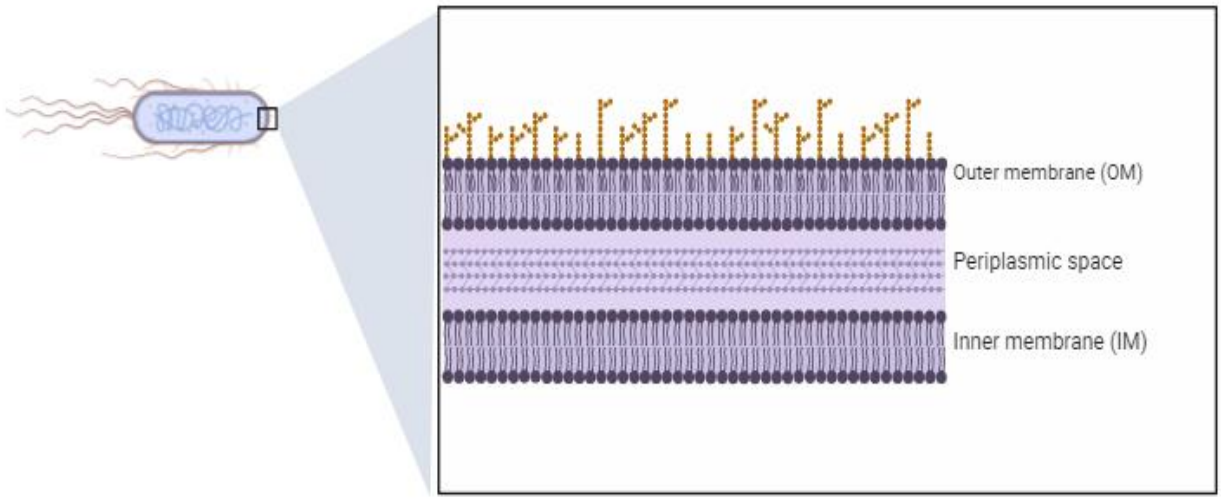

Figure 2: Structure of *E. coli* cell wall

The cytoplasmic organelles of gram negative species, such as *E. coli* are delineated by the inner membrane (IM), composed of a symmetric lipid bilayer. The outer leaflet of the bilayer is adjacent to the periplasmic space, an aqueous space which harbours the peptidoglycan layer of the cell wall. The outer membrane (OM) is an asymmetric lipid bilayer with phospholipids on the inner leaflet and lipopolysaccharides (LPS) on the outer leaflet. The outer membrane also contains the necessary lipoproteins and β-barrel proteins.

The rotating helical filaments, grouped in a bundle on *E.coli'*s surface termed flagella, are individually controlled by a rotating motor, which alternates between clockwise and counter-clockwise directions. When flagella rotate in the counter-clockwise direction, *E. coli* follows a

straight linear path known as “run”, whereas the clockwise flagellar rotation causes the bacteria to change the direction in the “tumble” position [27].

1.2.1.1 *E. coli* species variety

The *E. coli* species contains a variety of different strains which include both non-pathogenic and pathogenic bacteria. While a wide variety of different *E. coli* strains are used by researchers, the original *E. coli* K12 strain was isolated in 1922 at Stanford University [28]. The genome of this particular strain was first published in 1977 and the complete DNA sequence was determined by 1997 [29]. *E. coli* is an important contributor to the biosphere, colonizing the lower gut of animals, acting as a facultative anaerobe, and surviving in the environment allowing for its widespread dissemination. Through its widespread localization, multiple different strains of *E.coli* have been identified and isolated. Non-pathogenic strains provide host benefits such as vitamin K and B12 productions while pathogenic strains can cause serious disease.

1.2.2 *Staphylococcus aureus*

S. aureus is a gram-positive coccus which arranges in a grape-like cluster conformation and is a facultative aerobe, much like *E. coli*, *S. aureus* is both a human commensal and human pathogen with approximately 30% of the human population colonized with this bacterial species [30]. As the leading cause of bacteremia and infective endocarditis (IE), *S. aureus* infects 10-30 in 100,000 people annually [31]. In Quebec, the rates of *S. aureus* infection have risen since 1991, despite the stability of methicillin resistant *S. aureus* (MRSA) associated bacteremia infections [32]. MRSA is a significant public health problem and as the name indicates, is resistant to methicillin (formerly

the first line of therapy against *S. aureus* infections) making it much more difficult to treat. Infections caused by MRSA alone were calculated to cost 14.5 billion USD annualy to the health care system in hospital stays and treatment in 2003 in the USA [33]. Unfortunately, MRSA infections are not restricted to any particular geographic area with levels of incidence reaching 44% of nosocomial infections in Europe, with western European countries reporting 25% more prevalence [33].

1.2.3 *Clostridioides difficile*

Originally named *Bacillus difficilus* and described first in early 1930s, *C. difficile* is a gram positive, rod-shaped, obligate bacillus capable of spore formation [34]. Up until 2019, *C.* difficile was better known as *Clostridium difficile;* however this was a broad genera which encompassed many specific clostridial species and thus the European Committee on Antimicrobial Susceptibility Testing (EUCAST) had recently voted to change its name to *Clostridioides difficile. C. difficile* is the leading cause of HAI diarrhea with an estimated 250,000 cases annually in Canada alone [34]. HAI diarrhea is most detrimental in the elderly, those with weakened immune systems or young children with under developed immunity, and may occasionally result in death [35]. A marked increase in *C. difficile* infections has been reported since early 2000, yet the exact cause still remains to be determined [36]. As *C. difficile* is a sporulating species, hospitals have become increasingly contaminated with spores, increasing patient susceptibility to *C. difficile* infection [34]. *C. difficile* spores can resist a multitude of conditions including UV light, strong chemical agents and high temperatures as well as to certain antibiotics [37]. Individuals suffering from *C. difficile* infection (CDI) may exhibit a variety of symptoms that lie on the spectrum from being

asymptomatic, progressing to watery diarrhea to more extreme cases of life-threatening loss of bodily fluids [37]. In addition to colon inflammation, leaky pseudomembranous cells (pseudomembranous colitis) can illicit various immune responses leading to the formation of necrotic tissue [37]. According to Kujiper and colleagues, CDI can be defined as the presence of symptomatic diarrhea accompanied by three or more unformed stools in a 24-hour period, in addition to the presence of Toxin A/Toxin B as revealed by blood work or endoscopy [38]. Although *C. difficile* was first described in 1935, CDI gained much attraction in the mid 1950's, when metronidazole was being introduced in clinical practice to treat bacterial gut infections [39]. Since then, increased documented CDI cases have arisen in the 1990's and the introduction of a new hyper-virulent strain was described in the 2000's [40].

1.2.4 ***Helicobacter pylori***

H. pylori belong to the proteobacteria group and actively colonizes the gut microbiota. More than 20 different strains of the *H. pylori* species have been identified, some of which are still awaiting classification [41]. These microaerophilic organisms are both oxidase- and catalase-positive with a select few species being urease positive as well, and are capable of withstanding the low pH of stomach's acidity. A spirochete, this bacteria affects more than half the global population, and is the causative agent of peptic ulcer disease, chronic gastritis and has been classified as a type I carcinogen linking it to gastric cancer [42]. Gastric cancer is the 4^{th} and 5^{th} most prevalent cancer in women and men, respectively, with *H. pylori* infection associated with a two-fold increased risk of developing this cancer [43].

1.3 Mechanisms of Colonization and Infection

1.3.1 *E. coli and the gut microbiome*

While *E. coli* is well known to harbour in the gut of mammals, it not only colonizes in the guts of reptiles, birds and fish, but also found in the soil. In mammals, this bacterial species is responsible for the metabolism of lactose and composes 0.1-5.0 % of the total gut microbiome [44]. *E. coli* is predominantly found in the thin mucus lining of the lower intestine and thrives in complex multi-species biofilms, in which it competes for a vast variety of nutrients [45]. *E. coli* bacterial density is approximately 10^6-10^9 cells per gram of fecal matter with density being largely attributed to the variety of nutrients in the gut [46]. Recent metagenomic studies showed that *E. coli* colonization is significantly more abundant in young children than in healthy adults [47]. Unfortunately, the increase of *E.coli* population in older adults, which is not typically expected, could often be the result of increased pathogenic strains. Pathogenic *E. coli* is a major cause of diarrhea, peritonitis, colitis, bacteremia and urinary tract infections. The pathogenic strains of *E. coli* produce virulence factors, which may cause serious illness in the affected individuals. These strains are typically classified according to the location in which they cause disease, which includes enterohemorrhagic, uropathogenic, enterotoxigenic, enteroaggregative and enteropathogenic *E. coli*. The most well-known of these pathogenic strains is the enterohemorrhagic strain O157:H7, the causative of shiga-toxin [48]. *E. coli* O157:H7 is associated with severe vomiting, bloody-diarrhea, severe abdominal pains, severe dehydration and hemolytic uremic syndrome, and if left untreated it can result in death. O157:H7 resides asymptomatically in cattle; however, may find its way into the food chain through fecal contamination of meat in the packaging and handling process, causing severe

foodborne illness to humans. *E. coli* O157:H7 has caused multiple outbreaks, infecting 63,000 individuals per year in the United States alone with a healthcare burden of 405 million USD [49].

1.3.1.1 Pathogenic E. coli colonization

Once ingested, *E. coli* is able to withstand the strong acidity in the stomach with its capability to go into a stationary phase, enabling it to induce protective acid resistance mechanisms [50]. Once in the colon, *E. coli* must find nutrients that are embedded in the mucus lining, in order to propagate and grow rapidly. The important colonization properties of *E.coli* strain O157:H7 are on the locus of enterocyte effacement (LEE) pathogenicity island, which allows the specific attaching and effacing mechanism to take place [51]. Shiga-toxin *E. coli* (STEC) often carries the *eae* gene coding for the outer membrane adherence protein intimin [52]. The interaction of intimin with the translocated intimin receptor (Tir) allows for STEC attachment and effacement legions to be produced, which are critical for colonization and further pathogenesis (Figure 3) [53]. LEE-positive STEC strains display a type III secretion system which allows the formation of the EspA translocation tube and subsequent delivery of the Tir proteins into the host cell. This allows for downstream insertion into the plasma membrane, thus allowing its extracellular portion to bind to intimin. Together, intimin and Tir proteins form a multimeric subunit allowing for a signal transduction mechanism, causing the formation of actin assembly and pedestal formation (Figure 3) [54]. Long polar fimbriae (lpf) are also attributed to colonization, although they are less described than the LEE pathogenicity island mechanism. The *lpf* operon is located in an O-157 specific island of 5.9 kb, containing 6 genes (*lpfABCC"DE)* [55]. The regulation mechanism of the *lpf* operon is not well understood but various homologues have been identified and attributed as contributing factor to the attaching and effacing lesions caused by STEC. Attaching and effacing

lesions can also be facilitated by the presence of pili, such as the type 4 pili (T4P) which have been associated to *E. coli* adhesion, biofilm formation, bacterial aggregation, DNA uptake and cell signalling. 10 μm in length, T4P contains 19 kDa *hcpA* gene product that participates in adherence and host cell inflammation [56].

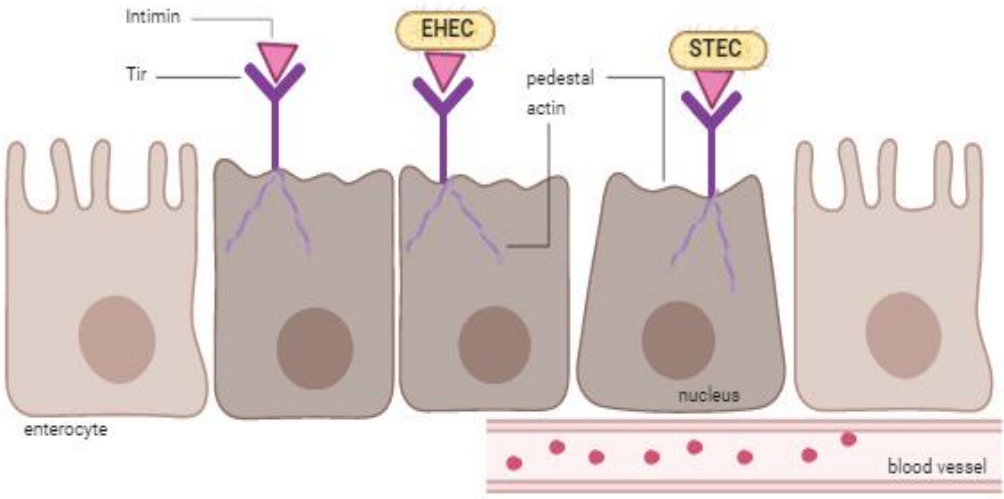

Figure 3: Attachment and effacing of pathogenic *E. coli*

Enterohemorrhagic *E. coli* (EHEC) and Shiga-toxin *E. coli* (STEC) attach and efface the microvilli of enterocytes. This process causes the formation of pedestals along the top of the enterocytes, ultimately damaging the cells. Attachment is mediated through the interaction of intimin with the Tir receptor. Further downstream phosphorylation events and recruitment lead to the internalization of the dimer. This process allows for the rearrangement of actin filaments and the effacing process to take place.

1.3.1.2 E. coli replication cycle

E. coli replication cycle can vary from several hours to less than 20 min. The cell-cycle of slow growing cells (> 1 hr of doubling time) can be represented in three phases: the pre-replication period, the DNA replication period and the cell division period. During the pre-replication period, cells increase their size without duplicating their DNA. During the replication period, DNA synthesis takes place, whereas the division period accommodates the termination of DNA synthesis and then cell division [57]. In fast growing bacteria, the pre-replication stage is omitted. Replication begins at the origin of DNA replication (*oriC*) and proceeds in a bidirectional manner on the circular chromosome until the replication forks meet at the opposite end of the chromosome. DNA replication is initiated by a constant mass/origin, called the initiation mass and requires the accumulation of a certain level of ATP bound to DnaA initiator [58]. At the initiation, the DnaA-ATP complex forms two filaments on *oriC* allowing for the assembly of two replication machineries. Since initiation happens once per cell cycle each initiation event will be consequently separated by one generation. Thus, cells with a rapid doubling time will contain multiple (up to 6) replication forks. Unfortunately, fast-growing bacteria will come at the price of leaving the chromosome unprotected, allowing DNA damage to occur.

1.3.2 *S. aureus clinical manifestations*

S. aureus and MRSA bacteremia are primarily caused by catheter-related infections, pleuropulmonary infections and osteoarticular related infection, as well as skin and soft tissue infections (SSTIs). SSTIs may be limited to the layers of the dermis or in more extreme cases, cause cellulitis and soft bone abscesses when travelled deeper. Group A streptococcal skin

infections will typically result in high fever, chills, bullae production and lymphangitis. MRSA when left untreated can further develop into streptococcal toxic shock syndrome (STSS) potentially leading to sepsis and death. IE is a primary disease associated with MRSA and often fatal. IE will develop on cardiac valves, often as a result of pacemakers or intravascular catheters [59].

1.3.2.1 MRSA colonization

Approximately one third of the global population is thought to carry *S. aureus*, and this bacterium is a colonizer of the interior nares as well as the skin surface. Airborn dissemination *via* droplets can be exacerbated with patients on respiratory ventilators, bridging the gap between healthy and infected individuals. The difficulty of treatment arises as there are currently very few antibiotics capable of penetrating the nares and effectively eliminating the bacterial populations. The use of certain antibiotics such as ceftazidime has been associated with an increase in MRSA colonization [60].

1.3.3 *Mechanisms of Colonization of C. difficile*

C. difficile colonization can occur even when a patient is presenting as asymptomatic. According to the Infectious Disease Society of America (IDSA) and the European Society of Clinical Microbiology and Infectious Diseases (ESCMID), CDI is acknowledged as positive when certain criteria have been met. The colonization criteria include identification through the presence of a toxigenic strain, toxin in the stool, histopathological evidence of pseudomembranous colitis, and exclusion of alternative etiologies for diarrhea [61]. Colonization occurs through the disruption of

the gut microbiota and leads to differences in bacterial composition which can be identified through luminal samples and specimen biopsy [62]. Low levels of species diversity and bacterial composition have been observed in *C. difficile*-colonized patients with a large decline of the *Bacteroidetes* phylum and increase in *Proteobacteria* respectively [63]. The *Firmicute* phylum is also impacted with a noticeable reduction in butyrate-producing bacteria and *Clostridia* species is also described [63]. The first step in colonization is the germination of spores which are stimulated through primary bile acid production [64]. Loss of secondary bile-acids and production of primary bile-acids have shown to be favourable conditions for *C. difficile* colonization. In addition to bile-acid composition, short-chain fatty acids (SCFAs) are important sources of gut microbiota composition, ultimately allowing *C. difficile* colonization to take place when alterations arise. Niche competition and nutrient availability also contribute to the colonization [65]. While the aforementioned factors promote *C. difficile* colonization, rapid responses of innate and adaptive immunity can generate antibody production against *C. difficile,* offering protection from colonization [66].

1.3.3.1 *C. difficile* Toxins

The majority of *C. difficile* strains produce two types of toxins, Toxin A (TcdA) and Toxin B (TcdB) [67]. These toxins are produced by the *tcdA* and *tcdB* genes, respectively, while certain strains express a binary toxin called *C. difficile* transferase (*cdt)* [67]. While the role of CDT toxin in CDI is still unclear, certain strains have been shown to produce CDT toxin in the absence of both toxin A and B [68].

1.3.3.2 Regulation of TcdA and TcdB production

Both TcdA and TcdB belong to a larger group of clostridial toxins called the clostridial glucosylation toxins or large clostridial toxins (LCT) [69]. Other toxin members are found in this family including the *Clostridium sordellii lethal* (TcsL), hemorrhagic toxin (TcsH) and *Clostridium perfringens* toxin (TpeL) which exhibits 26-76% conserved identity with modifications affecting their Rho or Ras protein domains [70]. Initially, TcdA was labelled an enterotoxin due to it actively contributing to mucosa damage, secretion and inflammation when compared with TcdB [71]. Conversely, TcdB was coined a cytotoxin due to its high levels of potency (100-1,000 fold) when compared to TcdA [72] . Much like other bacteria, *C. difficile* is no exception in the chronological order in which the toxins 1) Bind to target cells, 2) invaginate into the toxin-receptor complex, 3) translocate across membranes into the cytosol, 4) process to release the toxin subunit, and lastly 5) modify target proteins [69]. The *tcdA and tcdB* genes are found in the pathogenicity locus (PaLoc), a DNA segment spaning 19.6 kb present in toxigenic strains and absent in non-toxigenic strains [73] (**Figure 4**).

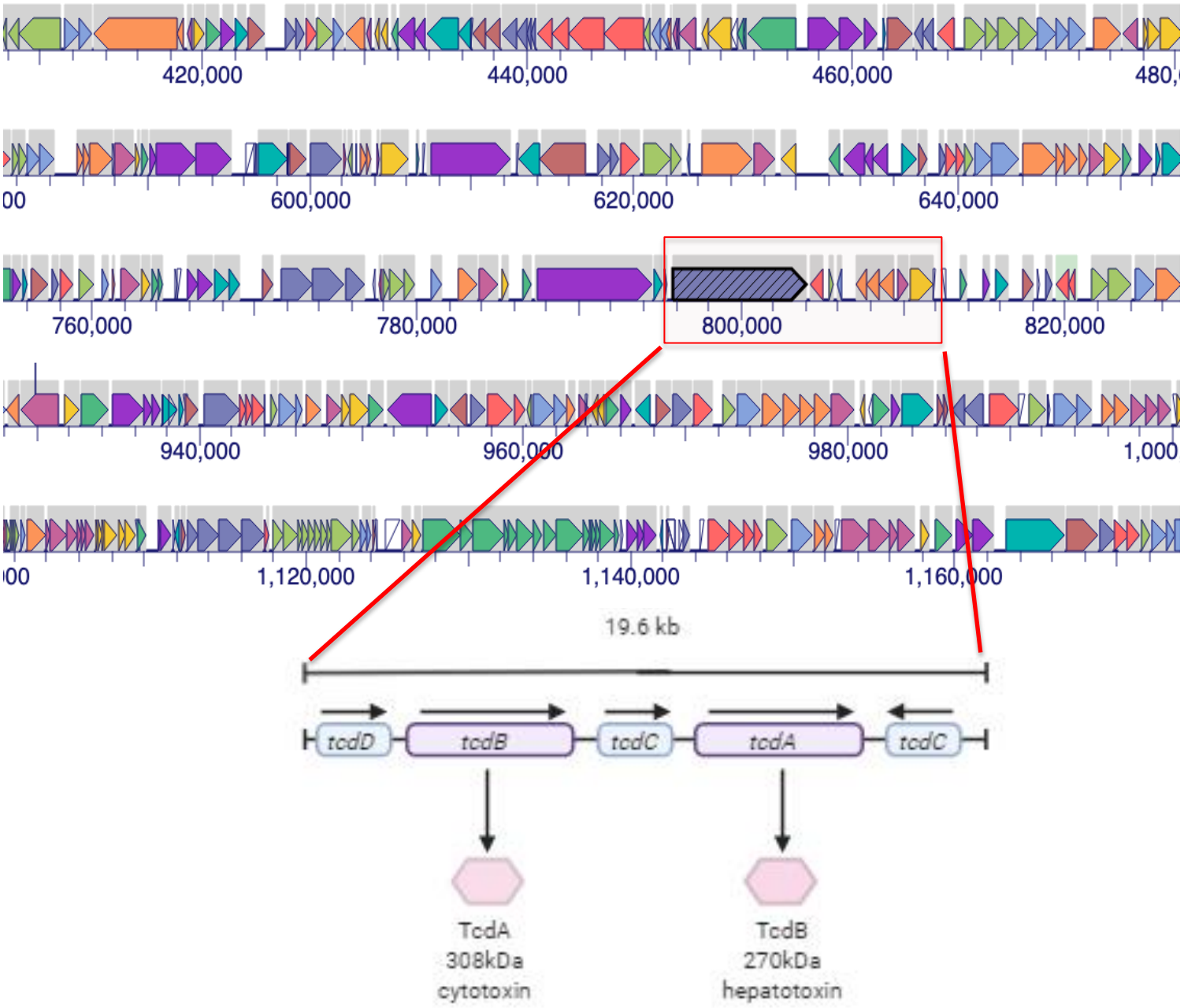

Figure 4: Genetic arrangement of *C. difficile* pathogenicity locus

Both *tcdA* and *tcdB* are located in the 19.6 kb pathogenicity locus in addition to three open reading frames: *tcdC*, *tcdD* and *tcdE*. Located at the Pa-Loc, *tcdA* and *tcdB* encode hepatotoxins and cytotoxins, respectively. Considered to be the primary virulence factors in CDI, these monoglucosyltransferases irreversibly modify proteins of the Rho family and other proteins leading to downstream pathway disruption and ultimately cell death.

The PaLoc also houses three other genes, the *tcdR*, *tdcC* and *tcdE*, which play a role in toxin regulation (*via* RNA polymerease), toxin repression or toxin secretion [74]–[76]. Toxin gene expression is bidirectional, which may be inhibited by various factors such as glucose production, certain amino acids or biotin, or facilitated in the presence of short chain fatty acids or elevated temperatures (37℃) [77]. In non-toxigenic strains, the PaLoc is traditionally replaced by a 115-bp non-coding DNA segment [78]. The PaLoc may also undergo mutation, such as insertions or deletions resulting in a multitude of toxinotypes associated with the *C. difficile* species [78]. Through PCR-based methods, the phylogeny of well-characterized *C. difficile* isolates were compared, which revealed that the population is divided into six clades (Clades 1, 2, 3, 4, 5 and C1) [79]. With the exception of C1, most clades contain strains which are toxin A^+B^+ or A^-B^+, and are predominantly found in clade 1 [80]. The genes *tcdA* and *tcdB* code for the TcdA and TcdB proteins with a molecular weight of 308 kDa and 270 kDa, respectively, and they also share a 48% sequence identity in their amino acid sequences (**Figure 4**) [73]. The N-terminal (A-domain) of the proteins contains the biologically active N-glycosyltransferase activity which is used to modify the Rho proteins, whereas the C-terminal (B-domain) of the protein is involved in the receptor binding [81, 82]. The proteins also contain two separate domains, the C-domain and D-domain responsible for protease activity and the delivery of the toxins, while working to maintain domain A and B stability, respectively [83].

1.3.3.3 Sporulation

The sporulation step is critical for *C. difficile* infection and host colonization. During CDI, *C. difficile* initiates a sporulation pathway, allowing dormant spores to be disseminated into patients.

While the triggers for sporulation have yet to be elucidated, it is postulated that sporulation may be a result of quorum sensing, nutrient starvation or other host limiting factors [84]. Other Clostridial bacterial species and Bacillus species are used to model the current *C. difficile* sporulation studies. Both the aforementioned species regulate their spore formation through the activation of specific histidine kinases, which in turn activate the phosphorylation of the transcriptional regulator, Spo0A [85]. While the mechanism by which Spo0A is directly phosphorylated prior to *C. difficile* sporulation is still unclear, a lack of *B. subtilis* phosphorylation transfer proteins suggests the phosphoryl group to be transferred directly from the histidine kinase to Spo0A [85]. Through the activation of Spo0A by histidine kinases, the activation of sporulation-specific RNA polymerase sigma factor genes take place [86]. Four sigma factors (σ^F, σ^E, σ^G, σ^K) are highly conserved amongst the *Clostridium* species and was modelled through the *B. subtilis* pathway. In *B. subtilis*, Spo0A activates σ^F, which in turn is necessary for the activation of the post-translational σ^G in a cascade reaction [87]. Contrary to *B. subtilis*, in *C. difficile* σ^E is dispensable for σ^G activation, σ^G is also not-necessary for σ^K activation and σ^K does not undergo proteolytic activation [88,89]. While differences have been noted between the regulation of the different sigma factors between *B. subtilis* and *C. difficile*, it has been shown that sigma factors in the *C. difficile* sporulation undergo compartment-specific activation, much like in *B. subtilis* [87]. It was noted that σ^F and σ^G are activated in the forespore, while σ^E and σ^K are activated in the mother cell [87]. The forespore represents a premature spore cell, receiving a copy of DNA from the mother cell (vegetative cell) during DNA replication. Structurally, *C. difficile* spores have morphology very similar to previously described endospore-forming bacteria, with the major differences occurring on the outer layer of the spore [90]. The spore contains numerous structural layers, with the innermost

compartment being the spore core, which harbours the spore genetic material [91]. Important factors that are necessary for spore resistance include low water content, elevated level of dipicolinic acid (DPA) chelated with calcium (Ca-DPA) and saturation with DNA soluble proteins, all of which are found in the spore core [91]. The core is further surrounded by compressed inner membrane protein composed of a non-permeable phospholipid layer, similar to that of vegetative cells [92]. The germ cell wall surrounds the inner membrane of the spore and eventually forms the cell wall upon germination. The following layer is a thick peptidoglycan layer which is surrounded by an outer membrane [93]. The final outermost layer is the spore coat or the exosporium (in certain species), allowing them to play an important role in pathogenesis [94]. Germination of *C. difficile* spores is an important step for CDI [95]. Spore germination occurs when specific germinant receptors (GRs) sense the presence of specific small molecules termed germinants. Binding of a germinant to a GR triggers the release of monovalent cations (K+, Na+, H+) and spore core stores of Ca-DPA [96]. Ca-DPA release in *B. subtilis* leads to the activation of cortex hydrolases allowing for the degradation of the peptidoglycan cortex layer and subsequent core hydration and resumption of core metabolism [96]. While *Bacillus* and *Clostridium* spores germinate in response to sugars, amino acids and specific ions, *C. difficile* may germinate in response to bile salt (cholate, taurocholate, glycocholate) and L-glycine as a co-germinant [97]. Through genomic sequencing analysis, it has been revealed that all sequenced *C. difficile* strains lack the homologues of the GR thus alluding to a different mechanism likely responsible for spore germination in *C. difficile* [79]. This mechanism relies on the activation of the CspC (one of three Csp serine proteases encoded by *C. difficile*) which acts as a bile salt germinant [64]. The precise signalling pathway that activates *C. difficile* cortex hydrolyzing through CspC bile salt germinant still remains to be elucidated.

1.3.3.4 Infections caused by *C. difficile*

C. difficile is most commonly associated with nosocomial infections, afflicting the elderly, the young and those with immunocompromised systems. While *C. difficile* infections are also present in the community, prevalence in a hospital setting accounts for 20%-40% of cases compared to 28% of cases in the community [98,99]. In 2001, the University of Pittsburgh in the USA noticed an increase in the incidence of *C. difficile* infections, leading to more stringent characterization and understanding of the bacteria [100]. The outbreak occurred in Pittsburgh, which was identified as the NAP1/B1/027 strain, also widely present in Canada and Europe during this time [100]. While the NAP1/B1/027 strain is typically associated with severe infection, across a multitude of demographics, at times carriers of *C. difficile* may present as asymptomatic.

1.3.3.4.1 Clinical manifestations

Certain individuals infected with *C. difficile* may not exhibit any symptoms or not required any treatment [101]. Twenty percent of adult carriers of *C. difficile* are asymptomatic, while the rate of asymptomatic carriers in long-term care facilities is about 50% [99], [102]. Symptomatic individuals may be classified into two categories: non-severe illness and severe illness. Those with non-severe illness will typically exhibit watery diarrhea, characterized by 3 > loose stools in a 24-hour period, in addition to possible low-grade fever, mucus or blood in stool, nausea and cramping [103]. CDI symptoms typically occur during the start of antibiotic therapy or shortly after (up to 1 month), and are most commonly associated with the use of fluoroquinolones. Lower intestinal

endoscopy may reveal mild erythema or pseudomembranous colitis. Those patients with severe illness are characterized as displaying clinical manifestations including severe hypotension or shock as well as ileus and megacolon [101].

1.3.3.4.2 Mode of transmission and diagnosis

C. difficile sporulation is the current mode of transmission of CDI. In health care settings, health care provider-to-patient as well as environment-to-patient are the most common modes of CDI transmission [104]. Studies have attributed certain antibiotic use and poor infection control practices as contributing factors to ongoing CDI in healthcare settings [91]. Diagnostic tests have recently evolved in CDI detection but ultimately the first step is the collection of stool samples from patients suspected of having been infected. Following this, positive detection of *C. difficile* toxin needs to be confirmed by enzyme-linked immunosorbent assay (ELISA) or polymerase chain reaction (PCR)-based methods [105]. Glutamate dehydrogenase, a bacterial cell wall protein, is produced in much higher levels than the *C. difficile* toxins, thus allowing for high sensitivity, rapidity and highly negative predictive values when using this method of detection [106]. When a positive glutamate dehydrogenase test is confirmed, a second ELISA may be completed against toxins A and B. If the toxin testing is confirmed as positive, in conjunction with the glutamate dehydrogenase test, a positive diagnosis of CDI may be established.

1.3.4 *H. pylori colonization*

The two most important factors for *H. pylori* colonization are urease and motility. Since *H. pylori* is not an acidophile, its ability to produce urease is essential for its colonization in the gastric mucosa. In the presence of urea, *H. pylori* can survive in the pH as low as 2.5 [107]. Sensitive to alkaline conditions, *H. pylori* ability to control the stomach pH is crucial for its ability to colonize and is the reason why it exclusively colonizes in this part of the body. The motility is another important factor for *H. pylori* colonization, through its polar flagella of which function is regulated by the expression of the FlaA and FlaB proteins [108]. Recently, *flaA* and *flaB* have been shown to be regulated by the autoinducer-2 (AI-2), through the expression of *luxS* gene [109]. A known quorum sensing molecule, AI-2, regulates the expression of the *H. pylori* flagellar genes in response to bacterial numbers and adapts to its environment through this mechanism.

1.3.4.1 **Gastric mucus penetration**

300 μm in thickness, the mucus lining of the stomach offers a modifiable barrier through the thioredoxin system which allows for disulphide bond disruption, reducing mucin formation and ultimately the elastic properties of the gastric layer [110]. The reduction in elastic properties enables *H. pylori* to move with ease and with greater speed through the mucus layer. MUC5AC, the predominantly secreted mucin, can be attributed to microcolony formation on the mucosal layer of the stomach lining [111]. *H. pylori* has also been shown to interact with MUC1, a membrane bound mucin mediated by *babA* and *sabA* [112]. This particular mucin, when overexpressed, has been shown to be an important modulator of *H. pylori* infection by blocking *H. pylori* stimulated

β-catenin nuclear translocation. MUC1 overexpression has also been shown to play a role in IL-8 production and neutrophil attenuation in gastric inflammatory responses.

1.3.4.2 *H. pylori* and epithelial cell interactions

As *H. pylori* rarely comes in contact with the gastric epithelial cells, its interaction with these cells can cause serious disease and a series of proteins have been identified as outer membrane adhesins which facilitate the attachment by *H. pylori*. Both BabA and SabA are well characterized *H. pylori* outer membrane adhesin. BabA, a 78 kDa protein, is highly conserved amongst various *H. pylori* species, whereas SabA displays a high degree of genetic variability [113]. SabA allows *H. pylori* to bind siyalated structures found on the gastric epithelium as well as those found on neutrophils in order to generate an oxidative-burst response [114].

1.4 Current Therapies

1.4.1 *β-lactam antibiotics*

Penicillin, a β-lactam antibiotic, was introduced at the clinical setting 12 years after it was discovered in 1921 by Alexander Flemming. Through the work of the Northern Regional Research Laboratory in England, various strains, culture conditions and media led to the formation of different penicillin analogues. These different analogues were later crystallized and their structure revealed a commonality: the β-lactam ring. Structurally, the four-membered heterocyclic β-lactam ring is fused to a five-membered thiazole ring (

Figure **1**). Since the discovery of the chemical structure, β-lactams have become some of the most highly prescribed agents to treat bacterial infections both in the community and at hospital settings due to their effectiveness and low toxicity. Although the initial β-lactams were the result of medicinal chemistry discoveries, newer β-lactams and derivatives are being generated through molecular organic chemistry methods.

1.4.1.1 The functional mechanism of β lactam-based antibiotics

β-lactam antibiotics are broad-spectrum antibiotics and may function by the following five different mechanisms: inhibition of cell wall synthesis, impairment of the cytoplasmic membrane, inhibition of protein synthesis, inhibition of nucleic acid synthesis, and as a metabolic antagonist [115]. The β-lactams primarily act by inhibiting transpeptidases, thus inhibiting cell wall synthesis. β-lactams work by mimicking the D-ala, D-ala sequence thus falsely substrating the D-alanyl, D-alanyl transpeptidases. The carbonyl of the β-lactam ring interacts with the serine residue of the transpeptidase deactivating the acyl enzyme. This is more commonly known as the penicillin binding pocket (PBP). Although they might follow the same broad tendencies, the mechanism of action is typically specific to the β-lactam sub-classes.

1.4.1.2 Subclasses of β-lactam antibiotics

β-lactam antibiotics are a large group of antibiotics that can be classified further based on certain specificities and characteristics. The major subclasses of β-lactams include the penicillins, penams, carbapenems, cephalosporins, monobactams and β-lactamase inhibitors.

1.4.1.2.1 Penams

The penam class of antibiotics is a large group which includes penicillins. Penicillin's structure, the prototype β-lactam ring, is composed of a dipeptide which is generated through the condensation of L-cystein and D-valine. The result is the formation of a β-lactam ring and an adjacent thiazolidinic ring. The β-lactam ring structure, however, makes it susceptible to various degradative processes. In order to be administered orally and bypass the stomach's acidity, β-lactam ring reconfiguration spontaneously takes place allowing for the protonation of the ring nitrogen with downstream nucleophilic attack. This process generates the formation of an oxazoline ring intermediate which may further produce penicillic acid [116]. Through the production of the natural penicillin G, semi-synthetic and synthetic forms of penicillin have been produced as second and third generation antibiotics. The first synthetic penam generated was methicillin, which was synthesized by substituting the benzene ring of penicillin with two methoxy groups, thus causing steric hindrance around the amide bond [117]. Downstream modifications were included in the development of second-generation penams to bypass β-lactamases. A substitution at the 5' methyl group allowes for the development of oxacillin, part of the second generation penams. In an effort to circumvent β-lactam resistance, third generation penams such as clavulanic acid, tazobactam and sulbactam have been developed to irreversibly bind to β-

lactamases thus inhibiting them [118]. Both ampicillin and amoxicillin belong to the penicillin-sensitive group of orally active penams, containing a phenylglycine in D-configuration instead of the phenylacetic moiety, which gives them a broader spectrum of activity.

1.4.1.2.2 Carbapenems

Imipenem, the first of the carbapenem family, displays broad activity against both gram-positive and gram-negative species. Due to its inactivation by renal tubules, imipenem is often administered in conjunction with peptidase inhibitors such as cisplatin [119]. Imipenem is able to penetrate fluids, tissues and cerebrospinal fluid but despite this, many species, such as *Pseudomonas sp.*, have developed resistance. Meropenem, although structurally similar to imipenem, is not inactivated by dipeptidases and is therefore more often used in the clinical settings.

1.4.1.2.3 Cephalosporins

Unlike the penam antibiotics, which were used in clinical practice prior to the identification of their functional mechanism, the cephalosporins underwent stringent testing and refinement before being introduced. With a similar structure to the penicillin but with generally better tolerance, cephalosporins have their C-side chain chemically removed in order to form 7-aminoacephalosporanic acid [120]. Mechanistically, cephalosporins are very similar to penicillin in their formation of covalent bonds with PBPs, resulting in cell lysis. The cephalosporins are now used as second, third, fourth and fifth generation compounds with each generation differing in their antibacterial activity, absorption, metabolism and side effects [121]. The fifth generation exhibits a broader spectrum of activity with the first generation displaying a more limited activity, being

directed towards gram-positive cocci (with the exception of enterococci). The first generation is also moderately active against *E. coli, Klebsiella* and anaerobic cocci, and is typically administered intravenously or intramuscularly, with none of the first generation compounds capable of penetrating the central nervous system (CNS) [121]. The third generation cephalosporins are the exception to the rule and exhibit decreased activity towards gram-positive cocci, although they do have increased efficacy against gram-negative rod shaped species, making them particularly useful in treating nosocomial infections [122].

1.4.1.2.4 Monobactams

The monobactams are a class of monocyclic β-lactams resistant to β-lactamases. Most active against gram-negative rods, the monobactams are ineffective against anaerobes and gram-positive species [123]. Aztreonam, the first monobactam, is well-tolerated in patients with allergies to penicillin, and only limited toxicity has been reported [124].

1.4.1.2.5 β-lactamase inhibitors

Due to the increased resistance to β-lactam antibiotics, the development of β-lactamase inhibitors were needed to circumvent this problem. β-lactamase inhibitors target specific classes of β-lactamases such as the serine β-lactamases. Clavulanic acid, produced by *Streptomyces clavuligerus*, is a selective β-lactamase inhibitor which causes the acylation of the enzyme and further opening of the oxazole ring in order to form an imine [125]. The imine will then proceed to rearrange into an enamine, which further arranges into a stable *trans* conformation to achieve

complete inhibition of β-lactamases [126]. Sulbactam, of the sulfones group of β-lactamases inhibitors, has a similar mechanism of action to that of clavulanic acid but with downstream compound improvements which brought about activity against Classes C and D β-lactamases [127]. Many other analogues of β-lactamase inhibitors have been generated through semi-synthetic organic chemistry methods with the major classes derived directly from natural products. Unfortunately, due to its natural product properties, many strains have developed resistance to β-lactamase inhibitors through acquisition of point mutations.

1.4.1.3 *S. aureus* and MRSA antibiotic treatment

S. aureus infections can be classified into two categories: uncomplicated and complicated ones. Uncomplicated infections must meet the following criteria: a catheter infection where the catheter is removed, a negative blood culture result on the follow-up, a fever resolution within 72 hrs, no abnormal findings on echocardiogram and no symptom of metastatic infection [128]. When the aforementioned conditions are not met, a complicated bacteremial case is diagnosed. Antibiotics should be taken for 14 days for uncomplicated bacteremial cases and for 4 to 6 weeks for complicated cases. For most cases of *S. aureus* and MRSA bacteremia, Vancomycin or Daptomycin are the recommended treatments, with linezolid and clindamycin being administered alternatively in the presence of a secondary infection contraindicating the use of the primary antibiotics [129]. The increase in Vancomycin resistant *S. aureus* (VRSA) has recently led to the development of alternative treatments such as vaccine-based and combinational therapies [130].

1.4.1.4 Current Therapies for CDI

Recommended treatments for CDI infection often vary based on the severity of the infection. The consensus therapy amongst healthcare providers is that stopping the course of the antibiotic causing this CDI should be the first and most important initiative. Broad-spectrum antibiotics, which impact the prevalence of CDI should be changed for a narrow-spectrum antibiotic, whenever possible [131]. Laxatives and antidiarrheal agents should be avoided due to patient fluid loss and electrolyte replacing fluids should be administered [131]. The current antibiotic therapies for CDI are the use of metronidazole and vancomycin. Powder vancomycin should be administered topically intraoperatively, orally or rectally as intravenous (IV) methods are ineffective [131]. Metronidazole may be administered orally or intravenously as similar levels of the antibiotic achieves equivalent bioavailability, although the oral route is preferred. While metronidazole is often administered prior to vancomycin use, vancomycin does exhibit superiority since *C. difficile* has acquired much resistance to metronidazole in recent years [132]. Due to the recent resistance to metronidazole, vancomycin is now becoming a first line therapy for CDI, especially in patients with severe cases [133]. A typical course of metronidazole for CDI treatment is of 10-14 days, although most cases resolve within 7 days of treatment [134]. In patients with moderate to severe cases, other strategies are often employed and include combination therapy, probiotic treatments and toxin binding resins [121]. Patients having multiple recurrences of CDI can explore alternative therapies such as fecal transplants [135].

1.4.1.5 Diagnosis and therapies for *H. pylori*

Diagnosis of *H. pylori* can be accomplished through invasive and non-invasive methods. Detection of *H. pylori* is sensitive and accurate although confirmation through various tests is required for accuracy. The most common invasive test is detection through endoscopy although it is expensive and generally unpleasant for the patients and carries the risk of perforation and hemorrhaging. New approaches such as confocal endomicroscopy and narrow band imaging allow the mucosal surface to be examined in greater detail [136]. Histologic tests are also used to reveal the presence of *H. pylori*. After obtaining a biopsy sample from the patient, a cut of tissue is stained with hemolin and eosin to see the spiral bacteria at the surface of the mucus layer and embedded in the gastric crypts [137]. The sensitivity of this test varies based on the level of bacterial colonization and the experience of the histologists. Stool culture testing or urease testing for the presence of ammonia are simple and rapid which can confirm the presence of *H. pylori*, although the most sensitive PCR or *in situ* hybridization methods allow for the detection of specific virulence markers [138]. Non-invasive testing is typically preferred by patients and includes serological tests such as the ELISA, the latex agglutination test and the Western blotting with gel electrophoresis. CagA, of which the gene is located on the pathogenicity island chromosome of *H. pylori*, is a 120 kDa protein associated with severe gastritis and increased probability of developing gastric atrophy, gastric metaplasia and a higher likelihood of developing cancer [136]. The vacuolating toxin, is not specifically located on the pathogenicity island but may be secreted by strains which generally contain a pathogenicity island. For real-time detection of *H. pylori* infection, the ^{13}C-urea breath test is based on the principle that urease activity is present in the stomachs of infected individuals; as *H. pylori* is a producer of urease which further dissociates into ammonia and carbon dioxide.

The hydrolysis occurs in the mucus layer of the stomach lining resulting in radio-labelled CO_2 being released into the epithelial blood vessels and further appearing on the patient's breath [138]. The first line of therapy for *H. pylori* infection has been the macrolide, clarithromycin but recently combination therapy is being promoted as the first line treatment. The combination of clarithromycin with proton-pump inhibitors in addition to metronidazole or amoxicillin as a triple therapy was previously included in the clinical guideline for managing the infection over a 7 day course [139]. However, the Canadian Association for Gastroenterology (CAG) has noted the growing prevalence of antibiotic resistant *H. pylori* and the increased failure of PPI triple therapies often requiring a quadruple therapy including Bismuth over a 14 day treatment [140]. With increasing resistance to clarythomycin and amoxicillin, tetracycline has been recently investigated as a combination treatment for the eradication of *H. pylori* [141].

The guideline also indicates that if amoxicillin resistance increases above 15%, a quadruple therapy with the addition of bismuth and substituting amoxicillin for tetracycline is to be employed. A 7-day course of the triple or a 14 day course of quadruple therapy is efficient in eliminating the infection.

1.4.1.6 *E. coli* ROS

Unlike its eukaryotic counterpart, *E. coli* DnaA may continue to initiate new rounds of replication despite the multiple strand breaks which may occur during exponential growth. Consequently, *E. coli* must repair its chromosome in a short time or risk turning the single strand breaks into double strand breaks (DSBs), ultimately leading to the bacterium’s death. There are many conditions

which may cause DSBs in *E. coli* such as the lethal oxidation of its DNA from the presence of molecular oxygen molecules. Molecular oxygen found in the environment can be converted into

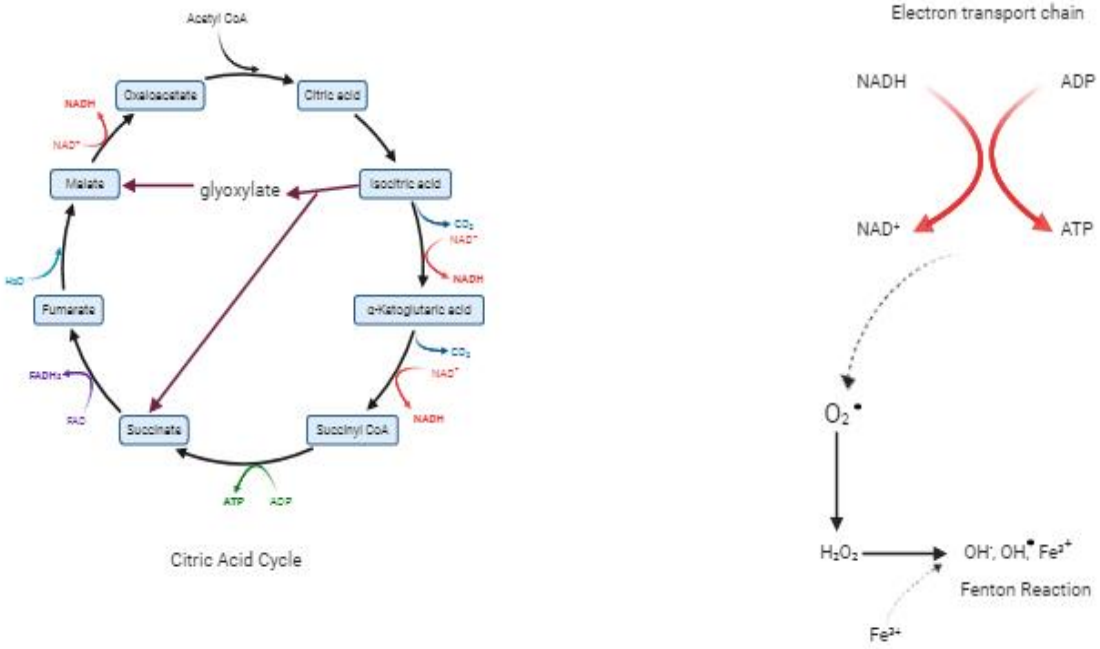

reactive oxygen species, with the most prevalent being the superoxide anions (O_2^-), hydrogen peroxide (H_2O_2) and hydroxyl radicals (OH^-). Although H_2O_2 is not a radical species, it has the ability to diffuse through biomembranes, reaching the cytoplasm and causing damage [142]. Importantly, H_2O_2 reacts with bioavailable iron (Fe) in the Fenton reaction allowing for the production of OH^- and further DNA damage (**Figure 5**) [143]. While O_2^- does not oxidize DNA directly, due to its dismutation into H_2O_2, it can contribute to the Fenton reaction.

Figure 5 : The ROS pathway in *E. coli*

Antibiotics such as compounds with β-lactams may activate the Citric Acid Cycle and, subsequently, hyperactivate the electron transport chain. Consequently, there is the production of oxygen radicals which can bind (dotted arrow) and destabilize the Fe-S

complex in which Mg^{2+} will outcompete Fe^{3+} binding. Free Fe^{3+} is now readily available to participate in the Fenton reaction. In order to circumvent ROS generation, the glyoxylate shunt (purple arrows) may be used to bypass the conversion of necessary NADH for the ETC.

1.4.1.6.1 Sources and Detection of ROS

E. coli often encounters ROS in its environment, especially in the gut, where H_2O_2 is occasionally the byproduct of lactic acid producing bacteria [144]. ROS are also produced endogenously, however, the respiratory chain accounts only for a minor quantity of *E.coli's* self-generated ROS [145]. The currently accepted model of bacterial ROS generation is that proteins containing exposed iron sulfur clusters are the main source of ROS. Under normal conditions, detection of ROS is achieved through superoxide dismutases (SOD), which are found in abundance in the eukaryotic and prokaryotic cells. *E.coli* harbours two systems to help it respond to ROS: the oxidative stress regulator (OxyR) responsible for mitigating high levels of H_2O_2, and superoxide response (SoxR/S) which reacts to elevated levels of superoxide generating molecules such as O_2^- [146,147]. With minimal overlap between the OxyR and SoxR/S regulons, a commonality presides over them: the induction of detoxifying enzyme catalases, peroxidases and dismutases. The reduction of the intracellular pool of Fe and the expression of oxidant-resistant isoenzymes are also additional commonalities shared amongst the two systems [146]. During normal growth conditions, SoxR is produced in a reduced state and activates simultaneously through the activation of *soxS* [147]. In turn, the SoxS protein activates the expression of *sodA, acnA, fumC, micF* and *zwF*. The OxyR regulon is primarily activated in the presence of H_2O_2, leading to the transcription of *ahpC, grxA, katG* and *oxyS* genes which increase hydrogen peroxide resistance [148]. ROS generating compounds can inactivate metalloproteins by promoting the dissociation of Fe atoms allowing the

apo-proteins to later reincorporate other metals such as Mg^{2+}, Fe and Zn^{2+}, allowing them to become resistant to H_2O_2 and O_2^- [149]. In order to reinstate metabolic activities, *E.coli* induces the expression of Mn^{2+} transporter causing an up-regulation of cytoplasmic Mn^{2+}. This increase in Mn^{2+} may outcompete Fe, leading to the accumulation of cytoplasmic Fe making it readily available to participate in the Fenton reaction [150].

1.4.1.6.2 **Response to ROS**

A variety of enzymes may be activated to scavenge ROS, which includes superoxide dismutases (SODs), peroxiredoxins (Prxs) and catalases. *E. coli* harbour three SOD variants including Fe-SOD and Mn-SOD, both found in the cytoplasm, as well as Cu-SOD located in the periplasm. The *sodA* gene codes for Mn-SOD, which allows the formation of H_2O_2 as a result of O_2^- dismutation [151]. Although H_2O_2 is one of the necessary compound in the Fenton reaction, alkyl hydroperoxide reductases are often up-regulated to circumvent the accumulation of the H_2O_2 byproducts. *ahpC*, a peroxiredoxins (Prxs) family, is a highly conserved enzyme in *E. coli*, and its conservation relies on only two specific amino acid residues [152]. The highly conserved nucleophilic cysteine residue becomes selectively oxidized to form the peroxidatic cysteine (C_p) - SOH intermediate. This allows for the resolving cysteine (C_R), located at the opposing C-terminus of the adjacent AhpC homodimer, to form intramolecular disulphide bonds [153]. The AhpC/Prx1enzymatic complex can modulate its quaternary structure depending on the redox state. When reduced, the complex becomes a doughnut-shape. In an oxidized state, weakening of the decamer interactions promotes dimerization [153]. In order to help maintain the intramolecular disulfide bond, AhpF (a bacterial AhpC reductase) enables the continuous peroxidase cycle. In contrast to mammalian cells, most

bacterial Prxs are resistant to elevated levels of H_2O_2. Bacterial Prxs are often up-regulated as a result of the increased levels of H_2O_2 in the cell [154].

1.4.1.6.3 Fenton Reaction

Under aerobic conditions, *E. coli* may reduce oxygen and generate water in a sequence of coupled proton and electron transfers to satisfy the necessary needs for ATP production. Similarly to the Haber-Weiss reaction, Fenton chemistry relies on the principle that the oxidant in the reaction does not necessarily need to be hydrogen peroxide but could also be substituted for chlorinated water [155]. The second rule of Fenton reaction is that a reduced form of a heavy metal is needed in moderate concentration, whereas the Haber-Weiss reaction involves an additional step, suggesting SODs are the generators of the oxygen necessary for the reaction. In scientific work, the Fenton reaction refers to the reaction between H_2O_2 and ferrous salts in order to produce superoxide radicals as shown below.

$$H_2O_2 + Fe^{2+} \rightarrow Fe^{3+} + OH\cdot + OH^-.$$

The biological targets of free radicals include DNA, RNA, proteins and lipids. The Fenton reaction is a major contributor to the lipid damage incurred at the cell wall through the production of free radicals. Free radicals generated in the cell are able to attack polyunsaturated fatty acids and initiate lipid peroxidation, resulting in a loss of membrane integrity [156]. DNA damage is also the result of free radical generation. Through the sugar moieties in the DNA backbone, free radicals will insert into the backbone causing single and double DNA strand breaks, which may block the progression of cellular replication.

1.5 Emergence of Antibiotic Resistance

1.5.1 *Current Status of C. difficile Antimicrobial Resistance*

Overprescription and misuse of antibiotics is thought to be the primary cause in patient acquired CDI [157]. Due to *C. difficile's* ability to produce spores, the bacteria will often persist through antibiotic treatments frequently causing relapse in patients with a previous CDI infection. It is known that *C. difficile* is resistant to many antibiotics such as penicillins, fluoroquinolones, aminoglycosides, clindamycin, tetracyclines, erythromycin and more, which are commonly used in clinical health care settings [158]. Recent studies have shown high levels of *C. difficile* resistance to first and second generation cephalosporins and fluoroquinolones (51% and 47%, respectively) according to the EUCAST and CSLI breakpoints [159]. Extended use of clindamycin, cephalosporins and quinolones have all been shown to promote CDI infection [160]. Resistance to commonly used antibiotics for the treatment of *C. difficile* not only promotes recurring CDI infection but also drives the emergence of new strains. The NAP1/B1/027 strain is a stereotypical example, having emerged in the last decade, becoming a predominant strain in North America associated with the overuse of fluoroquinolone antibiotics [161]. Metronidazole and Vancomycin remain the first line therapy for CDI although resistance to metronidazole is becoming increasingly apparent in the clinical setting [157]. Cephalosporin antibiotics are bactericidal β-lactam antibiotics, which act by inhibiting enzymes in the cell wall thus interrupting the synthesis of bacterial cell wall. Resistance to cephalosporin antibiotics is still poorly understood despite many strains displaying resistance to these antibiotics. *C. difficile* is often described as being "constitutively resistant" as overgrowth of the bacteria seems to occur after cephalosporin

treatment [162]. Sequence analysis of 630 genomes of *C. difficile* revealed the harbouring of several coding sequences similar to the β-lactam antibiotic resistance gene [163]. Much like the cephalosporin antibiotics, fluoroquinolone antibiotics are also classified as bactericidal antibiotics despite acting *via* the inhibition of type IV DNA topoisomerase (gyrase), which is required for bacterial mRNA synthesis and DNA replication [164]. DNA gyrase is responsible for introducing a negative helical twist in the DNA double helix thus allowing for the separation of the daughter chromosomes. DNA gyrase is composed of two protein subunits, GyrA and GyrB encoded by the *gyrA and gyrB* genes, respectively [165]. Topoisomerase IV is responsible for removing the linkages between the two daughter chromosomes thereby allowing the division into two separate daughter cells at the end of replication [166]. Fluoroquinolones will interact with the GyrA subunit of the enzyme bound DNA complex creating conformational changes, which results in the inhibition of normal enzymatic activity [167]. The enzyme still harbours the ability to cut DNA, however, lacks the ability to re-ligate DNA leading to eventual cell death [167]. Resistance to fluoroquinolones in *C. difficile* may be attributable to primary changes such as alterations in the drug target enzyme and alterations in access to the drug target enzyme. Previous studies have shown that *C. difficile* resistance to fluoroquinolones can be attributed to changes in the DNA gyrase subunits GyrA and/or GyrB [168]. Genomic analysis of *C. difficile* 027 ribotype revealed a single nucleotide polymorphism (SNP) in the quinolone resistance determining region (QRDR), specifically in the *gyrA* locus [169]. Through the identification of a mutation at the Ser-83 position in *gyrA* corresponding to fluoroquinolone resistance in *E. coli*, an ortholog for *C. difficile* NAP1/B1/027 has been identified as a mutation in the Thr-82 position [134]. Four different amino

acid substitutions have been identified in *gyrB*, with a substitution of the Asp426 residue to Val, being described in both toxin A and toxin B positive *C. difficile* strains [169].

C. difficile has developed multiple mechanisms of antibiotic resistance. They most commonly include: resistance associated genes, mobile genetic elements (MGEs), alteration to drug target and biofilm formation. An important mechanism of *C. difficile* antibiotic resistance is through the conjugation, transduction or transformation of MGEs [159]. *C. difficile* resistance to macrolide-lincosamide-streptogramin B (MLS_B) is mediated by four different transposons including: Tn5398, Tn5398-like derivatives, Tn1694 and Tn6215. Both Tn5398 and Tn6215 are known to integrate into the *C. difficile* genome *via* exchange of large genetic fragments [168]. Tn5298 will integrate into the genome through homologous recombination or site-specific integration whereas Tn6215 will integrate using a conjugation mechanism or phiC2 phage transduction [170]. These four transposons are responsible for the transfer of the tet class of genes (*tetM, tet44 and tetW*), promoting *C. difficile* resistance to tetracyclines. Resistance through biofilm formation is a common contributing factor in resistance of C. *difficile* to antibiotics. A multi-layered structure, the biofilm matrix is composed of proteins, DNA and polysaccharides. The formation of the *C. difficile* biofilm is largely due to intrinsic mechanisms including Cwp84, the flagella and the LuxS autoinducer [171]. Biofilms can protect *C. difficile* and other pathogenic bacteria from unfavourable conditions and have been proposed to play a role in Vancomycin and Metronidazole resistance [172]. Currently available data suggests that *C. difficile* Vancomycin resistance can be attributed to amino acid changes in the peptidoglycan biosynthesis through the MurG protein [173]. *C. difficile* resistance to rifamycin is proposed to be the result of mutations to the *rpoB* gene, which encodes a bacterial RNA polymerase. A similar mechanism of *C. difficile* resistance to

fusidic acid has been investigated by Tsutsumi and colleagues. They noted that *C. difficile* resistant strains carried a mutation in the *fusA* gene, which codes for bacterial proteins targeted by fusidic acid [174]. Although the exact mechanisms of resistance is poorly understood, the variety of antibiotics to which *C. difficile* is now resistant to, makes it increasingly difficult to control, and thus being responsible for many nosocomial infections.

1.5.1.1 Burden on Healthcare System

CDI places a significant burden to the healthcare system financially both in acute-care facilities as well as long-term care settings. Various studies have examined the attributable cost of CDI in acute-care facilities taking into account the costs of CDI as primary or secondary infections. O'Brien and colleagues determined the mean per patient cost of CDI in 2008 to be $11,498 USD for those diagnosed with a secondary infection, and $15,397 USD as a primary infection in acute-care facilities [175]. With the prevalence of CDI infection in the United States these costs can be translated into 4.9 billion dollars USD for 2008 alone [175]. According to the 2008 Healthcare Research and Quality Healthcare Cost Utilization Project (HCUP), 348,950 discharges in the United States were attributed to CDI in acute-care settings with the majority of these patients (340,401 patients) belonging to the adult (>18) age demographic [175]. While these studies examined the burden from a financial perspective, numerous indirect effects of CDI can also increase the cost to the health care system. Using appropriate contact precautions when possible, including isolation, suitable transfer of location and additional housekeeping measure are various approaches in order to help alleviate burden [176].

Despite no CDI burden study in long-term care facilities (LTCF) has been conducted, presumably the cost of CDI also extends into LTCF. Dubberke *et al.* found that 32% of patients diagnosed with CDI in an acute-care facility were discharged to a LTCF [176]. According to the HCUP data collected in 2008, this would equate to >30, 600 annual discharges of CDI positive patients transferred to a LTCF in the United States alone [177]. From a financial standpoint, this burden equates to $141 million USD in healthcare costs annually [177]. In addition to the cost of CDI patients in nursing homes, additional costs can be foreseen as a result of the accompanying ailments that are often found in an older demographic. The inability to control bowel movement and the increase in falls among the patients with *C. difficile* are additional contributing factors to the cost and burden to the healthcare system [178].

1.5.2 *Mechanisms of resistance*

With the β-lactams making 50% of the antibiotic market, it's no surprise that both gram-negative and gram-positive species have developed resistance to these antibiotics. Many mechanisms of resistance have been identified and have characterized the ways in which bacteria evade β-lactam antibiotics. The most common mechanisms include β-lactamase enzymes, target site alterations *via* the PBPs and efflux pumps.

1.5.2.1 **β-lactamase**

Predominantly found in gram-negative species, the β-lactamases represent a major source of resistance to β-lactam antibiotics. They do so by hydrolyzing the β-lactam ring of the antibiotic, making it ineffective [179]. β-lactamases are often encoded chromosomally but may also be

plasmid encoded for mobile genetic elements including transposons and integrons. The four molecular classes of β-lactamases are termed A-D, each class having specific substrate specificity and including metal-dependent and independent enzymes. Classes A and D are part of the extended spectrum β-lactamases (ESBL), which have broad substrate specificity and are capable of hydrolyzing many of the newer generations of antibiotics [180].

1.5.2.2 **ESBL Families**

Classical ESBLs which are found in Class A, have evolved from the TEM and SHV enzymes, whereas Class D has evolved from the OXA enzymes which have all derived from mutations associated with the use of narrow spectrum antibiotics [180].The most commonly reported microorganisms to have Class A ESBLs are *E. coli* and Klebsiella *sp.*; although other members of the enterobacteriacae family have been described [181]. Various amino acid substitutions are responsible for TEM and SHV resistance to specific antibiotics. Mutations at amino acid residues Gly238 and Glu240 of SHV-1 enzymes have been shown to confer resistance to ceftazidime and cefotaxime specifically [182]. The crystal structure for TEM and SHV enzymes revealed an enlarged binding cavity, which could accommodate bulky oxyamino substituents [183]. The OXA ESBLs are quite rare and are only found in the *Pseudomonas sp.* with the majority of the resistance conferred to oxyaminocephalosporins (such as ceftazidime) and often found chromosomally encoded or on plasmids (less so on integrons) [184]. Many ESBL strains also harbour AmpC in their genomes, conferring resistance to an even broader spectrum of β-lactam antibiotics. AmpC containing species belong to Class C ESBLs and are classified as cephalosporinases. Most AmpC containing microorganisms belong to the enterobacteriacae family and are highly resistant to

penicillins and cephalosporins [185]. AmpC ESBLs are encoded either chromosomally or on a plasmid, the former inducible by the AmpR regulator and ampD-cytosolic amidase [186,187]. On the contrary, plasmid AmpC is non-inducible due to the absence of AmpR, with alterations and mutations in the promoter as the suggested mechanism in AmpC plasmid positive species. The final class of ESBLs, Class B, is further subdivided into three classes (B1-B3) which are of particular concern as they are able to confer resistance to all classes of antibiotics. Found predominantly chromosomally encoded, Class B ESBLs are susceptible to metal-ion chelators, rendering metallo-β-lactams an attractive therapeutic alternative [188]. Unfortunately, metallo-β-lactamsases have surfaced in a number of organisms including *E. coli* (NDM-1 *E. coli*), *P. aeruginosa, K. pneumoniae* and others.

1.5.2.3 **Target site alteration**

While the major mechanism by which β-lactam resistance occurs is through the presence of β-lactamases, certain gram-negative species such as *Haemophilus influenzae* and *Neisseria sp.*, have been shown to display resistance as a result of alteration to their PBPs. Mutations in the *penA* gene of PBPs can be acquired through horizontal transfer and reduces PBP susceptibility [189]. Enterococci are intrinsically resistant to β-lactams because of their low PBP production. Gram positive species such as *Streptococcus pneumoniae* and *S. aureus* can almost exclusively attribute their resistance to β-lactams as a result of PBP alterations. Unlike *S. aureus* which only requires one PBP modification in order to exhibit resistance to all β-lactams, *S. pneumoniae* requires modification of all six PBPs, usually in the form of point mutations [190]. Resistance to β-lactams, such as methicillin, can result in the MRSA superbug as a consequence of a low-affinity PBP: PBP2a. PBP2a is encoded by *mecA* located on the novel staphylococcal chromosome cassette mec

(SCCmec) [191]. SCCmec also carries the *mecA* regulator genes, *mecI* and *mecR1,* and is horizontally transferred amongst MRSA species.

1.5.2.4 Efflux pumps

Efflux pumps have long been an antibiotic resistance mechanism. There are five well described classes of efflux pumps: the major facilitator superfamily (MFS), the ATP-binding cassette (ABC), the resistance nodulation division (RND), the multidrug and toxic compound extrusion (MATE), and lastly the small multidrug resistance (SMD) families [191]. The RND family is most prevalent amongst the antibiotic-resistant gram-negative species and is chromosomally encoded. The MexAB-OprM systems have demonstrated increased ability to confer carbapenem resistance to a variety of species including *E. coli, P. aeruginosa, S. enterica* and many others [192].

1.6 Novel Class of Antibiotics

1.6.1 *γ-lactam antibiotics*

In order to circumvent the widespread and increasing number of resistant strains to β-lactam antibiotics, new alternatives are being developed. γ-lactam antibiotics are a novel class of antibacterials with a similar backbone to the β-lactam structure. The traditional 4-membered ring of the β-lactams is altered to a cyclopentane moiety with PBP-like activity (Figure 6). The first described γ-lactam compound was in 1986 by Williams and colleagues who had documented increased molecular strain on the bicyclo ring, which resulted in its instability and ultimately associated with poor antibacterial activity [193]. That same year, Baldwin *et al.* synthesized stable

variants of the γ-lactam; however, the authors only vaguely mentioned the novel compounds being weak antibacterial activity against gram-positive species as their work focused primarily on the chemistry [194]. The work by Baldwin and colleagues claimed that they tested their γ-lactam compounds on *E. coli* and *Bacillus subtilis*. However, the authors did not provide with any specific antibacterial results. Thus, chemical synthesis of γ-lactam compounds have been described; however, their antibacterial activities and the mechanism of action are not yet known.

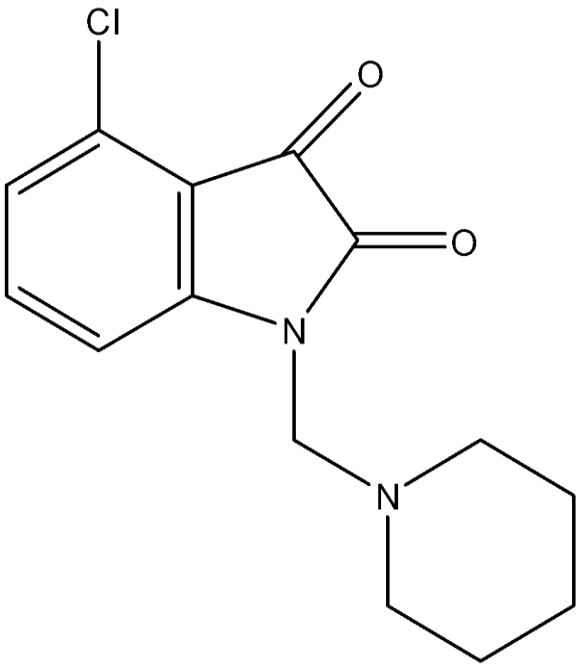

Raja 42

Figure 6: Chemical structure of Raja 42

Much like β-lactams, the γ-lactam backbone is composed of a cyclopentane fused to an aromatic ring, forming isatin. As is the case for Raja 42, it contains Isatin, an organic

compound derived from indole as well as a terminal chlorine (Cl) substituent in the 4th position. In addition, the backbone for Raja 42 contains a piperidine-ring.

1.6.2 *Raja 42*

Initially developed as a novel anticancer therapeutic agent, 4-Chloro-1-(1-piperidinylmethyl)-1H-indole-2,3-dione (Raja 42) is one of the 211 compounds from a chemical library generated through hybrid approach as described [195] (Figure 6). Raja 42 contains a basic CQ scaffold, an isatin moiety, and a terminal chlorine group in addition to a piperidine ring. The IC_{50} values of Raja 42 on non-cancer cell lines are 70-90 μM; thus, its cytotoxicity on normal human cells is not very high. In this thesis, I will describe Raja 42 as a promising lead for an effective and potentially safe antibacterial agent.

1.7 Thesis Overview

1.7.1 *Summary of work presented in this thesis.*

With the ongoing global threat of antibiotic and multi-drug resistant microorganisms, the development of novel alternative therapeutics is an urgent matter. The work described in this doctoral thesis aims to determine the spectrum of activities of novel compounds, and to elucidate the mechanism of action of one of these compounds. This thesis comprises two aims, with the first aim to focus on the characterization of the Raja 42 novel compound against prevalent bacterial species. This initial work led to the second chapter of my thesis in which I questioned and identified the mechanism by which Raja 42 exhibits its antibacterial activity. Through bacterial genomic sequencing and further analysis, it was determined that the citric acid cycle and Fenton reaction (generating ROS) played an important role in the Raja 42-mediated cell-killing mechanism. In

particular, the data revealed an important deletion in the gene neighbourhood of *ghrA.* Complementary experiments further highlighted the importance of this deletion in the development of bacteria resistant to Raja 42. This study further sought to determine the spectrum of activity of Raja 42 against *C. difficile* clinical patient samples obtained from Health Science North Hospital in Sudbury, Ontario. Through this work, a novel mechanism of action against anaerobic species has been postulated. In conclusion, this work suggests a novel mechanism of action which Raja 42 exhibits, to inhibit aerobic bacterial species. Through the activation of the citric acid cycle and further hyper-activation of the electron transport chain, Mg^{2+} may out-compete Fe^{3+} when binding to the superoxide dismutase. Consequently, the free floating Fe^{3+} may be readily available for the Fenton reaction which further produces reactive oxygen species capable of causing downstream DNA, RNA and protein damage. This postulated novel mechanism and extended spectrum of activity make Raja 42 an attractive novel antibacterial compound.

2.0 Materials and methods

2.1 Aerobic Bacterial Culture

E. coli K12 (New England Biolabs, Ipswich, MA) was used primarily for all spectra analysis and mechanistic studies. NDM-1 *E.coli* ATCC BAA 2469 and *E. coli* DH5α were grown in Luria-Bertani Broth (LB) dehydrated media and LB-agar (7.5g/lt) according to the Becton-Dickinson methodology as previously described [196]. *E. coli* K12 and NDM-1 *E. coli* were also grown on LB Chromo Select Agar purchased from Sigma Millipore (Darmstadt, Germany). Kanamycin resistant *E. coli* ATCC 55244 and ampicillin-resistant *E. coli* ATCC 39936 were grown in LB supplemented with 50 µg/mL and 100 µg/mL of kanamycin and ampicillin, respectively. *S. aureus* ATCC 10832 and methicillin-resistant *S. aureus* (MRSA) ATCC BAA-44 were both grown in Nutrient broth or Nutrient agar plates (ATCC, Manassas, U.S.A), whereas *Saccharomyces cerevisiae* ATCC S288c was grown in Yeast-Extract-Peptone-Dextrose (YPD) purchased from Sigma (Basingstoke, UK). Vancomycin-resistant *Enterococcus faecalis* (VRE) ATCC 51299 was grown in Tryptic-Soy Broth (TSB) (Basingstoke, UK). All plates were grown at 37 °C in aerobic conditions and liquid tube cultures were grown in 5 mL of broth (unless stated otherwise) at 37 °C in aerobic conditions shaking at 200 rpm (Thermo Scientific Max Q 2000). Bacterial medium containing 0.5% the agar content was used to create a soft- top for bacterial plating.

2.2 Antibiotic Susceptibilities of C. difficile isolates

The 200 clinical *C. difficile* samples collected from Health Sciences North by Dr. Nokhbeh and his group, are listed in (Table 2) of the appendix section. Quality Control (QC) validation was

performed comparing the MIC of our clinical isolates against that of EUCAST published values for *C. difficile* ATCC 700057, *C. difficile* ATCC 9689, *C. difficile* ATCC 42596, *C. difficile* ATCC 43598 and *E. faecalis* ATCC 29212 strains respectively. All *C. difficile* strains were grown in Columbia broth (Oxoid Ltd., Basingstoke, Hampshire, England, Cat: CM0331) to allow for sporulation and further growth in Brain Heart Infusion Broth (BHI) (Nutri-Bact, Terrebonne, Quebec, CA, Cat: QB-48-0305). Bacteriological Agar (BA) (Quelab, Montreal, Quebec, CA, Cat: QB-46-0221) was used to prepare solid agar plates (15g/lt) for MIC testing against the *C. difficile* isolates. BHI agar plates were supplemented with Hemin (from Bovine origins, with >90% purity) (Sigma-Aldrich, Saint Louis, MO, USA, Cat:H9039-1G), Vitamin K1 (Sigma-Aldrich, Saint Louis, MO, USA, Cat: V3501-1G) and laked, defibrinated sheep blood (NutriBact, Terrebonne, QC, CA) and pre-reduced in the anaerobic chamber prior to inoculation with bacteria. *C. difficile* cultures were grown in anaerobic conditions in an 855-AC controlled atmospheric chamber (Plas Labs, Lansing, USA). Standard microanaerobic conditions were met (85% N_2, 10% H_2, 5% CO_2). Visualization of bacteria was made possible using the Axioscope A1 fluorescent microscope and by the use of phase contrast mode and 40x objective lens (Carl Zeiss Microscopy, Thornwood, USA). FloQSwabs were used to create uniform and even bacterial lawns in order to complete antibiotic susceptibility testing. Bacterial culture optical density was determined using a 96 well NUNC plates which were visualized in the TECAN Spectra computerized plate reader at an absorbance of 540 nm.

2.3 Cryopreservation

Working plates of each strain were maintained at 4 ^{o}C for daily culturing and short term storage. Cryopreservations of all bacterial stocks were completed by growing 5 mL of culture for 18 hours and further peletting the cells at 3200 ×g for 15 min. The supernatant was discarded and spun down cell pellets were resuspended in 10% sterile glycerol prior to being transferred to cryovials. Cryovial stocks were stored in the -80 °C freezer for long term storage and preservation. Inoculation of broth and plates media used sterile, plastic 1 µL inoculating loops (Sarstedt, Germany, Cat: 86.1562.010).

2.4 Aerobic Antibiotic Susceptibility Testing

Cryopreserved isolates (*E. coli, S. aueus,* MRSA, *H. pylori* and *S. cerivisciae*) were grown in LB, YSB, Nutrient Broth, YPD or agar plate equivalents at appropriate atmospheric conditions. Turbidity of cultures was standardized to 1 McFarland turbidity index and adjusted by adding LB (De Backer et al., 2006; bioMérieux, 2012b). The turbidity adjusted bacterial cultures were streaked on the surface of 100 mm petri plates containing, 4 mm thick agar media (supplemented with or without Kanamycin or Ampicillin) three times, rotating the plate 90°-180° and allowing the plate to sit 3-5 min at RT to allow it to dry. 6.5 mm Kirby-Bauer Disks were impregnated with a volume of 20 µL of various synthetic novel chemical compounds to deliver 200 µg of each compound and subsequently the equivalent to MIC value for 27 active compounds and deposited onto the plate using a pair of sterile forceps and gently tapping in place, according to the ASM guidelines [197]. All novel compounds, as well as test compounds were in powder form and 20

mg mL^{-1} stock solutions were prepared by dissolving in dimethyl sulfoxide (DMSO) as listed in 6.2 Antimicrobial activities of 27 active synthetic compounds

Table 3 of the Appendix section. DMSO was used as negative control (150 µg mL^{-1}). Plates were inverted and stacked no higher than five plates per stack and kept under aerobic conditions at 37 °C for 18-24 hours. Diameters of inhibition zones were assessed by measuring the spanning region across the filter disk, absent of bacterial growth. Assays were completed in triplicate, for accuracy, as showin in Figure 7, **Error! Reference source not found.**, and Figure 9.

2.5 Anaerobic Antibiotic Susceptibility Testing

C. difficile Antibiotic susceptibility testing was performed using an Epsilometer test (E-test), with strips purchased from bioMérieux Canada Inc. (St. Laurent, QC, Canada) according to the Clinical Laboratory Standard Institute (CSLI) and European Committee on Antimicrobial Susceptibility Testing (EUCAST) guidelines (Clinical and Laboratory Standards Institute, 2004). Through those standards, *C. difficile* testing was carried out on 100 mm round Petri dishes containing 4 mm thick Brucella agar supplemented with 5% laked sheep blood, 5 mg/L hemin and 1 mg/L vitamin K1 (BBA). The panel of E-test strips included Metronidazole MZ 256 US S30 (Cat: 412403) as well as Vancomycin VA 256 US S30 (Cat: 412486). In order to confirm the accuracy of testing, quality control (QC) strains *E. faecalis* ATCC 29212, *C. difficile* ATCC 700057, *C. difficile 9689, C. difficile* 43596 and *C. difficile* ATCC 43598 were plated using standard conditions (De Backer et 52 al., 2006; bioMérieux, 2012b; Schuyler et al., 2016). Cryopreserved isolates were grown in CB or CB agar plates and colony purified prior to being grown in BHI medium at appropriate atmospheric conditions. Turbidity of cultures were adjusted to 1 McFarland turbidity index by

diluting the cultures with pre- reduced BHI (De Backer et al., 2006; bioMérieux, 2012b). BBA plates were reduced by leaving them for a minimum of 24 hours under anaerobic conditions in order to equilibrate the media to the atmosphere. The standardized bacteria were streaked on the surface of pre-reduced BBA plates 3 times, using sterile cotton swabs, rotating the plate 90°-180° accordingly thus creating a uniform lawn. E-test strips were acclimated to ambient temperature for a minimum of 30 min prior to their application on the plates. E-test strips were applied according to manufacturer instructions followed by plate inversion (bioMérieux, 2012a). Plates were stacked no more than five plates and kept under anaerobic conditions at 36.8 ℃ for 24-30 hours. Qualitative assessment was carried out by comparing the MIC of clinical isolates to that of QC strains and of published MIC values according to the EUCAST guidelines. Antibiotic susceptibility testing was further performed using plate microdilution assay adapted to 96-well plates and dilutions of our novel compound, Raja 42. Raja 42 testing was first performed against *C. difficile* strain ATCC 9689 to identify the Minimum inhibitory concentration (MIC).

Plate microdilution assay was completed as previously described by Garcia, with the following adaptations [198]. Innoculum suspensions and inoculum panels were completed inside the anaerobic chamber. In the anaerobic chamber, 1 mL samples were collected from each culture in order to verify culture contamination using the Axioscope A1 fluorescent microscope with the use of phase contrast mode and 40x objective lens (Carl Zeiss Microscopy, Thornwood, USA). In the anaerobic chamber, 100 µl of each culture was added, in triplicate, to a sterile 96-well plate in order to determine bacterial culture optical density using the TECAN Spectra computerized plate reader at an absorbance of 540 nm. Appropriate culture dillutions to 1 McFarland Turbidity were calculated and dillutions were performed accordingly in the anaerobic chamber. Raja 42 serial

dilutions were performed in a 96 well sterile plates, and 5µl of each 1 McFarland bacterial culture was added to the 96 well sterile plate, containing the Raja 42 serial dilutions, in triplicate rows. Plates were left in anaerobic chamber for 24-48 hours at 36.8 ℃. Turbity was measured using the TECAN Spectra computerized plate reader at an absorbance of 540 nm, in order to determine the MIC of each respective cultured isolate.

2.6 Time kill study

E. coli K12 cells were grown to logarithmic (log) phase and bacterial suspensions were diluted to standard 1 McFarland using the spectrophotometer at 600 nm wavelength. A total volume of 5 mL of culture had various treatments including Raja 42 (50 µg mL^{-1} (12.5 µL from a 20 mg mL^{-1} stock)), kanamycin (100 µg mL^{-1} (5 µL from a 100 µg mL^{-1} stock), clindamycin (100 µg mL^{-1} (5 µL from a 100 µg mL^{-1} stock), and untreated control, in a 50 mL tube. These concentrations were chosen to be equal to the MIC values of antibiotics against the *E.* coli strain used. Treated cells in liquid culture were incubated for various time points: 0 min, 15 min, 30 min, 60 min, 2 hours, 4 hours and 6 hours at 37 ℃ and shaking at 250 rpm. At appropriate time intervals, 5 µL of culture was diluted by a factor of 1/1000 in LB broth. Although multiple dilutions were examined, 1/1000 was shown to give the most optimal results. 100 µL of the diluted sample was plated on LB agar plates and incubated for 24 hours at 37 ℃ and colony forming units (CFU/mL) were determined in triplicate experiments.

CFU/mL = number of colonies × dilution factor × volume factor

2.7 Membrane Depolarization Assay

Five µL of broth cultures of *E. coli* strain K12 was grown in L.B, in a 50 mL tube at 37 °C, shaking at 200 rpm (Thermo Scientific MaxQ 2000) for 18 hours. Bacterial cells were harvested by centrifugation (rotating at 10,000 ×*g* for 1 minute) (Thermo Scientific Sorvall Legend Micro 17) and washed 2 times (*via* pipetting) with Hepes buffer (20 mM of glucose and 5 mM of Hepes at pH 7.3). A volume of 1 mL of fractions from the cell suspensions were diluted with Hepes buffer to achieve a final bacterial concentration ranging between 0.085 and 0.05 at an A_{600}. The suspensions was briefly mixed by quick vortexign and 200 µL was added to the wells of a black 96-well plate. 5 µL of $DiSC_3$ (3,3'-dipropylthiacarbocyanine iodine) dye (1 mg mL^{-1}) was added to a final concentration of 0.4 µM and 0.2 mM of EDTA was added to each well and incubated at 37 °C for 60 min in the dark. 100mM of KCl was added to equilibrate cytoplasmic K+ concentrations. Depolarizing agents were added in triplicate wells at the desired final concentration. The plate was rapidly placed into the reader for monitoring using the monochromater UV-Vis absorbance optics filter. Changes in fluorescence occured at the excitation wavelength (622 nm) and the emission wavelength (670 nm). The fluorescence intensity was measured for cells treated with 0.1% Triton-X (negative control), and the cells treated with 30% hydrogen peroxide (positive control), the untreated culture, and culture treated with the MIC equivalent concentration of drug (50 µg/mL). A_{670} was measured at 60-second intervals for 10 min using the Biotek Synergy H4 Hybrid Reader, as shown in Figure 12.

A blank with only cells and the dye was used to subtract the background.

2.8 Flow Cytometry

The percentage of live and dead cells following treatment with Raja 42 was assessed by flow cytometry and was carried out as follows. 1 mL of overnight Raja 42 treated and untreated *E. coli* K12 were diluted to 5×10^5 bacteria/mL in staining buffer (Phosphate-buffered saline, 1 mM EDTA, 0.1% sodium azide, Tween-20 at 0.01%, pH 7.4). Bacterial suspension was vortexed and subsequently diluted 1/10 in staining buffer. 200 µL of diluted bacterial suspension was added to a 12 × 75 mm polystyrene tube in addition to 0.5 µL of propidium iodide (PI) (Life Technologies, Burlington, ON, Canada) and thiazole orange (TO) to each tube in order to achieve a final concentration of 420 nM for TO and 48 µM for PI. The stock PI solution contained 0.1% v/v PBS, 0.3% v/v Nonidet P-40, 100 µg/mL RNase A and 100 µg/mL propidium iodide. The samples included untreated *E. coli* K12, Raja 42 treated with ½ of the MIC value of *E. coli* K12, Kanamycin ½ of the MIC of *E. coli* K12 as well as the necessary controls (DMSO, T.O alone, P.I alone, unstained sample and ddH2O). The samples were vortexed and incubated for 5 min at RT, protected from light. 50 µL of BD Counting Beads were reverse pipetted into the staining tube in order to determine the concentrations of live and dead cells. Samples were then analyzed using a Beckman Coulter Epics Elite FC 500 Flow Cytometer (Mississauga, ON, Canada). Forward Scatter and Side Scatter (FSS/SSC) were used to exclude potential doublets and debris while the FL1 vs FL3 plot was most representative for the discrimination of the live vs dead populations. Data was generated from at least three biological replicates, as shown in Figure 13.

2.9 2D Gel electrophoresis

2D gel electrophoresis was carried out with log-phase growing *E. coli* K12 treated with ½ of the MIC of Raja 42 or untreated. Cells were centrifuged at 13,000 ×*g* for 10 min using a benchtop Sorvall Legend Micro T17 (Thermo Scientific) and washed twice with 1× PBS. Cultured bacterial cells were resuspended in chilled lysis buffer (7M urea, 2M thiourea, 30 mM Tris, 4% CHAPS, pH 8.5) and sonicated on ice for 30-second pulses at 7 micron amplitude using a sonic dismembrator, model 100 (Thermo 54 Fisher Scientific). Protein extracts were obtained through further centrifugation at 12,000 ×*g* for 10 min and resuspended in 100 µL of an isoelectric-focusing (IEF) rehydration buffer containin 7M urea, 2M thiourea, 4% CHAPS, 1% ampholyte and 1% bromophenol blue (GE Healthcare, Amersham). Proteins were quantitated using the A_{260}/A_{280} ratio feature on the NanoDrop 2000c UV-Vis spectrophotometer (Thermo Scientific, Wilmington, DE, USA) and adjusted to 100 µg/mL in IEF rehydration buffer. Samples were loaded on a 7 cm imobilline dry strip pH 6-10 (ZOOM IPG Strip) and 4-7 (ZOOM IPG Strip), purchased from Thermo Scientific (Carlsbad, California). Strips were transferred to the manifold and 50 µg of samples were overlaid and ran at the following conditions: 300 volts for 3 hours, 600 V for 3 hours, 1000 V for 3 hours, 8000 V for 4 hours and 500 V for 48 hours. Strips were equilibrated with 10-15 mL of equilibration solution 1 (50 mM Tris-HCl pH 8.8, 6 M urea, 30% [v/v] glycerol, 2% SDS, 0.5% DTT) for 10 min and solution 2 (50 mM TrisCl pH 8.8, 6 M urea, 30% [v/v] glycerol, 2% SDS, 4.5% iodoacetamide) for 10 min with gentle shaking. Strips were trimmed to 7 cm and the second dimension was run in precast acrylamide gels (12.5% resolving and 4% stacking gels) with the first lane containing a broad range protein marker (Thermo Scientific). Gels were run in 1× running buffer (25 mM Tris, 192 mM glycine, 0.2% SDS) for 18 hours at 12V. Gels were

stained with 60 mL of Sypro Ruby overnight and imaged on the FluorChem FC3 imaging system using the AlphaView Software. The corresponding results are shown in Figure 14.

2.10 Hydrogen peroxide Assay

Detection of hydrogen peroxide levels in *E. coli* K12 following treatment with Raja 42 was determined using a Hydrogen Peroxide Assay Kit from Abcam (ab102500). *E. coli* K12 was treated with 25 µg mL^{-1} of Raja 42, DMSO (negative control), a combination of thiourea (positive control) and ½ of the MIC of Raja 42 or ½ of the MIC of ampicillin by adding to the culture for 30 minute or 60 minute timepoint. A standard curve was generated by preparing a 0.1 mM H_2O_2 standard and completing serial dilutions to obtain final concentrations of 0, 1, 2, 3, 4, or 5 nM per well. 1.5 mL of mid-log phase bacterial cultures were harvested by centrifugation at 10,000 ×*g* for 1 min using a Thermo Scientific Sorvall Legend Micro 17, and then washed with phosphate buffer saline (PBS). Cells were resuspended in 500 µL of assay buffer (included in the kit) and lysed, on ice, using sonic dismembrator for 30-second pulses at 7 micron amplitude (Thermo 54 Fisher Scientific). Cells were centrifuged at 5000 ×*g* for 1 minute and supernatant was collected. Ice cold 4 M HCl was used for the deproteinization of samples to achieve a final concentration of 1M (contrary to the suggested PCA) and incubated on ice for 5 min. Deproteinization of samples helped minimize erratic readings and HCl was used, contrary to PCA, as our fume hood was not calibrated to support PCA use. Samples were centrifuged at 13,000 ×*g* for 2 min at 4 °C (Sorvall™ Legend™ Micro 21R centrifuge). The supernatant was collected and neutralized with 34 µL 2 M KOH per 100 µL of sample. The samples were further centrifuged at 13,000 ×*g* for 15 min at 4 °C (Sorvall™ Legend™ Micro 21R centrifuge). Once equilibrated at room temperature (RT), 50

µL of sample was dispensed into wells of 96-well plate with 50 µL of reaction mix (46 µL of assay buffer, 2 µL of oxired probe and 2 µL of HRP), followed by incubation at RT for 10 min. The OD_{570} was measured using Biotek Synergy H4 Hybrid Reader. Assay was carried out in triplicate and calculations to determine the concentration of H_2O_2 used the average triplicate readings. The corrected absorbance was determined by subtracting the value of the blank absorbance from standards and samples. The corrected standards were plotted and the best smoothe curve fit generated by the Excel software. The concentration of H_2O_2 was determined using the following formula, as shown in Figure 15.

Sample amount from the standard curve was calculated using the following formula:

$$\text{Sample amount from standard curve} = (\text{corrected absorbance} - (\text{y-intercept})\ \text{slope}^{-1})$$

$$[H_2O_2] = \text{Sample amount from standard curve}\ (\text{sample volume}^{-1})$$

2.11 Live Cell Microscopy

E. coli K12 and NDM-1 *E. coli*, were grown overnight. 10 µL of turbid culture was deposited onto a glass slide and ½ of the MIC of Raja 42 was added to the culture or left untreated. A glass cover slip was added to the slide and time lapse microscopy was carried out with an Axio Scope.A1 at 400× magnification. Cell morphology was observed, and images were captured using the phase contrast setting of the microscope. Time points for the time-lapse study were: 0 min, 5 min, 10 min, 15 min, 30 min and 60 min. Data was generated from three biological replicates, as shown in Figure 16.

2.12 Live/Dead BacLight Fluorescent Microscopy

The Live/Dead Fluorescent microscopy was carried out using the Live/Dead BacLight Bacterial Viability Kit from Thermo Fisher Scientific (L7007). 30 mL of *E. coli* K12 cells were grown to log phase and centrifuged at 10,000 ×*g* for 10 min in the benchtop Sorvall Legend Micro T17 (Thermo Scientific). Cell pellet was resuspended in 2 mL of wash buffer (0.85% NaCl) and 1 mL of concentrated suspension was added to 20 mL of 0.85% NaCl and incubated at RT for 1 hour. Cells were centrifuged at 10,000 ×*g* for 10 min and resuspended in 10 mL of wash buffer. An equal volume of SYTO9 and PI were combined and 3 µL of dye mixture was added per mL of sample. Sample and dye mixture alone were incubated at RT for 15 min and 5 µL was pipetted onto a glass slide with the addition of 25 µg mL^{-1} of Raja 42. Subsequently, cells were imaged at various time intervals: 0 min, 5 min, 10 min and 30 min. Cells were imaged on the Axio Scope.A1 fluorescent microscope (Carl Zeiss Microscopy, Thornwood, USA). The experiment was performed in triplicate, as shown in Figure 17.

2.13 Western Blotting

Protein extraction was carried out on *E. coli* K12 and NDM-1 *E. coli* grown to log phase, which had been treated with or without ½ of the MIC of Raja 42 during growth. 1 mL of turbid culture was centrifuged at 10,000 ×*g* for 2 min and supernatant decanted and kept the pellet on ice. The pellet was resuspended in 200 µL of Lysis buffer (100 mM PO_4^{3-}, 300 mM NaCl, 10% (v/v) glycerol and 1 mg/mL of lysozyme, pH 8.0) and sonicated on ice for 30-second pulses, with 60-second rest intervals, at 7 micron amplitude (at a frequency of 20kHz), for a total of 6 cycles, using a sonic dismembrator, model 100 (Thermo 54 Fisher Scientific). Crude cell lysate was centrifuged

at 16,000 ×*g* for 10 min using the benchtop Thermo Scientific Sorvall Legend Micro 17. Supernatant was collected and transferred to a new 1.5 mL Eppendorf tube for downstream application. Protein concentration was determined using the NanoDrop 2000c UV-Vis Spectrophotometer and normalized using 5× SDS PAGE loading buffer (312.5 mM Tris-HCl, pH 6.8, 10% v/v glycerol, 11.5% v/v sodium dodecyl sulphate (SDS), 0.05% (v/v) bromophenol blue, 5% β-mercaptoethanol) and equal amounts of proteins (25-40 µg/mL). Protein extracts were denatured by boiling samples for 2 min and immediately put them on ice. Samples were loaded into precast 4-12% gradient NuPage SDS-PAGE gels or precast 10% NuPage SDS-PAGE polyacrylamide gels. Proteins were separated at 75 volts in 1× Tris-glycine running buffer (25 mM Tris, 192 mM glycine, 0.1% w/v SDS) for 1 hour. Using the Bio-Rad semi-dry trans-blot SD cell (Bio-Rad, Mississauga, ON, Canada), proteins were transferred to 0.45 µm-diameter pore nitrocellulose membrane (Amersham Biosciences through Cedarlane) in transfer buffer (50 mM Tris, 40 mM glycine, 0.04% w/v SDS, 20% v/v methanol) at 15 V for 30 min. Membranes were "blocked" for 1 hour at RT with 5% weight/volume (w/v) skim milk powder (Carnation) in TBS, followed by addition of a 1/1000 dillution of primary antibody (5% [v/w] skim milk in TBS with respective antibody) overnight at 4 °C with slow rotation. Membranes were washed three times for 5 min each with TBST (TBS with 0.05% Tween-20) and incubated for 1 hour with a 1/1000 dillution of secondary antibody (TBST with 5% [v/w] skim milk powder and secondary antibody conjugated to HRP). Membranes were then washed again 3 times for 5 min each, and imbued with 1 mL of enhanced chemiluminescence (ECL) prime or select reagent. Signals were visualized by exposing the membrane to X-Ray film or with the FluorChem FC3 imaging system using the AlphaView Software from 30-second to 120-second intervals.

2.14 RNA Electropherogram

RNA extraction from *E. coli* K12 and NDM-1 *E. coli* was carried out using a miRNeasy kit from Qiagen (Mississauga, ON, Canada). Protocol was adapted from Bacteria Reagent Handbook (Qiagen) for Gram negative species. *E. coli* K12, Raja 42-resistant *E. coli* and NDM-1 *E. coli* were grown to log phase (OD_{600}) with an addition of the MIC of kanamycin (negative control), ½ of the MIC of Raja 42, rifamycin (positive control) or untreated (control). 500 µL of bacterial broth was added to an RNeasy microcentrifuge tube and centrifuged at 5000 ×*g* for 10 min. The supernatant was decanted and 200 µL of lysozyme-TE buffer (30 mM Tris-HCl, 1 mM EDTA with 15 mg/mL lysozyme, pH 8.5) with 10 µL of proteinase K was used to resuspend the pellet. Samples were vortexed for 10 seconds and incubated at RT for 10 min. 700 µL of proprietary RLT buffer (included in the kit) and 7 µL of β-mercaptoethanol (BME) was added to each sample and vortexed. 500 µL of 100% ethanol was added to each sample and 700 µL of lysate was transferred to an RNeasy mini spin column (Fisher Scientific, Ottawa, ON). The columns were spun for 15 seconds at 8000 ×*g* and 350 µL of proprietary RW1 buffer (included in the kit) was added, spun once more. The flow-through was discarded and 80 µL of DNase1 (1kunitz) was added to the column for 15 min at RT. 500 µL of RPE wash buffer was added to the spin columns and centrifuged for 15-seconds at 10,000 ×g, and carried out for two independent wash steps. 50 µL of RNase-free water was added to the column membrane and spun at 8000 ×*g* for 1 minute to elute the RNA. Electropherogram was analyzed using capillary gel electrophoresis. Samples were loaded into an RNA Nano chromatin immunoprecipitation analysis (Chip) (Agilent Technologies, Santa Clara, CA) and further analyzed using the Agilent 2100 Bioanalyzer (2100 Expert software,

Agilent Technologies, Santa Clara, CA). RNA integrity was assessed through the resultant electropherogram in Figure 19.

2.15 Generation of bacteria resistant to Raja 42

To help identify a possible Raja 42 mechanism of action, *E. coli* K12 DH5α and NDM-1 *E. coli* bacteria resistant to Raja 42 were generated by growing them in liquid L.B medium containing ¼ of the MIC of Raja 42 (12.5 µg/mL) and further plated on L.B agar plates containing 12.5 µg/mL of Raja 42. Plates were incubated for 18 hours at 37 °C and individual colonies assessed the following day. Colonies were subsequently plated on LB agar plates that contained ¼ of the MIC of Raja 42 (12.5 µg/mL) for an additional 3 passages prior to being plated on LB agar plates that contained ½ of the MIC of Raja 42 plates (25 µg/mL). Subsequent to 3 passages at ½ of the MIC of Raja 42, individual single colonies were streaked onto LB agar plates that contained ¾ of the MIC of Raja 42 plates for an additional 3 passages. Colonies were finally streaked on LB agar plates that contained equivalent to one MIC of Raja 42 (50 µg/mL) plates and resistant bacteria were subculted three additional passages. Finally, individual colonies resistant to Raja 42 were isolated and grown in liquid L.B broth containing the MIC of Raja 42 for 18 hours at 37 °C. 1 mL of fully grown culture was cryopreserved in a 10% glycerol stock, and remaining culture stored at -20°C, in a 10% glycerol stock, if downstream applications were not immediately carried out.

2.16 Bacterial Genomic DNA extraction and sequencing

Genomic DNA extraction was carried out with a bacterial genomic DNA kit which was purchased from Norgen Bioteck Corp. (Thorold, ON, Canada). The purity of DNA was assessed using the A_{206}/A_{280} ration function on the NanoDrop 2000c UV-Vis spectrophotometer, and subsequently checking DNA integrity on an agarose gel. Additionally, DNA purity was confirmed through fluorometric quantification using the Quabit dsDNA BR Assay kit and the Qubit 2 fluorometer (Thermo Scientific), as previously described [199]. Library creation and sequencing were completed by Genome Quebec, using pair end-labelling and 250 bp reads through the Ilumina Mi-Seq platform (McGill University and Génome Québec Innovation Centre). The technical control for clustering reactions, sequence accuracy and sequencing diversity in low complexity libraries was done using two parental *E. coli* K12 and NDM1 strains and five clones for each parental strain, respectively. Samples were demultiplexed, and fastq files were produced.

2.17 *E. coli* K12 genomic assembly and annotation

The bioinformatic pipeline was generated and used at the office of Bioinformatics and Genomics at the Health Sciences North Research Institute. The Bioinformatics and Genomics office performed the quality control of the Illumina data, genome assembly and single nucleotide polymorphisms identification, comparison and annotation. Sequence quality control (QC) was performed using the program FastQC ver. 0.11.5 [241]. Trimmomatic ver. 0.39 [200] was used to remove adaptors and trim the sequences using the parameters: ILLUMINACLIP: TrueSeq3-2.fa:2:30:20 LEADING:3 SLIDWINDOW: 4:15 MINLEN: 36. The program Kraken2 ver. 2.0.8-beta [201] was used to confirm the identification of all contigs as *E. coli*. assembly of sequences

was completed using Spades ver. 3.13.1, and error corrections were completed in order to improve the alignment of the contigs [202]. The parameters used in Spades were: --careful -k 33,55,91 –cov-off auto. The scaffolds of the reference genomes were ordered based on the genome reference from NCBI with accession number NC_000913.3 *Escherichia coli* strain K12 substr. DH5α, using the program Mauve mover, part of the program Mauve ver. 2015-02-13 build [203]. The contigs were joined in one fast file using Artemis ver. 16.0.0 [204]. Annotations of wild-type and mutant genomes were completed using the software Prokka ver. 1.14.6 [205]. The program Snippy ver. 4.4.3 [206] was used to determine the single nucleotide polymorphisms (SNPs) among the samples using the default settings (--mapqual 60) and using parental sequences ordered by Mauve mover. The core SNPs, all the single nucleotide polymorphisms shared by each of the five clone samples with their parental *E. coli* genome as a reference, were obtained using Snippy-core ver. 4.4.3, part of the Snippy package [206]. The SNPs were also annotated by the program Snippy, including their position; type of mutation: SNP, deletion or complex variations (ex. frameshift); the level of evidence, based on the SNP sequence coverage; direction of the strand; nucleotide and amino acid position; and if the sequence variance produced a synonymous, nonsynonymous substitution, frameshift or non-coding variation. Snippy also reports structural variations, like deletions and insertions, to report this results we used bcftools ver. 1.9 (bcftools consensus –sample test –fasta-ref ref.fa snps.vcf.gz –o test.fasta)[207]. Finally, it also indicates the gene involved in the mutation and the gene product, if any. The ECOCYC *E. coli* database [204, 205] platform from the Biocyc and Kegg databases [210] were used to correlate SNPs and sequence deletions with metabolic pathways.

2.18 Bacterial Transformation

YcdW (GrhA) and AceA plasmids were generous gifts by Dr. Heribert Warzecha at TU Darmstadt, Germany. The *aceA* and *ycdW* sequences were modified with a His-tag and inserted into a pSB1C3 plasmid, as described by the iGEM group [211]. *E. coli* K12 and Raja 42-resistant *E. coli* K12 were grown to mid-log phase and 25 µL of cells were incubated on ice with 100 ng of YcdW or AceA (negative control) pSB1C3 plasmid DNA for 30 min. NEB 5-alpha Electrocompetent *E. coli* (C2989K) were used as a positive control. Following incubation, cells were heat shocked for 60 seconds by placing tubes in a 42 °C water bath and placing them back on ice for 2 min. 1 mL of SOC outgrowth medium (NEB, B9020S) was added to the cells and incubated at 37 °C for 45 min with shaking at 250 rpm. 50 µL of cells were plated onto LB chloramphenicol plates (150 µg/mL) as the plasmids contained a chloramphenicol selectable marker [211]. Plates were incubated overnight at 37 °C for colony formation. Transformed colonies of *E. coli* K12 (pSB1C3) and Raja 42-resistant *E. coli* K12 (pSB1C3) were grown in liquid culture until log phase, and plasmid DNA was extracted using a NEB Monarch Plasmid miniprep extraction kit (NEB, T1010). 1 mL of bacterial culture was spun down at 12,000 ×*g* for 30 seconds and resuspended in resuspension buffer (B1) included in the kit. Cells were then lyzed with lysis buffer (B2) and further neutralized with plasmid neutralization buffer (B3), both of which were included in the kit. The lysate was calrified by spining at 12,000 ×*g* for 30 seconds and transferring to a new spin column and centrifuging once more. Flow-through was discarded and column was reinserted into collection tube and washed thrice with alcohol-based plasmid washing buffer supplied, prior to centrifugation. Plasmids were eluted from the column membrane with 50 µL of nuclease free

H_2O. Recovered plasmid DNA was quantified using the NanoDrop 2000c UV-Vis spectrophotometer.

For electroporation, SOC medium was placed in a 37 °C water bath and pre-warmed for 1 hour, and then electroporation cuvettes were placed on ice. Positive control, PUC19, was diluted ⅕ to a final concentration of 10 pg/uL using nucleotide-free water. 25 µL of NEB 5-alpha electrocompetent *E. coli*, *E. coli* K12 and Raja 42-resistant *E. coli* K12 were added into chilled electroporation cuvettes, to which 1 µL of AceA or YcdW plasmid DNA was also added. Electroporation was carried out under the following conditions: 1.7 kV, 200 Ω and 25 µF for an electroporation time of 4.8 milliseconds per sample. 975 µL of pre-warmed SOC medium was added immediately following the electroporation, and then contents of the cuvette were transferred into a 1.5 mL Eppendorf tube. Tubes were incubated at 37 °C for 1 hour with rotation at 250 rpm. 100 µL of transformed cells at 1/100 dilution was found to be optimal for plating onto LB agar plates containing Raja 42 (50 µg/mL). Plates were incubated at 37 °C for 18 hours.

2.19 Genomic DNA extraction

Phenol/chloroform extraction method was used to isolate genomic DNA from bacteria, prior to obtaining commercial kits. 1.5 mL of fully grown *E. coli* K12 was centrifuged at 20,000 ×*g* for 1 minute using the benchtop Sorvall Legend Micro 17. The supernatant was decanted and 600 µL of Lysis buffer (for 10 mL: 9.34 mL of TE buffer (10 mM Tris HCl, pH 8.0, 1mM EDTA pH 8.0), 600 µL of 10% SDS and 60 µl of proteinase K [20 mg mL^{-1}]) was used to resuspend the pellet, and then incubated at 37 °C for 1 hour. An equal volume of phenol/chloroform was added and the mixture was spun at 20,000 ×*g* for 5 min at RT. The upper aqueous phase was transferred to a

new 1.5 mL Eppendorf tube and an equal volume of chloroform added. Contents were spun at 20,000 ×*g* for 5 min at RT, and the aqueous layer transferred to a new 1.5 mL tube. The DNA solution was mixed with 2.5 × of cold 200 ethanol, and incubated at -20 °C for 1-2 hours. Contents were spun for 15 min at 20,000 ×*g* at 4 °C using a benchtop Sorvall Legend Micro 21R centrifuge. The supernatant was discarded and the pellet washed with 70% ethanol and further spun at 20,000 ×*g* for 2 min at 4 °C. The pellet was air dried and resuspended in 50 µL TE buffer. DNA was quantified using a NanoDrop 2000c UV-Vis spectrophotometer, and then stored at -20°C.

2.20 PCR and QPCR analysis

E. coli K12 specific PCR and QPCR oligonucleotide primers are listed in Table 4 of the Appendix section. SodA, AhpC and CysG (housekeeping gene) were used to assess the effects of Raja 42 on *E. coli* K12, and GhrA and rrsA (housekeeping gene) were used to examine the upregulation and downregulation in response to Raja 42 treatment in *E. coli* K12. Total RNA template volumes, extraction as described above, varied around 1-4 µL of DNA in order to achieve 0.1 µg of DNA per reaction. Thermo Scientific Superscript III Mastermix for cDNA first strand synthesis included 2× First Strand Synthesis Mix (10 mM $MgCl_2$ and 1 mM of dNTP) and Superscript RNase Out Enzyme mix. 5 µL of total RNA (1 µg), 1 µL of random hexamer oligonucleotides (2.5 ng/ µL), 1 µL of annealing buffer and nuclease free water up to 8 µL were added into a PCR tube and incubated in the PTC-100 Programmable Thermal Controller Thermal Cycler at 65 °C for 5 min. The reaction was terminated by placing tubes immediately on ice for 1 minute and adding 10 µL of 2× First strand synthesis mix (2.5 µM oligo (dT), 2.5 ng/µL of random hexamers, 10 mM $MgCl_2$) and dNTPs) and 2 µL of Superscript RNase out (2 units (U)) Enzyme mix. The reaction

mixture was briefly vortexed and then incubated at 50° C for 60 min. Finally, the reaction was terminated by incubating it for 5 min at 85 °C. PCR was carried out using a Thermo Scientific Taq DNA Polymerase kit, to which adding 5 µL of 2 mM dNTP mix, 5 µL of 10× Taq buffer, 1 µL of forward gene specific primer, 1 µL of reverse gene specific primer, 8 µL of 2.5 mM $MgCl_2$, 1 µL of template cDNA, 1.25 units of Taq DNA polymerase and nuclease free water to 50 µL in a PCR tube on ice. The following polymerization conditions were used for PCR reactions: initial denaturation step at 95 °C for 5 min, denaturation at 95 °C for 30 seconds, annealing at 55 °C for 30 seconds and extension at 72 °C for 60 seconds for a total of 30 cycles, and final extension step at 72 °C for 5 min. QPCR reactions were carried out on the Agilent AriaMx QPCR and included additional no-template buffer controls and reference ROX dye control.

2.21 Statistical Analysis

Values are expressed as mean ± standard error, unless otherwise stated. Every assay was carried out in triplicate, unless otherwise indicated. Biological data were acquired through three independent experiments. Comparison between experimental groups was made by *p*-value determination using one-way ANOVA or student t-test. The p-value <0.001 is considered to be statistically significant. Analyses were performed using GraphPad Prism software, version 8.2.1 (San Diego, CA).

3.0 Results

3.1 Raja 42, which induces cell death in both Gram-positive and Gram-negative bacteria, is equally potent against antibiotic resistant strains.

A chemical library comprising 211 novel compounds was previously generated by the Lee laboratory. Although the chemical library was originally created with the intention of developing effective anticancer agents, we hypothesized that they might also possess antibacterial activity since most of them include the quinoline or quinolone scaffolds, which often demonstrate antibacterial activity[212]. By screening this library against *E. coli* K12 bacteria, I identified 27 compounds (Figure 7) that are active against the bacterial species examined (Table 3, located in the Appendix section). To determine the activity spectrum of the 27 active compounds, I examined their bactericidal activity against *E.* coli DH5α, NDM-1 *E. coli*, ampicillin-resistant *E. coli*, kanamycin-resistant *E. coli*, *S. aureus* Wood 46 and MRSA HPV107, as noted in

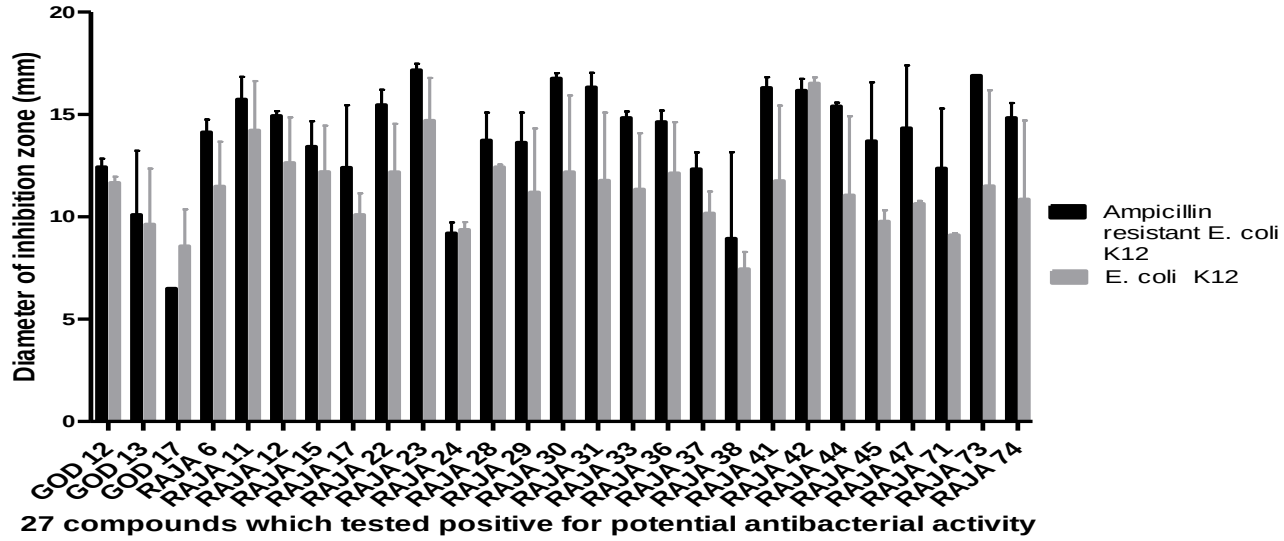

B

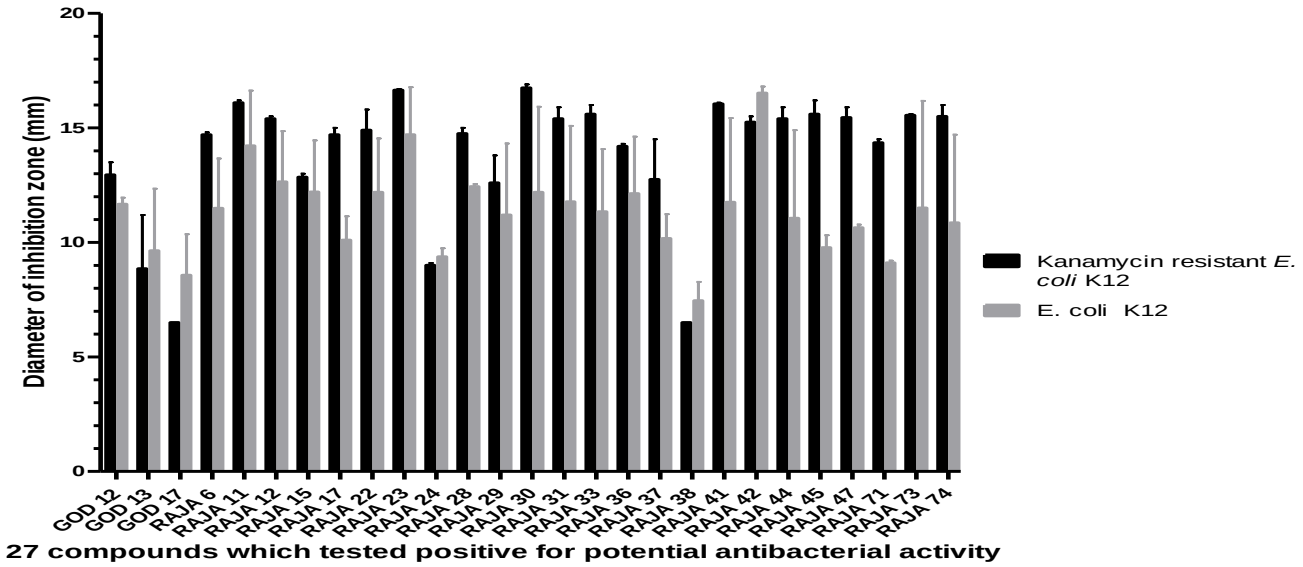

Figure 8 and Figure 9. The most promising compound, Raja 42, was further characterized including its MIC against *E. coli* DH5α. Determining the MIC and molarity of Raja 42 indicated that this novel compound was as effective as ampicillin or kanamycin in impeding *E. coli* growth. Raja 42 was most notably active against *C. difficile* and displayed some activity against *H. pylori*, as displayed in Figure 10.

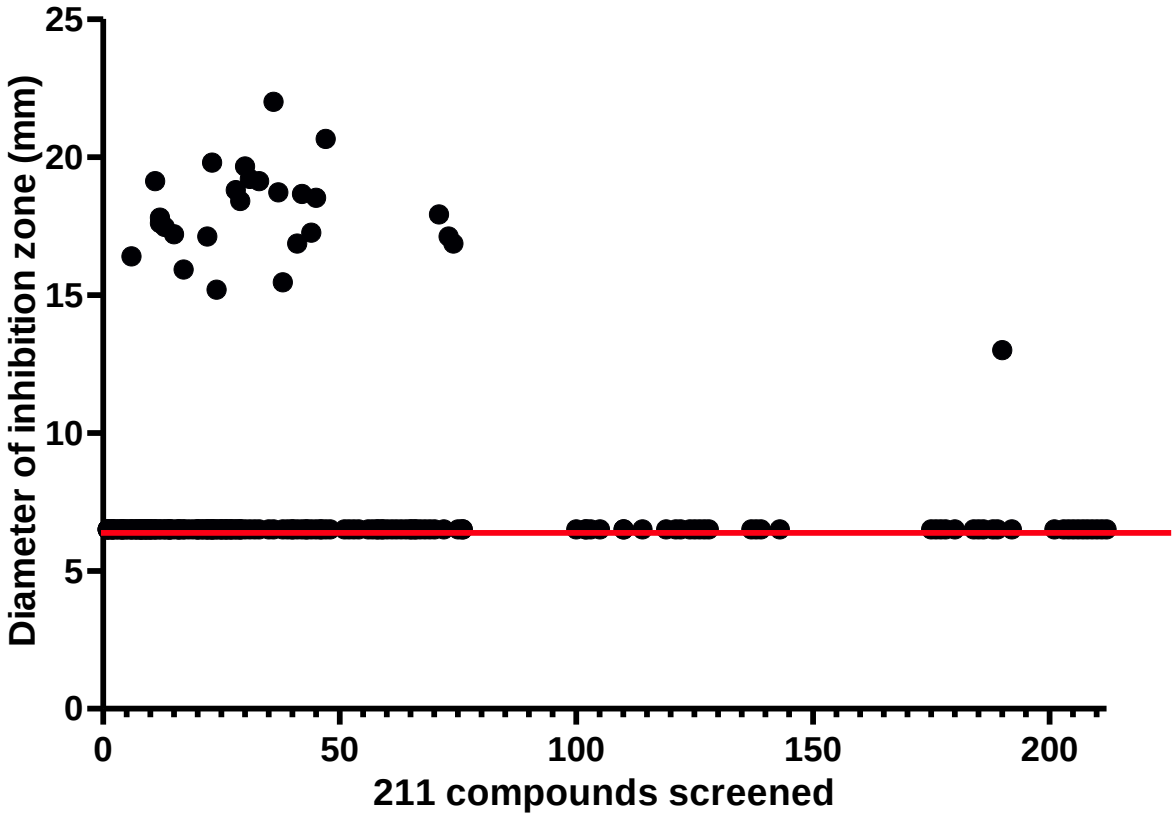

Figure 7: Screening of 211 novel compounds revealed 27 active compounds

211 compounds were examined for their antibacterial activities against *E. coli* DH5α by growth- inhibition zone assay using 200 μg of each compound. The average diameter of the inhibition zone was calculated by measuring across the zone including the diameter of the filter disk (6.5 mm). The diameter of 6.5 mm is represented by the red line.

A

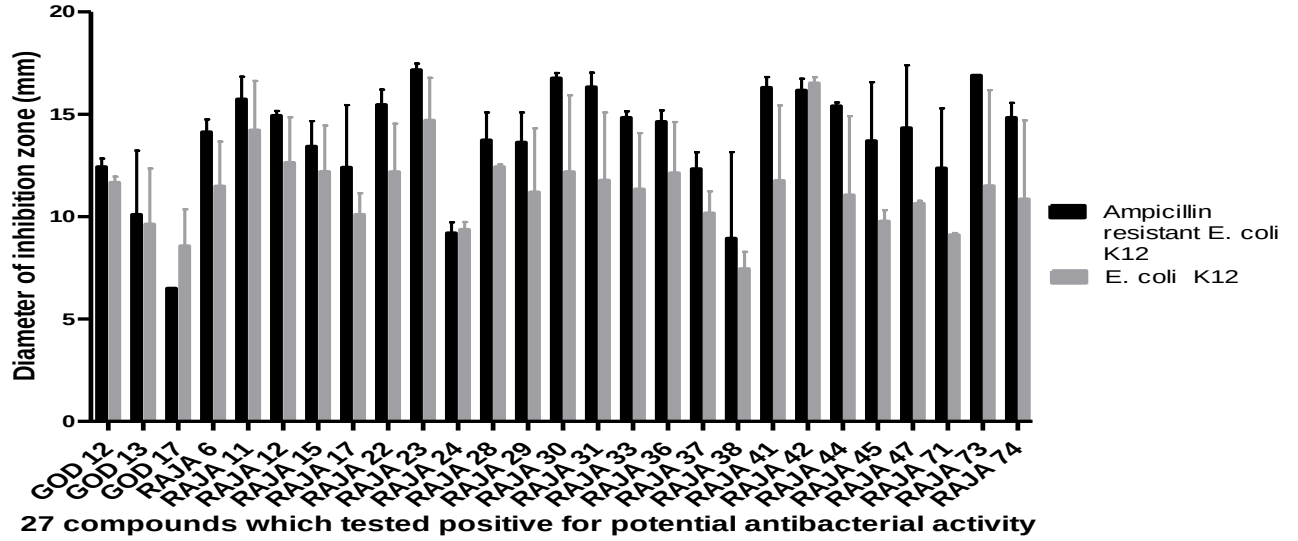

B

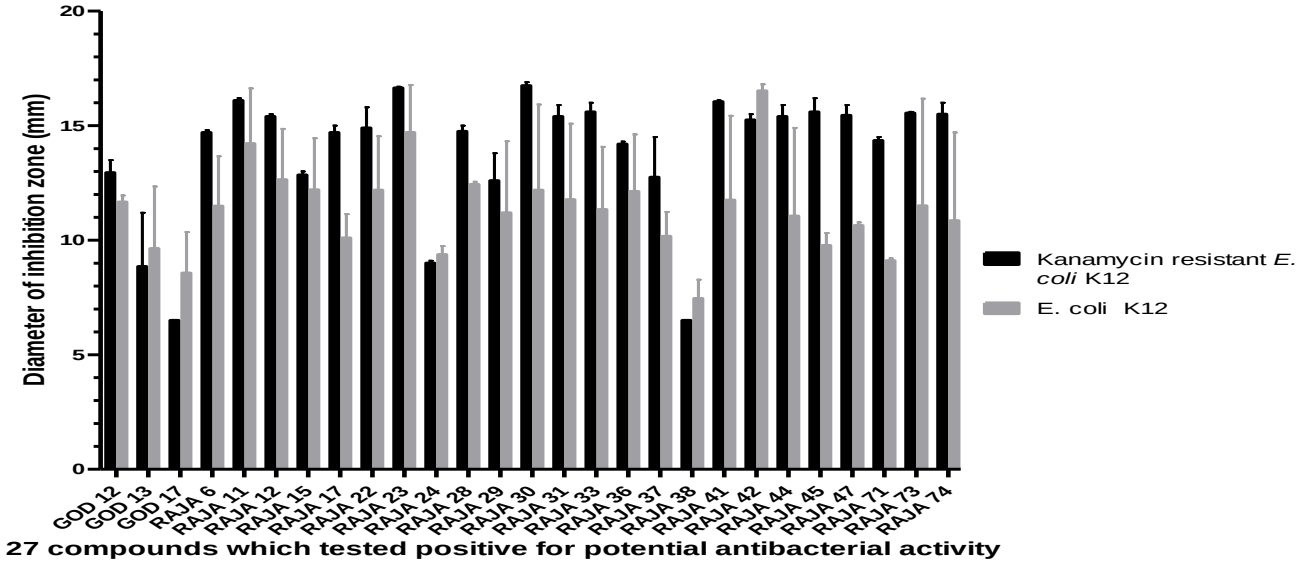

Figure 8: 27 compounds displayed antibacterial activity against antibiotic-resistant strains of *E. coli*.

Average diameters of inhibition zones plotted for each of the 27 compounds. Triplicates were performed for each compound and the diameters were expressed by average ± standard deviation (P <0.001). P values were calculated using GraphPad Prism software version 8.2.1.

A: Average diameter of inhibition zones for 200 μg of the 27 compounds with antibacterial activity against ampicillin-resistant *E. coli* K12 (K12 + plasmid) and *E. coli* K12

B: Average diameter of inhibition zones for 200 μg of the 27 compounds with antibacterial activity against kanamycin-resistant *E. coli* K12 (K12 + plasmid) and *E. coli* K12

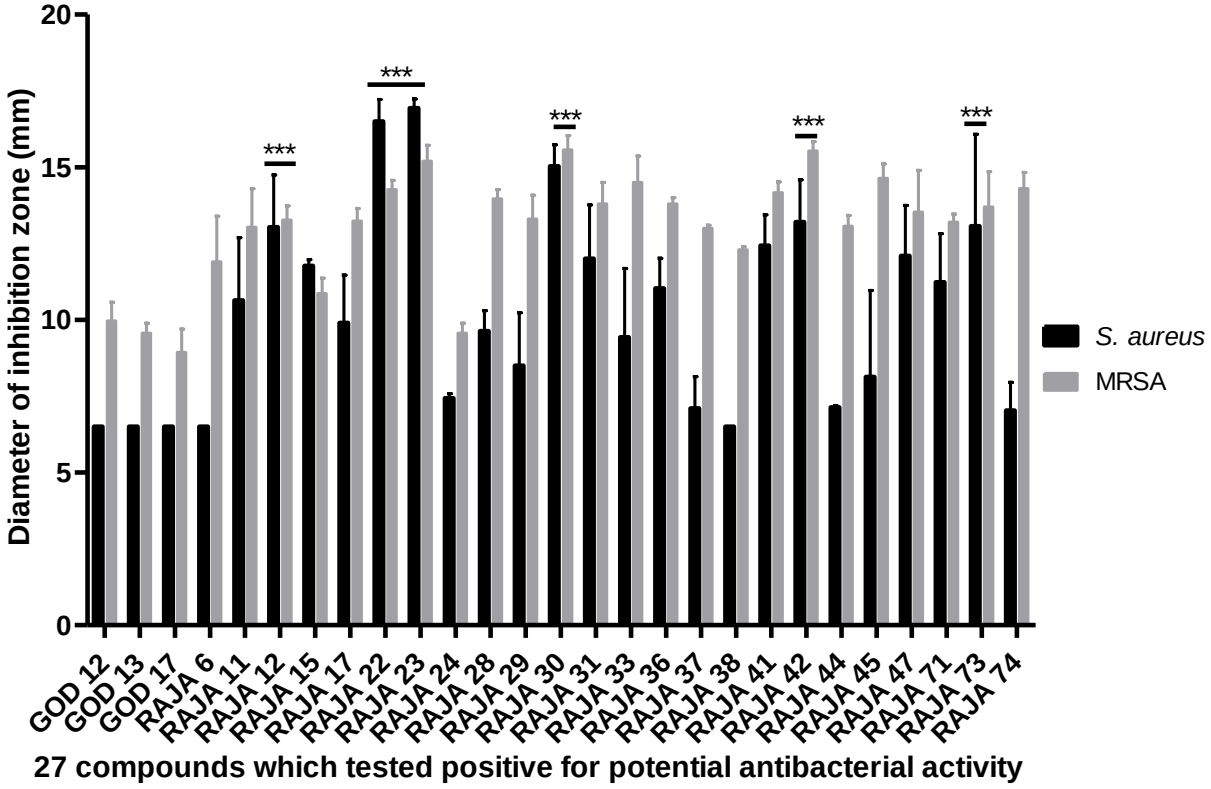

Figure 9: 27 compounds displayed antibacterial activities against antibiotic-resistant strains of gram-positive *S. aureus* and MRSA.

Average diameters of inhibition zones plotted for each of the 27 compounds against *S. aureus*Wood 46 and MRSA HPV107 are shown. Triplicates were performed for each compound and the diameters were expressed by average ± standard deviation (P <0.001). P values were calculated using a student T-test in GraphPad Prism software (v.8.2.1).

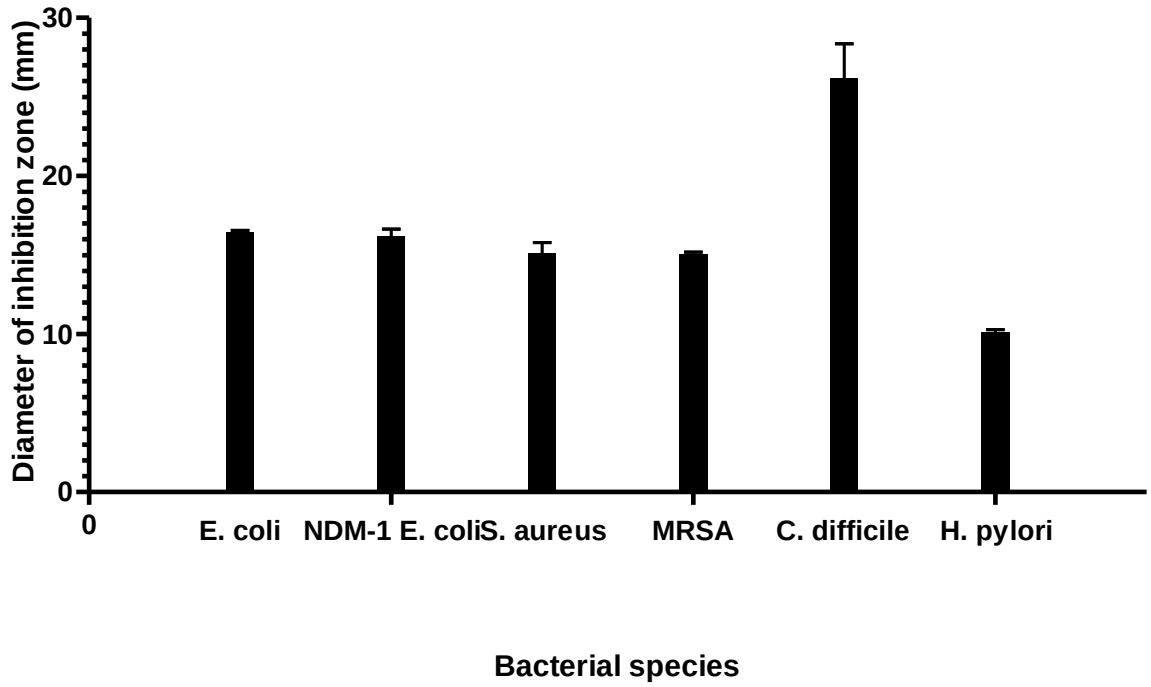

Figure 10: Antibacterial activity of Raja 42 against *E. coli, S. aureus, H. pylori* and *C. difficile*.

Raja 42 compound was further characterized. The minimum inhibitory concentration (MIC) of Raja 42 was initially determined against *E.* coli DH5α, by Tube Broth Dilution method as well as by a 96-well plate-based serial dilution method, and further determined for the other species. The MIC was determined to be 50 µg/mL against the wild-type *E.coli*, 100 µg/mL against NDM-1, 200 µg/mL against *S. aureus*, 200 µg/mL against MRSA and 4.6 µg/mL against *C. difficile.*

3.2 The mechanism of action of Raja 42 against facultative anaerobes

3.3 Raja 42 exhibits rapid bactericidal activity

As Raja 42 was identified as a promising new antibacterial compound, I carried out experiments to unravel its functional molecular mechanism. Data from a time-kill assay indicated that Raja 42 is bactericidal as it killed bacteria very rapidly. Raja 42 did not cause a slow cell death, often attributed to bacteriostatic antibacterials (Figure 11). Clindamycin and Kanamycin were used as bacteriostatic and bactericidal controls, while untreated cells were used as a positive control allowing to accurately measure the kinetics of cell killing by Raja 42. The treatment of bacteria with Clindamycin, a bacteriostatic compound, led to a stagnant population at 30 min, however, slow growth resumes at 60 min, as displayed by the area under the curve (AUC). Kanamycin, a bactericidal agent, causes rapid cell death within 30 min of treatment. The linear slope of the Kanamycin curve demonstrated significant declines in the CFU, indicative of bactericidal activity. Raja 42 mimicked the monoexponential killing curve of Kanamycin, with rapid decline in CFU at 30 min, ultimately reaching 0 CFUs after 2 hours. This data indicates the bactericidal nature of Raja 42, as it displayed similar killing kinetics to a known bactericidal agent, Kanamycin.

To further determine its functional mechanism, membrane integrity, RNA damage and changes in protein levels were assessed following the treatment of cells with Raja 42. Membrane integrity was assessed using a membrane depolarization assay conducted on *E. coli* K12 cells. The resultant data provides further evidence that Raja 42 is compromising membrane integrity (Figure 12).

In another experiment, bacteria were incubated with a membrane permeable fluorescent dye, $DiSC_3$, allowing for its uptake into the live cells. Successful uptake of the dye was confirmed by

the absence of free dye in the surrounding media, which corresponded to a decrease in detectable fluorescence. As a positive control, cells were treated with 0.1% Triton X-100, a known membrane-disrupting agent. The increase in fluorescence in response to Raja 42 indicated that Raja 42 compromises bacterial cell wall similarly to Triton X-100.

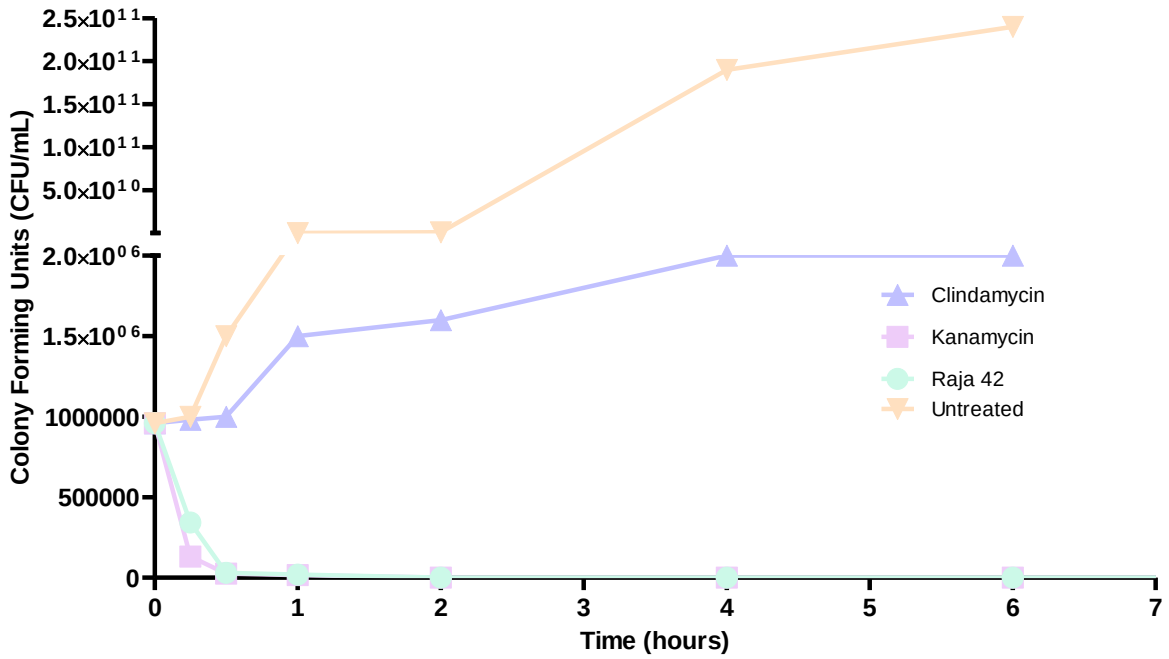

Figure 11: Time-kill assay of Raja 42 against *E. coli* K12 strain.

E. coli colony forming units were counted at 15 min, 30 min, 60 min, 2 hours, 4 hours and at 6 hours. It should be noted that the killing of the entire colonies was completed within 2 hours.

A

B

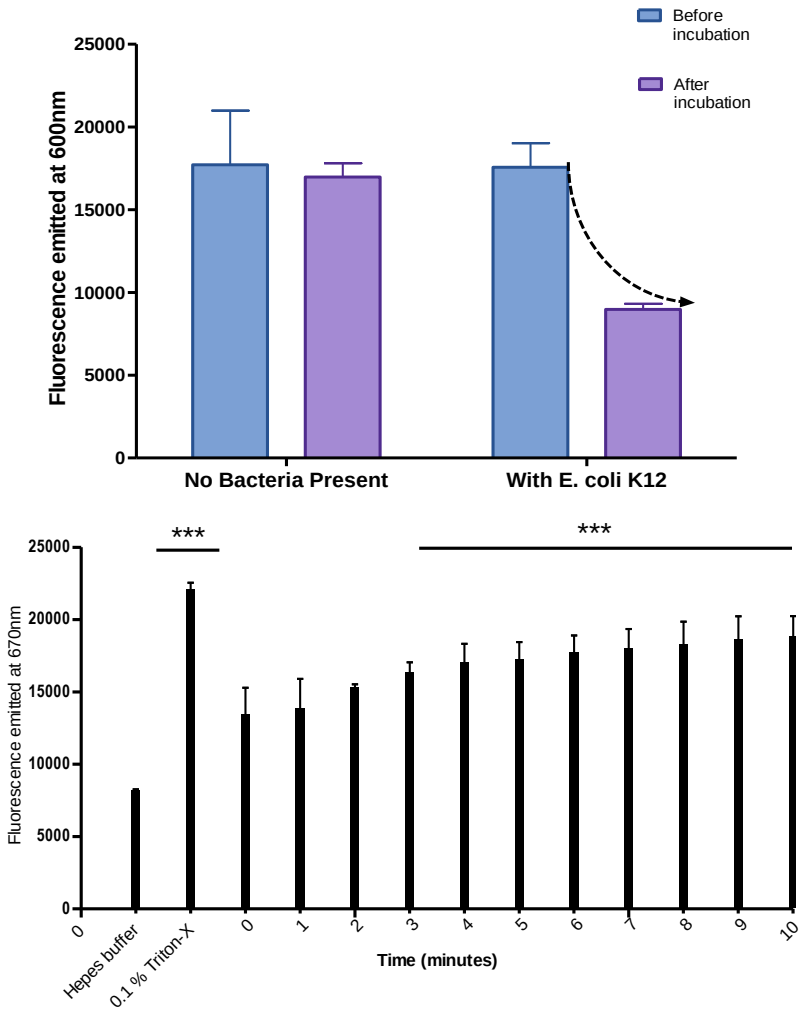

Figure 12: Membrane depolarization assay against *E. coli* K12 strain.
E. coli culture was incubated at 37 °C for 1 hour allowing DiSC3(5) dye absorption prior to treatment with the MIC of Raja 42, a positive control Triton X-100 (0.1%) or a negative control Hepes with 20 mM glucose. Triplicates were used for each compound, and the diameters are expressed in average ± standard deviation (P <0.001). P values were calculated using Prism software (v.8.2.1).
A: Addition of *E. coli* bacterial culture results in a decrease in fluorescence emitted as the cells have taken up the dye during the incubation period. The dotted arrow signifies a decrease in detectable DiSC3.
B: Treatment of *E. coli* K12 with Raja 42 reveals a gradual increase in the levels of emitted fluorescence over time as bacterial membrane integrity is compromised allowing fluorescent dye to be detected in the supernatant. The p-values were determined by Dunnett test, and the values presented are mean ± SEM (n=3). *** p <0.001, which denotes significant differences from the Hepes buffer group, the Triton X-100 (0.1%) group and treatment groups from 3 min to 10 min time points.

Flow cytometric analysis of propidium iodide stained cells demonstrated that ½ of the MIC of Raja 42 (25 μg/mL) treated cells undergo rapid cell death within 30 min of treatment, as displayed by the increased population of dead cells (Figure 13). To examine the percentage of the population being impacted by Raja 42, three subgroups were chosen. Live (pink), injured (green) and dead (blue) cell populations were gated, allowing for flow-cytometric discrimination through forward scatter and side-scatter plots. Note that Kanamycin treated cells display a larger population of injured cells in the flow cytometry profile by 30 min post-treatment.

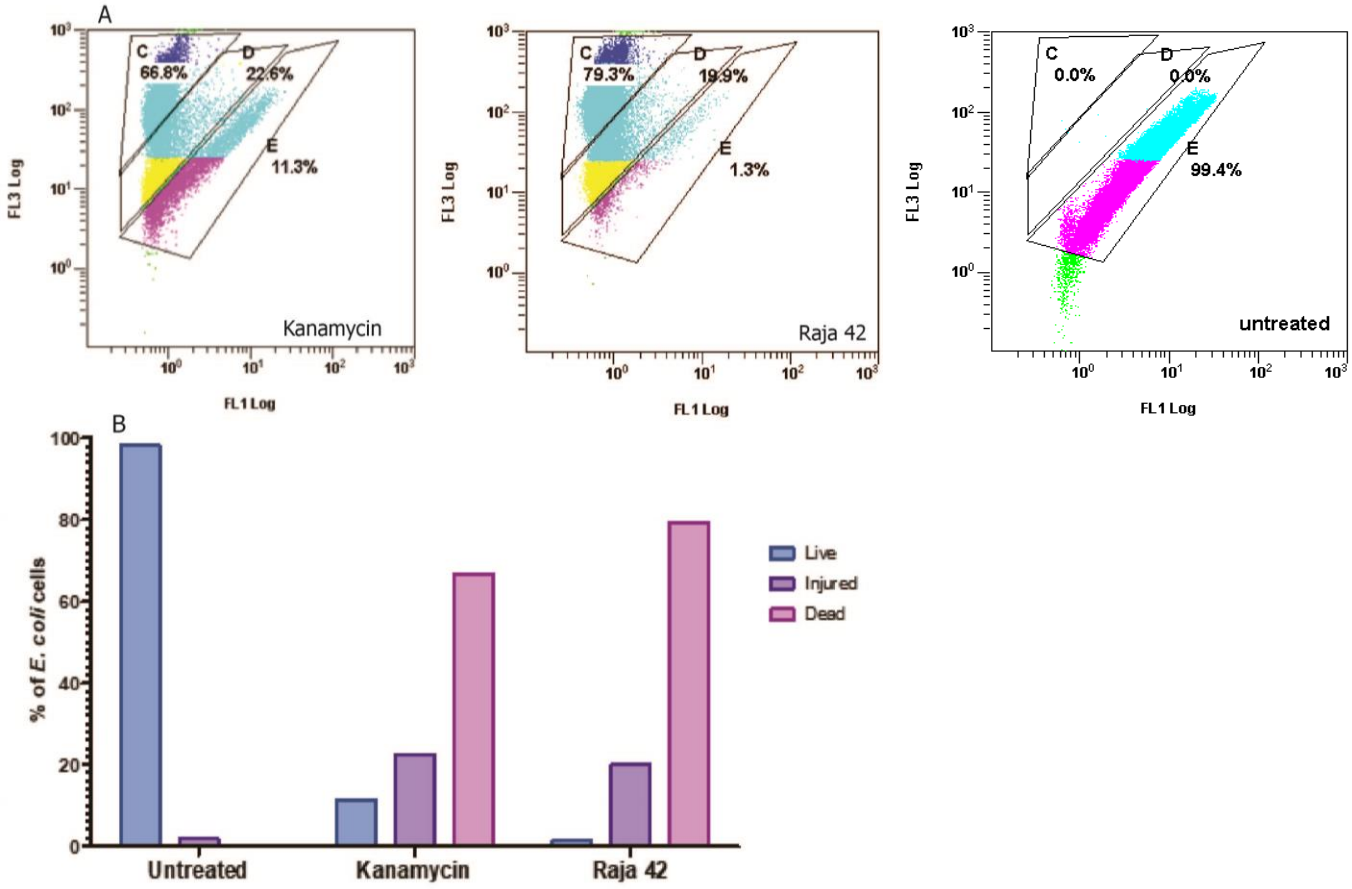

Figure 13: Flow Cytometric analysis of *E. coli* K12 treated with Raja 42

Three distinct populations, live, injured and dead bacteria, were gated according to BD Bioscience guidelines. Flow cytometric analysis of 1.3 µg mL^{-1} PI and 8.1 µg mL^{-1} TO stained cells revealed a higher percentage of dead *E. coli* K12 cells when treated with Raja 42, compared to clindamycin.

A: Raw flow cytometry data displaying three gated populations and percentage of cells in each population. Navy blue gated population corresponds to dead cells, fuchsia gated population represents live cells, and intermediate green population represents injured cells. ½ of the MIC of Kanamycin was used as a positive control.

B: Bar graph summarizing data from experiments for Raja 42 at MIC (25 µg mL^{-1}) treated and the MIC Kanamycin (positive control) treated *E. coli* K12. Exponentially growing bacteria were treated for 30 min prior to flow cytometry analysis.

3.4 Two dimensional (2D) gel electrophoresis with whole cell extract (WCE) proteins

The 2D SDS-PAGE would allow for the necessary resolution in order to identify which proteins might have been altered in response to Raja 42. Two-dimensional difference gel electrophoresis (2D-DIGE) separates proteins in the first dimension to their isoelectric point (pI). The second dimensional separation is according to their sizes. 2D-DIGE can make use of fluorescent probes to identify and to quantify proteins with appropriate software. Figure 14 shows an example of 2D-based separation of *E. coli* K12 proteins with or without treatment with Raja 42. A pH gradient of 3-6 was used and a few proteins can be seen in the untreated sample, with some having good resolution. Conversely, in the sample treated with Raja 42, the appearance of seven additional proteins, absent from the untreated sample, is shown.

Protein identification through mass spectrometry confirmed the upregulation of metabolic proteins: SodA and AhpC. Other proteins were identified as conserved non-essential proteins. The findings suggest an overall increase in expression level of metabolic proteins, although there are few proteins where the expression level seems to remain the same. This provided initial evidence that Raja 42 interferes with bacterial metabolic pathways. Future work would need to examine the impact of Raja 42 treatment on the downregulation of bacterial proteins.

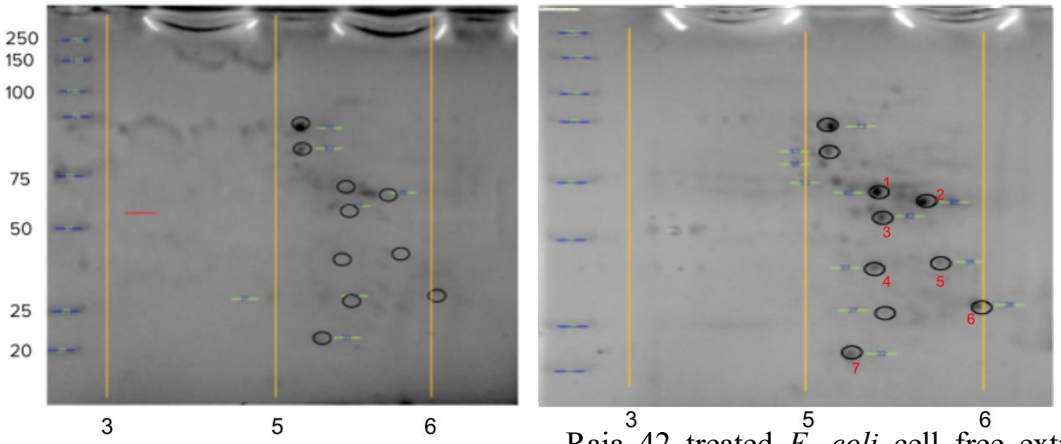

Untreated (control) *E. coli* cell free extract (CFE)

Raja 42 treated *E. coli* cell free extract (CFE)

Figure 14: Separation of *E. coli* K12 proteins by 2D gel electrophoresis.

As compared to untreated control, cells treated with Raja 42 at the ½ MIC concentration displayed an upregulation of seven proteins. Proteins separated by 2D-gel can be visualized by staining them with Sypro Ruby. The identities of the proteins were determined later by mass spectrometry, by which SodA (denoted by number one) and AhpC (denoted by number three).

Raja 42 caused statistically significant (>0.05) increase in the production of ROS (H_2O_2), compared to the sham-treated control (Figure 15). Bacteria treated with ampicillin resulted in the elevated level (0.35 nmol) of H_2O_2 within 1 hour of the treatment. Dwyer and colleagues investigated the potential of various bactericidal antibiotics including ampicillin, and concluded that treatment with these compounds led to detectable levels of various ROS using a combination of fluorescent dyes [213]. The authors also noted ampicillin's involvement in the activation of the SoxR SOS pathway, often leading to downstream citric acid cycle activation. Treatment with Raja 42 alone resulted in similarly increased levels of H_2O_2 (0.30 nmol) over 1-hour. This provides evidence that bacteria produce similar levels of ROS in the presence of Raja 42 and other

antibiotics known to generate ROS. To confirm this conclusion, bacteria were treated with Raja 42 in the presence of an ROS scavenger, thiourea. The treatment of bacteria with the Raja 42 in combination with thiourea decreased the ROS production level to half (0.15 nmol), compared to the level treated with Raja 42 alone. This data is consistent with the notion that bacteria produce substantial amounts of ROS in the presence of Raja 42.

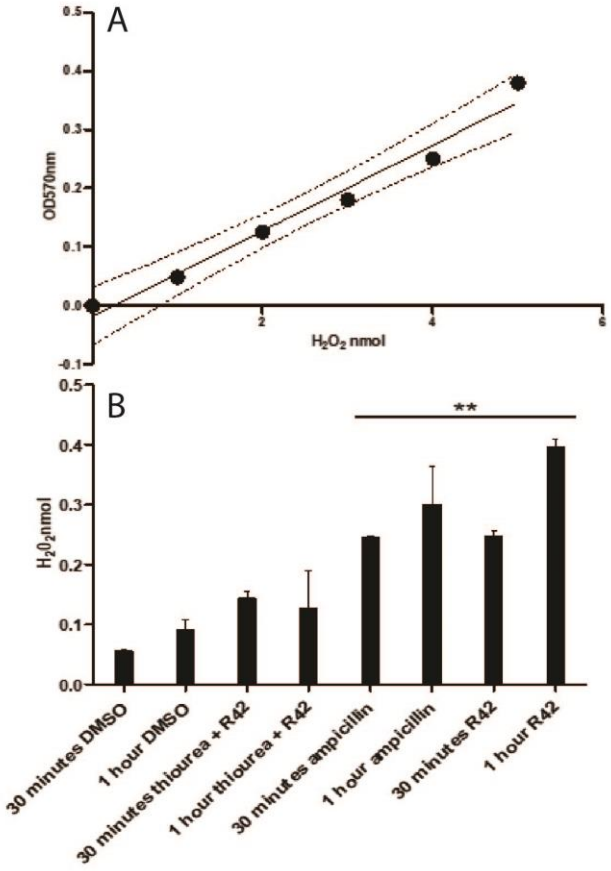

Figure 15: Treatment of *E. coli* K12 by Raja 42 produces the elevated level of H_2O_2
A: Standard curve of H_2O_2 (nmol) against OD_{570}nm with coefficient values and intercepts displayed.
B: DMSO (negative control), thiourea (ROS scavenger) with ½ MIC of Raja 42, ampicillin (positive control) and ½ MIC of Raja 42 treatments of *E. coli* K12 at 30-minute and 60-minute time points. OD_{570} nm was measured and correlated to the levels of H_2O_2 (nmol) using the standard curve. The *p*-values were determined by Dunnett test, and the values presented are mean ± SEM (n=3). ** $p < 0.05$, which denotes significant differences from the DMSO or thiourea groups and Raja 42 alone or ampicillin groups.

3.5 Some E. coli cells become elongated in response to Raja 42, which appears to rapid cell death

Through live cell imaging, changes in the morphology of *E. coli* K12 bacterial cells in response to Raja 42 were studied. Raja 42 treatment caused an increase in abnormally elongated cell morphology (Figure 16). A number of cells appeared to be elongated and thicker in morphology, with increasing evidence of this abnormal morphology occurring at later time points. The elongated morphology may be in accordance with previously published reports, which indicated that this kind of altered morphology occurs when cell-wall synthesizing enzymes is compromised [214]. β-lactam antibiotics target PBP proteins that help mitigate cell elongation, cell shape and cell division. Gin and colleagues reported previously that piperacillin β-lactam treatment of *E. coli* leads to the formation of altered cell shape and division, as the antibiotic has a specific affinity for PBP2 and PBP3 [214]. The incidence of altered phenotype varies among cells and depends on the stage of the cell cycle following Raja 42 administration. If cells are not in mid-log phase when treatment is administered, bacteria may not actively grow and division would be impaired. Consequently, if cell divition is not active during administration of Raja 42, inhibition of elongation will ensue. If the stage of bacterial cell division in not accurately determined, prior to administration of the compound, inaccurate findings could be reported.

To visualize the real-time impact of Raja 42 treatment on *E. coli* cells, fluorescence microscopy using Cyto9 and PI was conducted (Figure 17). Log-phase growing *E. coli* are motile and actively tumble and swim in various directions. The motility of free-swimming *E. coli* is well

characterized. Treatment of motile bacteria by bactericidal antibiotics can cause alterations to the cell wall proteins, such as those necessary for bacterial flagellar movement. I therefore investigated the cessation of bacterial motility upon treatment with Raja 42 in order to determine if Raja 42 is impacting cell wall integrity. When bacteria were treated with Raja 42 at the MIC concentration cells became completely immobile within a few seconds. This observation strongly agrees with the previous reports that when the cell wall is substantially disrupted, it causes rapid loss of flagellar motility [215].

A LIVE/DEAD BacLight bacterial viability kit uses a combination of Cyto9 green-fluorescent nucleic acid stain and PI red-fluorescent nucleic acid stain. Cyto9 stains cells with both intact and damaged membranes. PI penetrates only bacteria with damaged membranes. Consequently, when both dyes are used in a 1/1 ratio, a reduction of Cyto9 fluorescence may be observed if dead cells are present in the population. Bacteria with intact membranes will stain and fluoresce in green, whereas bacteria with damaged membranes stain in fluorescent red. Of note, since the excitation and emission for these dyes are 480/500 nm, the background remains virtually nonfluorescent.

I observed that following treatment with Raja 42, cells are alive and intact for 5 min as demonstrated by the fact that cells are fluorescing in green (Figure 17). At the 15- and 30-minute time points, cells are no longer viable, as they are fluorescing red. Microscopy images, using the 480 nm and 500 nm filters, were taken of the same frame in order to maintain accuracy and allow

for comparisons in live and dead cell populations. These results are indicative of the ability for Raja 42 to damage bacterial membranes, ultimately contributing to cell death.

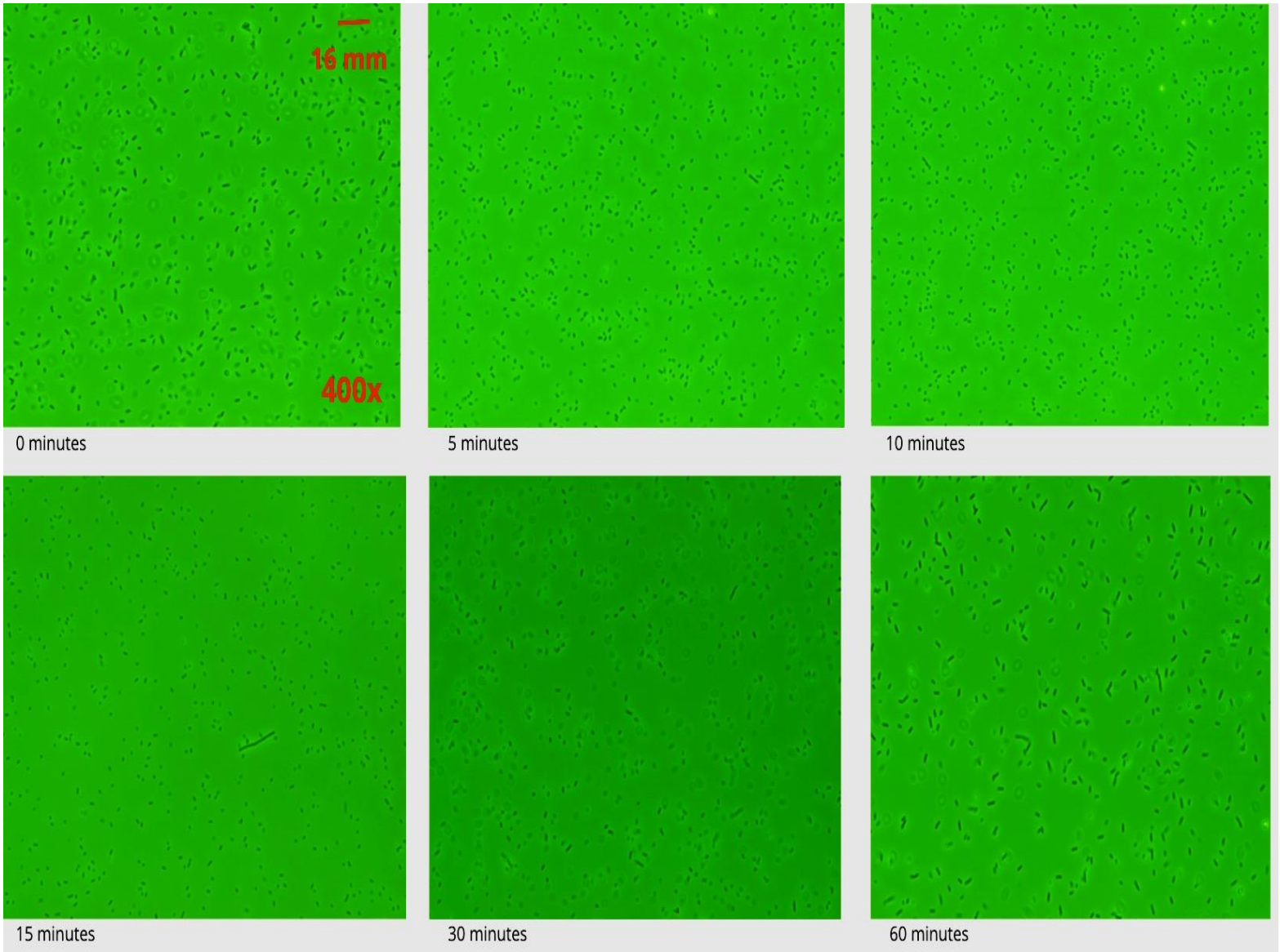
16 mm
400x
0 minutes
5 minutes
10 minutes
15 minutes
30 minutes
60 minutes

Figure 16: Raja 42 treatment caused the appearance of elongated bacteria in later time points.

E. coli K12 cells were treated with Raja 42 at ½ MIC and time lapse images were obtained at 0, 5, 10, 15, 30 and 60 min to examine morphological changes of *E. coli* K12 in the presence of Raja 42.

A

B

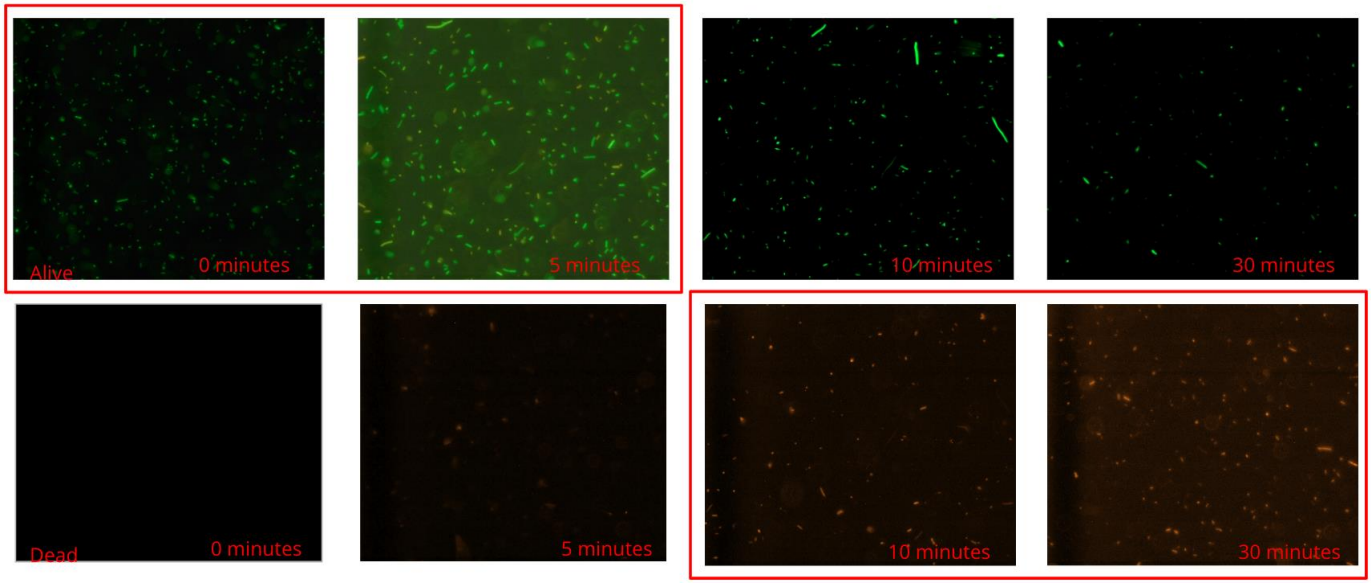

Figure 17: Raja 42 treatment caused rapid cell death, as determined by uptakes of dyes.

Cells were treated with Raja 42 at the MIC concentration and imaged at time points of 0 min, 5 min, 10 min and 30 min. Cells were stained with an equal volume of propidium iodide (30 μM) and Cyto9 (6 μM) to visualize dead cells.

A: Live cell fluorescence was detected using the green panel setting of the AxioScope.A1 fluorescent microscope.

B: Dead cells were detected using the red panel setting of the AxioScope.A1 fluorescent microscope. All time points were taken at the same frame for both live and dead cells for comparison.

3.6 The effect of Raja 42 on expression levels of select proteins in E. coli K12

To confirm the data from the 2D gel electrophoresis, immunobloting experiments with antibodies specific to metabolic proteins was carried out. Data shown in Figure 18 demonstrate the dramatic increase of SodA protein in *E. coli* K12 cells upon treatment with Raja 42 at the ½ MIC concentration for 18 hours. Figure 19 also includes immunoblotting data with anti-Ftsz antibody, which functions as a control as its banding pattern is consistent across all treatments. The immunoblot of *E. coli* K12 cells having undergone treatment with Raja 42 is displayed in both upper and lower panels in Figure 19. The similar band size and location of the SodA purified protein and *E. coli* K12 treated with ½ of the MIC of Raja 42 cells suggest that Raja 42 is upregulating SodA expression in treated cells. As the cells are still viable after 18 hours with a sub-MIC dose of Raja 42, perhaps, once could speculate that this may be indicative that cells are utilizing a mechanism of transient drug defence in order to circumvent death.

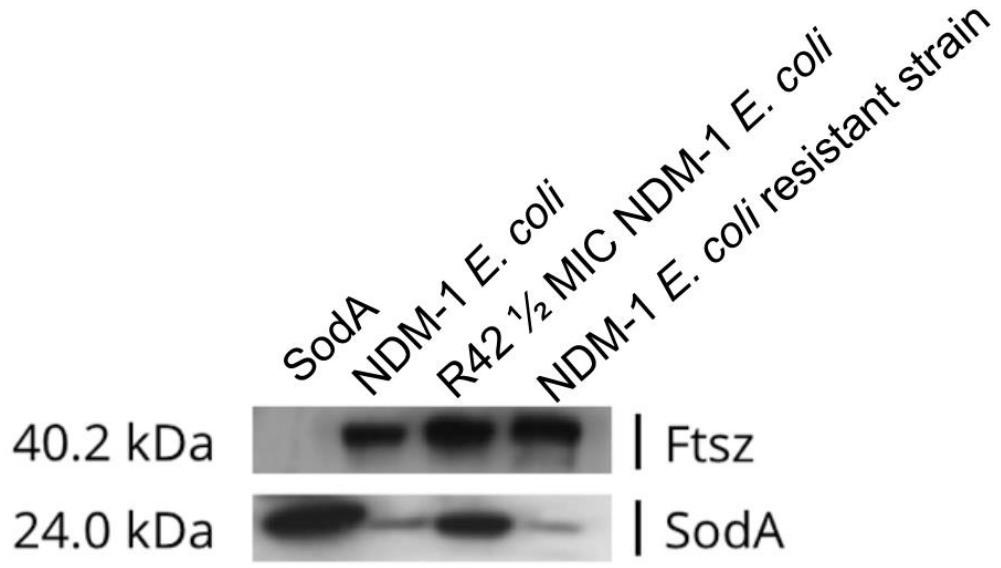

Figure 18: Raja 42 treatment of NDM-1 *E. coli* dramatically increases the level of SodA protein.

In this Western blot, Ftsz protein was used as a loading control, corresponding to the 40.2 kDa size marker. Subsequent immunoblotting of SodA against resistant NDM-1 *E. coli* and the parental strains are displayed below, at the 24.0 kDa size marker. The first lane contains 50 ng of purified SodA protein while the second lane contains untreated *E. coli* K12 cells. The third lane contains cells treated with ½ of the MIC of Raja 42 with the last lane containing *E. coli* resistant to Raja 42. The relative amounts of SodA proteins of cells treated with Raja 42 (½ MIC) was compared with 50 ng of purified SodA protein (lane 1).

3.7 Effect of Raja 42 on the ribosomal RNA integrity

To determine if Raja 42-caused ROS production in bacteria leads to certain cellular damage, *E. coli* K12 cells were treated with Raja 42 (25 μg/mL) for 18 hours. Bacterial cells were harvested, lysed, and then RNA was isolated using a Qiagen miRNeasy kit. The profile of total RNA obtained from *E. coli* K12 bacteria is shown in Figure 19, which was generated by capillary electrophoresis using an Agilent 2100 bioanyalyzer. As expected, the total RNA profile clearly displayed typical 23S and 16S ribosomal RNA (rRNA). The *E. coli* K12 contained the typical band pattern of high quality total bacterial rRNA. Cells treated with Kanamycin, an aminoglycoside, which binds to the 30S RNA subunit, displayed no RNA degradation as a similar banding pattern to the parental treatment is displayed. In *E. coli* K12 cells treated with ½ of the MIC of Raja 42 (25 μg/mL), it can be seen that there are elevated amounts of degradation bands below the 16S RNA, with a smeared pattern being observed. In Raja 42-resistant *E. coli* treated with ½ MIC of Raja 42 (25 μg/mL), a similar banding pattern is observed, however, the smeared banding pattern occurs slightly over the 23S rRNA band and continues until the 16S rRNA. Treatment of *E. coli* K12 with Rifamycin, an RNA binding agent not known to cause RNA degradation, displays a similar band pattern found in untreated *E. coli* K12 cells and Raja 42-resistant *E. coli* K12 cells.

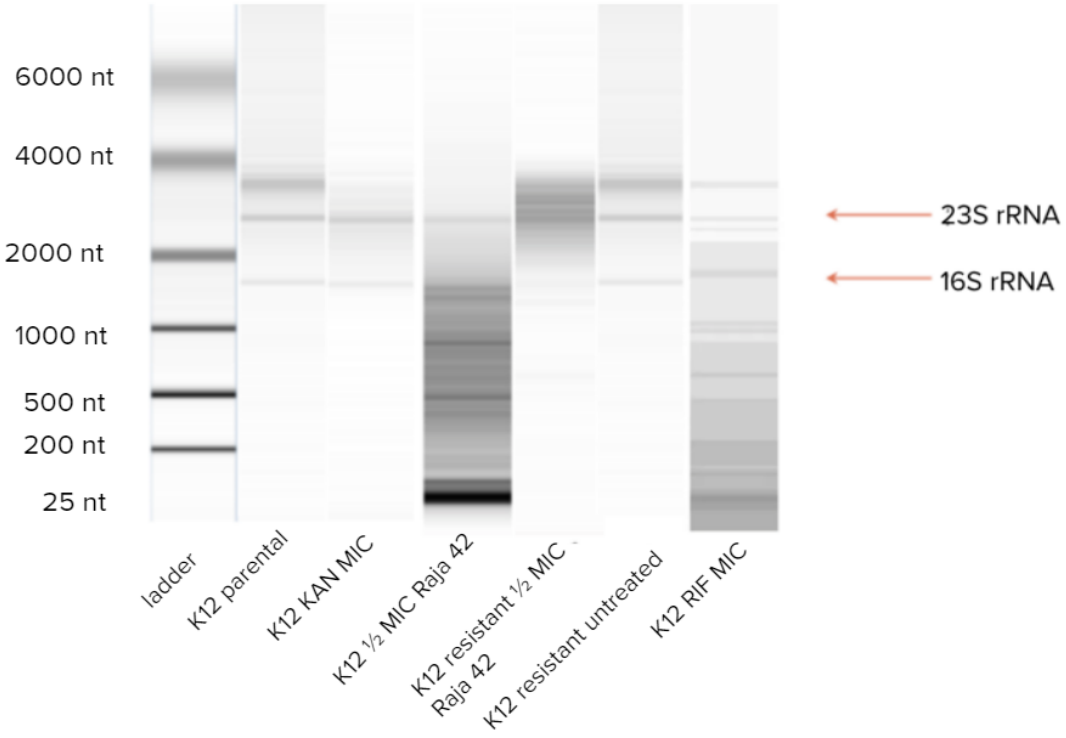

Figure 19: Raja 42-sensitive, but not Raja 42-resistant bacteria show high degrees of rRNA degradation in the presence of Raja 42.

RNA electropherogram of bacteria treated with MIC of Kanamycin (negative control), MIC of Rifampicin (positive control) or ½ of the MIC of Raja 42. Total RNA isolates were resolved by capillary electrophoresis using an Agilent 2100 bioanyalyzer. RNA samples were loaded onto an RNA Nano Chip (Agilent, Technologies, Santa Clara, CA) as directed by the manufacturer's protocol and analyzed with the Agilent 2100 Bioanylizer.

3.8 Raja 42 causes metabolic shift in citric acid cycle of E. coli K12

In order to determine the functional mechanism of Raja 42, I have generated Raja 42-resistant bacterial clones by growing *E. coli* K12 and NDM-1 *E. coli* in various sub-MIC concentrations of Raja 42, followed by picking up a number of individual resistant colonies. Several individual colonies were expanded after three rounds of selection process. The genomes of the two parental strains (*E. coli* K12 DH5α and NDM-1 *E. coli*) and five resistant colonies per cell line were subjected to determine their nucleotide sequences using an Illumina Mi-Seq platform. Subsequently, the resultant DNA sequences were assembled into multiple contigs as described in sections 2.16 and 2.17. Although the genome gaps were not fully filled, overall interpretation was possible. The genomes ranged in size from 4.5 Mbp to 4.6 Mbp, as anticipated, with CG contents of 40.0%. The nucleotide sequences with potential protein coding capacities accounted for 80% of the genomes corresponding to 4,251 CDS (coding sequences). Phylogenetic comparison, based on 16S rRNA gene sequences of the genomes, revealed the 10 Raja 42 resistant colonies and two parent lines sequence identity to be 99% *E. coli* K12 strain DH5α and NDM-1 *E. coli*, respectively. Following phylogenetic analysis, comparative genomics analysis of the parental strains against the resistant clones allowed for detection of SNPs, deletions of complex variations. A 27 bp deletion of 5'-CGGTGAGGGGGGGATTGACTCGCTTCG-3' was consistently found in all of the Raja 42-resistant clones (Table 5 of the Appendix section). The deletion occurring at the position 954546 was analyzed using the EcoCyc *E. coli* database, Kegg and Snapgene software version 5.1[216] (Figure 20). The sequence comparision between Raja 42-sensitive and Raja 42-resistant bacteria revealed that the deletion occurs directly upstream of serX, which encodes for a tRNA-serine. Having previously identified the metabolic pathway as a potential mode by which Raja 42

was killing bacteria, I sought to examine the *serX* gene neighbourhood to identify possible metabolic genes which may be impacted by Raja 42. I noted that the deletion was 317 bp upstream of the ghrA gene and 195 bp upstream of its promoter region respectively. Figure 20 depicts the gene neighbourhood of the ghrA gene as well as nucleotide position within the *E. coli* K12 substr. DH5α genome.

A

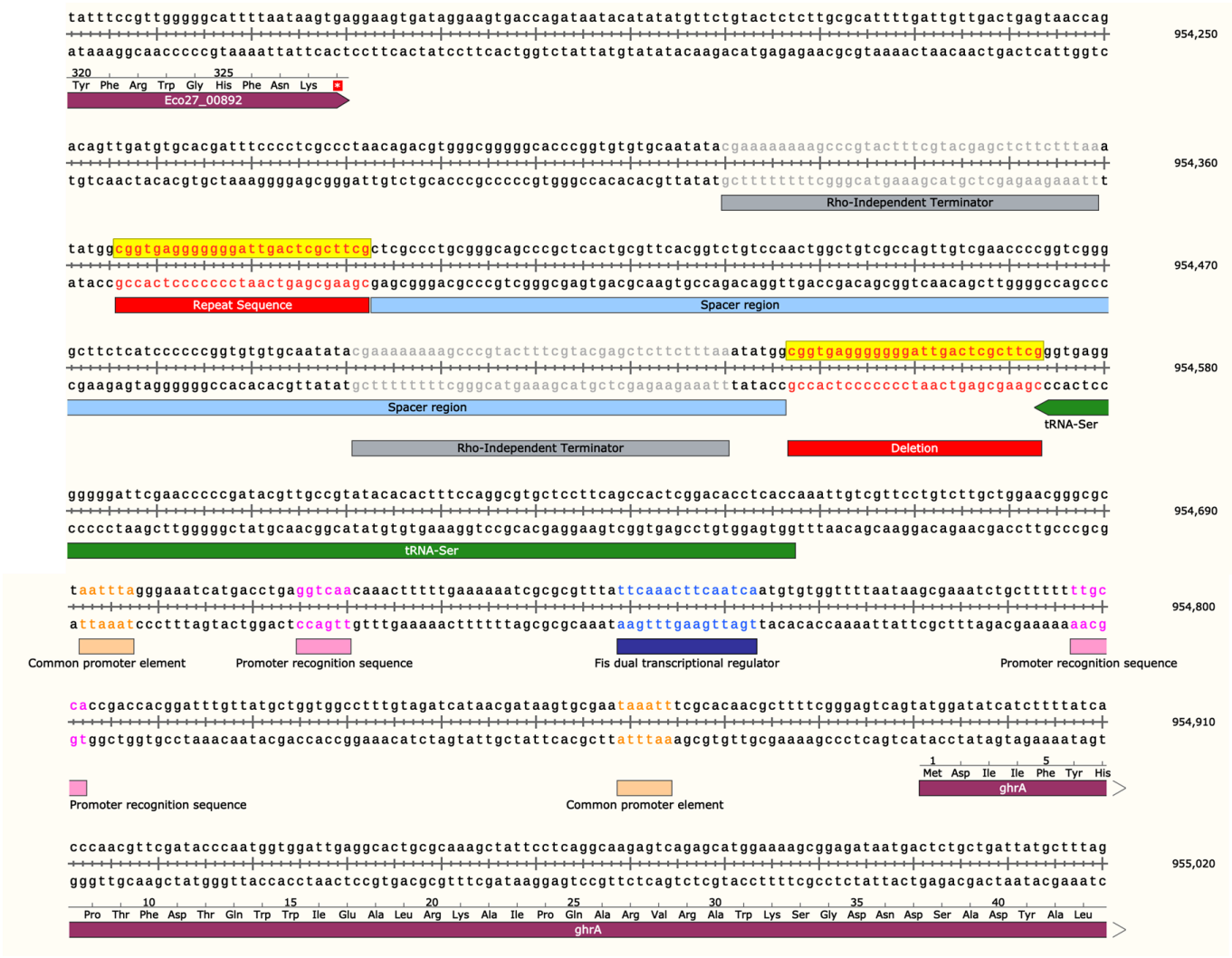
954,250
320 325
Tyr Phe Arg Trp Gly His Phe Asn Lys
Eco27_00892
954,360
Rho-Independent Terminator
954,470
Repeat Sequence
Spacer region
954,580
Spacer region
tRNA-Ser
Rho-Independent Terminator
Deletion
954,690
tRNA-Ser
954,800
Common promoter element
Promoter recognition sequence
Fis dual transcriptional regulator
Promoter recognition sequence
954,910
1 5
Met Asp Ile Ile Phe Tyr His
ghrA
Promoter recognition sequence
Common promoter element
955,020
10 15 20 25 30 35 40
Pro Thr Phe Asp Thr Gln Trp Trp Ile Glu Ala Leu Arg Lys Ala Ile Pro Gln Ala Arg Val Arg Ala Trp Lys Ser Gly Asp Asn Asp Ser Ala Asp Tyr Ala Leu
ghrA

B

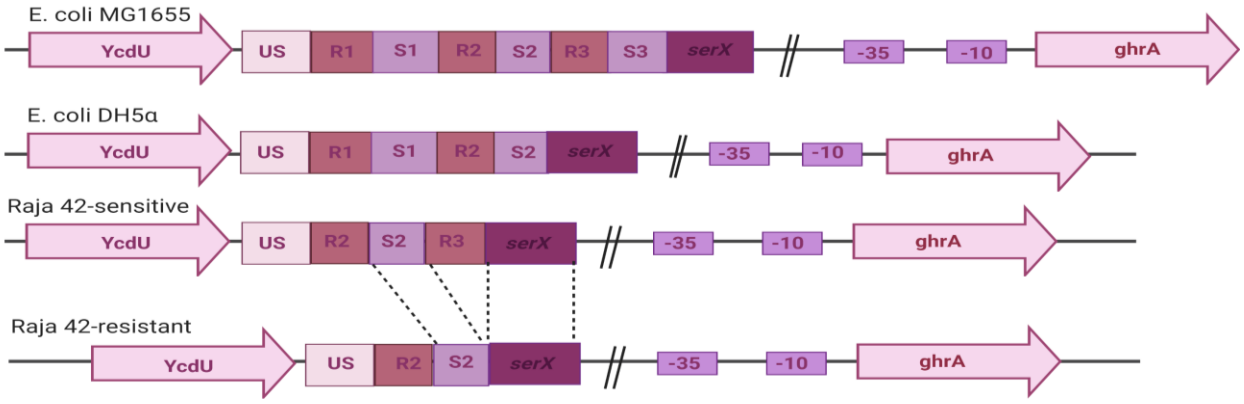
E. coli MG1655
YcdU
US
R1
S1
R2
S2
R3
S3
serX
-35
-10
ghrA
E. coli DH5α
YcdU
US
R1
S1
R2
S2
serX
-35
-10
ghrA
Raja 42-sensitive
YcdU
US
R2
S2
R3
serX
-35
-10
ghrA
Raja 42-resistant
YcdU
US
R2
S2
serX
-35
-10
ghrA

Figure 20: Raja 42-resistant bacteria revealed a deletion upstream of promoter region of ghrA gene.

A: Parental genome alignment to resistant isolates revealed a 27 bp deletion (red), in the repeat sequence downstream of the *serX* gene. The gene neighbourhood includes the upstream Eco27_00892 hypothetical protein, the *serX* gene and the downstream *ghrA*. Repeat sequences are denoted in red, while spacer regions are denoted in blue. Rho-Independent Terminators are highlighted in grey and are associated with Eco27_00892. Although both *serX* and *ghrA* have two different promoter regions, they share a common δ70 factor sequence, TAAATT, denoted in beige, each of which has a specific promoter recognition sequence (pink). Both promoter recognition factors for *serX* and *ghrA* are regulated by Fis, a dual transcriptional regulator (dark blue). *ghrA* is located at nucleotide position 954,841 to 955,829 and its promoter region commences at 954,797. The 27 bp deletion occurred at nucleotide position 954,547, which is located 317 bp upstream of ghrA.

B: Comparison of NCBI published *E. coli* K12 substr. MG1655, substr. DH5α, parental DH5α and mutant DH5α genomes. The upstream sequence (US) from repeats and spacers is identical in all genomes. Spacer regions, with sequence similarity, are found interspersed among repeat sequences. The NCBI published MG1655 substr. has three repeat sequences (R1, R2 and R3) and three spacer regions (S1, S2 and S3) present. In the NCBI published DH5α substr., two repeat sequences (R1 and R2) and two spacer regions (S1 and S2) can be found at nucleotide positions 997,923 and 998,105 respectively of *serX*. The parental DH5α has lost the first repeat and spacer (R1 and S1) section starting with R2 and S2. The parental strain has a second repeat (R3), however, no subsequent spacer. In the Raja 42 resistant strain, a single repeat and spacer are found at positions 954,366 and 954,393 relative to *serX* as it contains a 27 bp deletion, corresponding to an entire repeat section.

To accurately measure the upregulation and downregulation of *sodA* and *ghrA* transcript in the presence of Raja 42, the levels of their RNA transcripts were determined both by RT-QPCR (Figure 21). The resultant data showed that RNA transcript expression level of *sodA* in wild-type strain (sensitive to Raja 42) was increased by 5,600 fold in the sample treated with 25 μg/mL of Raja 42 in comparison to the *E. coli* K12 untreated sample. In contrast, the level of *sodA* RNA in Raja resistant mutant cells did not increase in the presence or absence of Raja 42. Thus, these results allow us to conclude that *sodA* is inducible by Raja 42 treatment in wild-type *E. coli*, whereas induction of this same gene in Raja 42-resistant strain is lost. When quantifying the levels of *ghrA* RNA, the baseline level was low as GhrA is involved solely in the TCA. However, the level was further downregulated in the bacteria resistant to Raja 42: in Raja 42-resistant cells, *ghrA* is decreased 4,500 times below the baseline level. In the presence or absence of Raja 42, the *ghrA* transcription level did not change in the wild-type strain. In comparison, Raja 42-resistant bacteria treated with Raja 42 also displayed significantly lower expression levels of GhrA, as levels were similar to those of resistant cells without Raja 42 treatment. Therefore, based on these findings, unlike *sodA, ghrA* is not inducible in wild-type strains and is downregulated in resistant mutants. *Together*, these data are in line with expectations, as a deletion upstream of ghrA led to the substantial or complete decrease of GhrA expression. During the progression of the TCA, production of NADH is required to stimulate the ETC, which results in the production of H_2O_2.

SodA that encodes for superoxide dismutase is an essential regulator for scavenging the superoxide radical (O_2^-). Through a separate mechanism, the glyoxylate shunt diretly interferes with the TCA cycle, limiting its ability to produce NADH necessary for the activation of ETC. GhrA is responsible for the catalytic conversion of glyoxylate to glycolate allowing the TCA cycle

to bypass the glyoxylate shunt with normal progression to the ETC. Together, both ghrA and sodA work independently; with sodA aiming to minimize the cells exposure to ROS and ghrA to avoid activation of the glyoxylate shunt. As both ghrA and sodA are integral components of bacterial metabolism, a deletion causing a downregulation in ghrA activity would have no impact on the sodA pathway, as is observed in Figure 21. However, an upregulation in sodA should neither have an impact on ghrA expression, as sodA is independent of ghrA function.

A

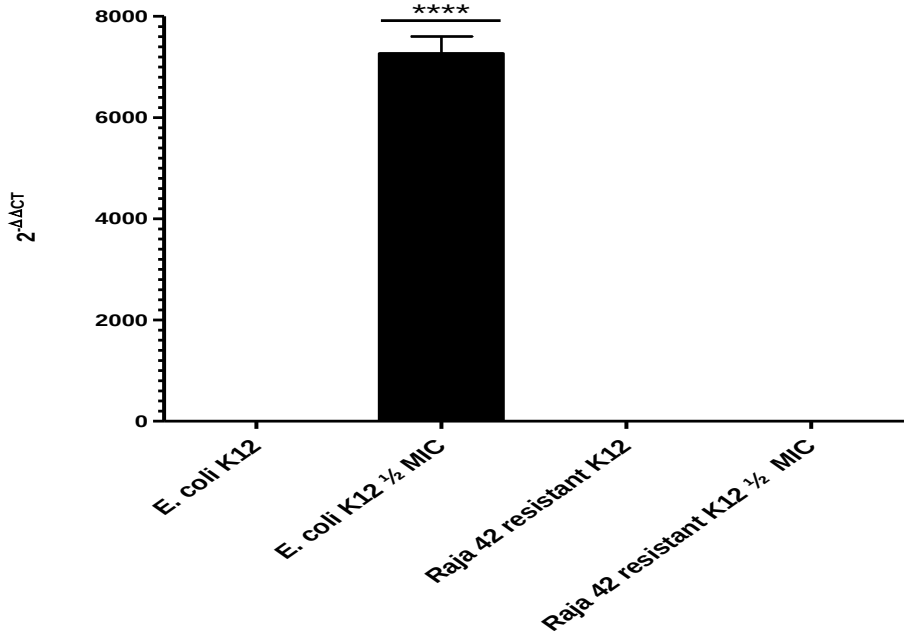
8000
6000
4000
2000
0
$2^{-\Delta\Delta CT}$
****
E. coli K12
E. coli K12 ½ MIC
Raja 42 resistant K12
Raja 42 resistant K12 ½ MIC

B

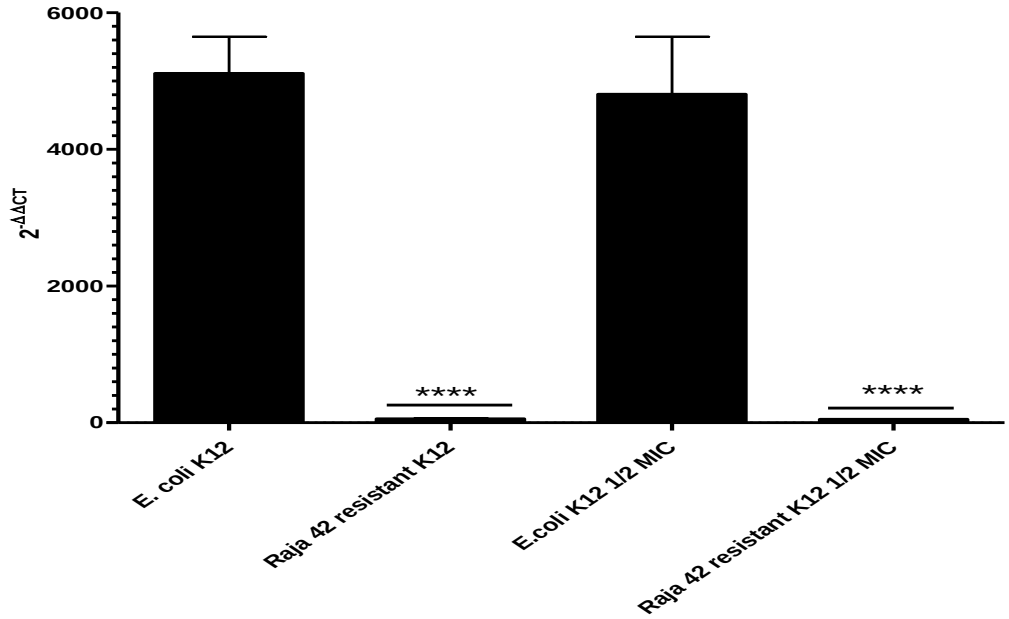
6000
4000
2000
0
$2^{-\Delta\Delta CT}$
****
****
E. coli K12
Raja 42 resistant K12
E.coli K12 1/2 MIC
Raja 42 resistant K12 1/2 MIC

Figure 21: *E. coli* DH5α upregulates *sodA* and downregulates *ghrA* in response to Raja 42 treatment, while Raja 42-resistant K12 strain does not express ghrA mRNA.

A: QPCR analysis of *E. coli* K12 following treatment with Raja 42. When treated with Raja 42 at the ½ MIC concentration, sodA transcript level was significantly upregulated. Shown are the levels of *sodA* in the whole cell extract (WCE) of *E. coli* K12 and Raja 42-resistant *E. coli* K12 cells treated with Raja 42 (25 μg/mL) for 18 hours. $2^{-\Delta\Delta CT}$ corresponds to the final product of the Livek method resultant in the fold increase or decrease in transcription of the gene of interest (*sodA*) compared to the housekeeping gene. ΔΔCT shows the difference in expression levels of two genes: the gene of interest and the housekeeping gene (*cysG*). The values presented are mean ± SEM (n = 3). The comparisons between groups were made using one-way ANOVA. The "n = 3" shown above denotes three independent experiments with samples from three different bacterial populations. **** $P < 0.001$.

B: QPCR analysis of *E. coli* K12 following treatment with Raja 42. When treated with ½ of the MIC of Raja 42, ghrA is significantly reduced. Shown are the levels of *ghrA* transcript in the WCE of *E. coli* K12 and Raja 42-resistant *E. coli* K12 cells treated with Raja 42 (25 μg/mL) for 18 hours. $2^{-\Delta\Delta CT}$ corresponds to the the final product of the Livek method resultant in the fold increase or decrease in transcription of the gene of interest (*ghrA*) compared to the housekeeping gene (*rrsA*). ΔΔCT shows the difference in expression levels of two genes: the gene of interest and the housekeeping gene. The values presented are mean ± SEM (n = 3). The comparisons between groups were made using one-way ANOVA. The "n = 3" shown above denotes three independent experiments with samples from three different bacterial populations. **** $P < 0.001$.

3.9 The combination of Raja 42 and clinically used antibiotics effectively kills Raja 42-resistant bacterial strain

Multidrug resistant organisms are becoming more prevalent in clinical settings, often requiring the use of combinational therapy. The generation of Raja 42-resistant *E. coli* may provide insights into the Raja 42 mechanism of action. Therefore I sought out to test whether the intentionally generated Raja 42-resistant *E. coli* was susceptible or resistant to various antibiotics used at clinics

Figure **22**). Raja 42-resistant bacteria were treated with a variety of different antibiotics including: clindamycin, neomycin, kanamycin, ampicillin, vancomycin and metronidazole. Antibiotics were used to treat bacteria using the respective MIC for each compound against Raja 42-resistant *E. coli* K12. Assays were carried out on agar plates and drug treatment was performed, as outlined in section 0. After 18 hours, plates were assessed and diameters of inhibition zones measured. Raja 42-resistant *E. coli* K12 was susceptible to all treatment groups with the exception of Kanamycin treatment. Diameters of inhibition zones measured were similar or slightly better to that of Raja 42 measurement against *E. coli*. Raja 42-resistant *E.coli* was completely resistant to Kanamycin treatment as no diameter of inhibition zone appeared and bacterial lawn was very dense.

In order to determine if combinational therapy enhances the susceptibility of Raja 42-resistant bacteria, the Raja 42-resistant *E. coli* K12 clones were treated with a combination of Raja 42 and clinical antibiotics. Half the MIC of both Raja 42 and the respective antibiotic was used for the combination therapy. As expected, all antibiotics, which had shown efficacy in treating Raja 42-resistant *E. coli* K12, were also efficient when used in a combination therapy with half of the MIC of Raja 42. However, most combinations did have an additive effect as the diameters of inhibition zones were greater than treated alone. To my surprise, the combination of Raja 42 with Kanamycin efficiently killed Raja 42-resistant *E. coli*, although kanamycin or Raja 42 alone did not effectively kill the bacterial clone. It is to be noted that the aminoglycoside antibiotics in particular, kanamycin and neomycin, did exhibit a synergistic effect in the treatment of Raja 42-resistant *E. coli*. The diameters of inhibition zones by the aminoglycosides were greater when used in combination compared to either one alone.

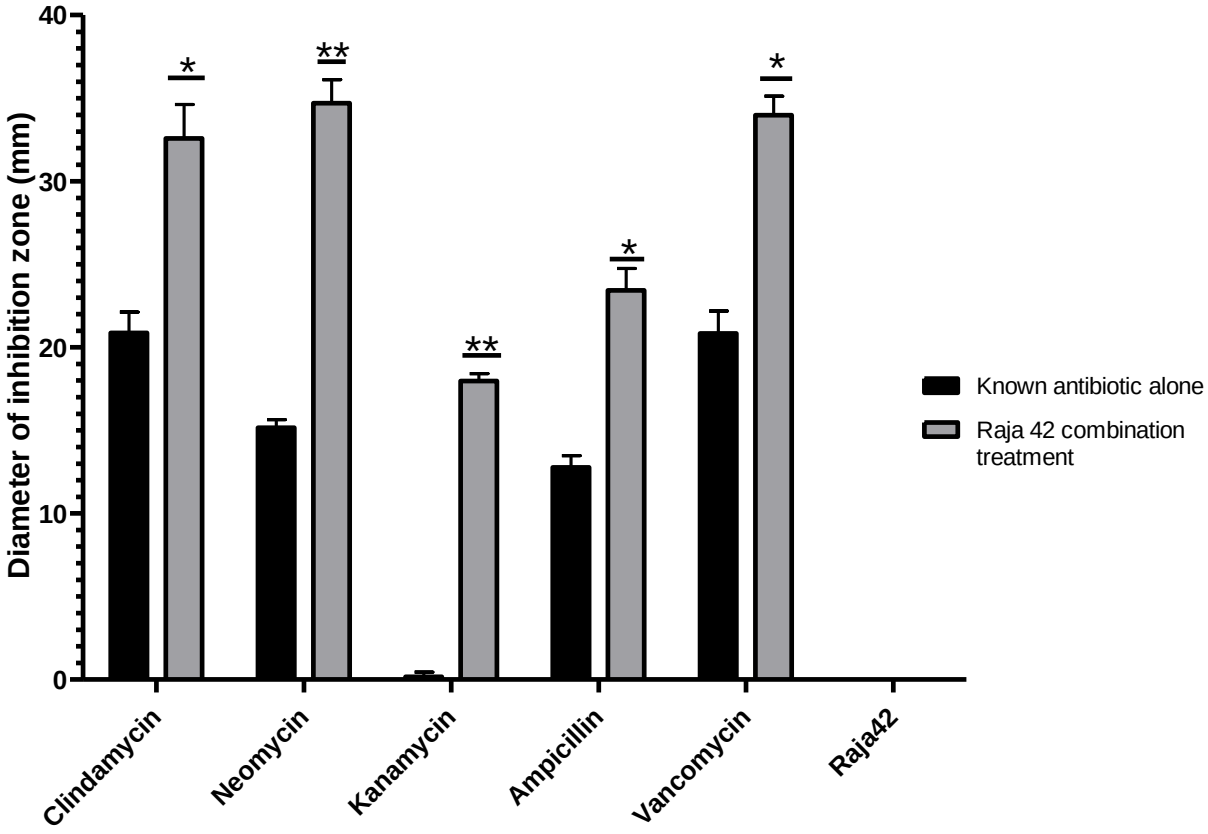

Figure 22: Raja 42-resistant *E. coli* K12 becomes sensitive when treated with Raja 42 in combination with other antibiotics, although either alone is not effective

Clindamycin, Neomycin, Kanamycin, Ampicillin, Vancomycin and Raja 42 were used to treat Raja 42-resistant *E. coli* K12. Raja 42-resistant *E. coli* K12 was treated with antibiotics alone or in combination with Raja 42 at each MIC concentration. Diameters of inhibition zones were measured. Combination effects of Raja 42 and clinical antibiotics were determined using three biological replicates.

3.10 Raja 42 mechanism of ROS generation requires functional ghrA

Bacterial transformation of Raja 42-resistant *E. coli* K12 showed that *ghrA* may be a necessary component of the MOA for Raja 42 antibacterial activity. Bacterial transformation of Raja 42-resistant clones were carried out using the pSB1C3 plasmid harbouring *ydcW* (*ghrA)* or *aceA* (housekeeping gene) donated by Dr. Warzecha's lab from TU-Darmstadt, Germany. Plasmids were concentrated and electroporated in Raja 42-resistant clones and subsequently, cells regained their susceptibility to Raja 42 as displayed in Figure 23. Sub-culturing of the PSB1C3 plasmid allowed for increased copy numbers to be generated for bacterial transformation. PSB1C3 plasmid DNA was introduced into Raja 42-resistant *E. coli* K12 cells by electroporation as described in section 2.17. The PBSB1C3 plasmids containing the *aceA* gene were used as positive control as *aceA* is a housekeeping isocytrate lyase gene in *E. coli* K12. The plasmids also contained a chloramphenicol selection marker. Following electroporation, cells were grown on Raja 42 containing plates and further propagated for multiple generations in order to confirm successful plasmid uptake within the bacteria. *E. coli* K12 cells containing the *aceA* gene did not undergo metabolic pathway modification and thus were susceptible to Raja 42 (Figure 23), as was evident by the absence of bacterial colonies on the agar plates. Raja 42-resistant *E. coli* still remained resistant to Raja 42 if AceA is not restored, since this gene is not essential for the TCA and downstream generation of ROS. This was confirmed through a confluent lawn on the agar plate following incubation. *E. coli* K12 cells, transformed with the *ghrA* plasmids, have maintained their susceptibility, as noted by the absence of colonies on the plates Raja 42-resistant *E.* coli K12 cells transformed with the ghrA containing plasmids had regained their susceptibility to Raja 42. The absence of colonies observed on the Raja 42-resistant *E. coli* plate was similar that of Raja

42-susceptible bacteria, thus confirming that cells had regained their susceptibility to our novel compound. This leads us to conclude that *ghrA* may be essential for bacteria to maintain their sensitivity to Raja 42 and plays an important role in the mediation of bacterial intracellular ROS responses. The importance of ghrA in the mechanism of Raja 42 lethality is spported by the data shown in Figure 24, which demonstrate that GhrA is highly expressed in the parental DH5α, but not in the Raja 42-resistant bacteria. Following transformation with *ghrA* plasmid, Raja 42-resistant bacteria express GhrA and became sensitive to Raja 42. This data clearly shows that *ghrA* plays a critical role in conferring the sensitivity of bacteria to Raja 42.

E. coli K12 expressing wild-type AceA

Raja 42-resistant *E. coli* K12 expressing wild-type AceA

E. coli K12 expressing wild-type YcdW

Raja 42-resistant *E. coli* K12 expressing wild-type YcdW

Figure 23: Expression of YcdW (ghrA) gene in Raja 42-resistant *E. coli* K12 restores its susceptibility to Raja 42

GhrA (YcdW) plasmid or *aceA* (housekeeping gene) plasmid transformed parental *E. coli* K12 and Raja 42-resistant *E. coli* K12. *ghrA* plasmid transformed Raja 42-resistant *E. coli* regain their susceptibility to Raja 42.

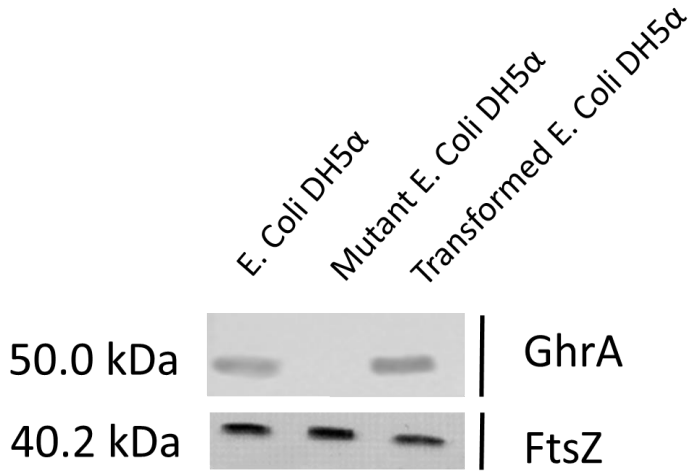

Figure 24 : GhrA protein detected in parental DH5α and transformed cells, while being absent in Raja 42-resistant bacteria.

Parental *E.* coli DH5α, Raja 42-resistant *E. coli* and GhrA plasmid transformed parental *E. coli*. *ghrA* plasmid transformed Raja 42-resistant *E. coli* express ghrA protein, compared to Raja 42-resistant bacteria which do not express detectable levels of GhrA.

3.11 The efficacy of the first or second line therapy against C. difficile isolates that were collected from patients treated at HSN

In order to determine the efficacy of Raja 42 as a novel antibacterial agent, it needed to be tested in a clinical setting. Therefore, the second aim of this thesis focuses on the Raja 42 activity on the killing of clinical *C. difficile* isolates, which were collected previously by the Nokhbeh group at HSNRI. Antibiotic susceptibility profiles were determined against the *C. difficile* collection and the reference strain *E. faecalis* ATCC 29212 using E-test strips. Clinically relevant first and second line therapies, Metronidazole and Vancomycin, respectively, were the antibiotics chosen for Epsilometer testing. The application of E-test strips onto the *C. difficile* or *E. faecalis* ATCC 29212 lawn was carried out as described in section 2.4. Breakpoints were determined according to the CLSI and EUCAST guidelines and defined by the presence of an ellipse of an inhibition zone surrounding each E-strip (Figure 25). Following the E-test guidelines, the MIC values were read at the point of intersection of the E-strip with the bacterial lawn at the edge of the zone of inhibition (bioMérieux, 2012c). Since both Metronidazole and Vancomycin are bactericidal towards *C. difficile*, MIC values were read at 100% bacterial growth inhibition at the edge of the strip.

A

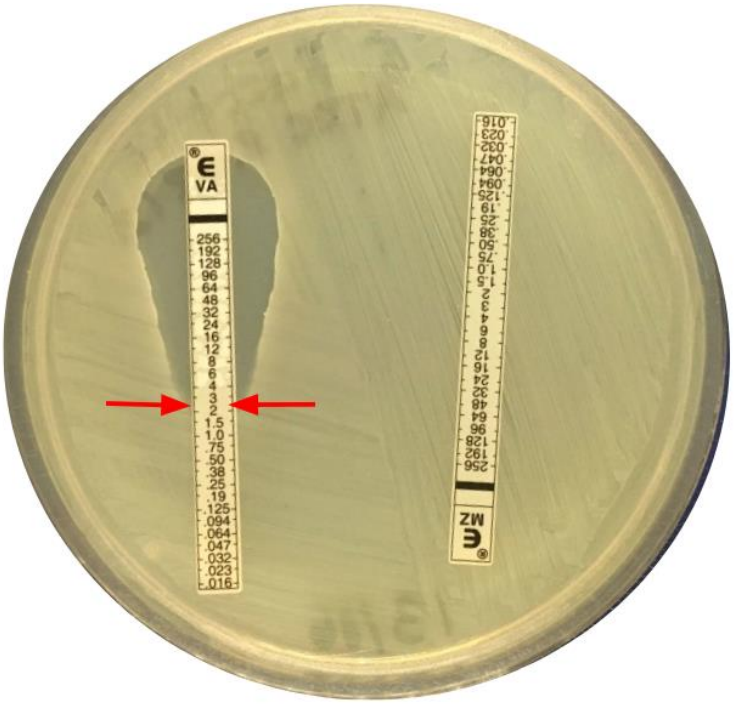

B

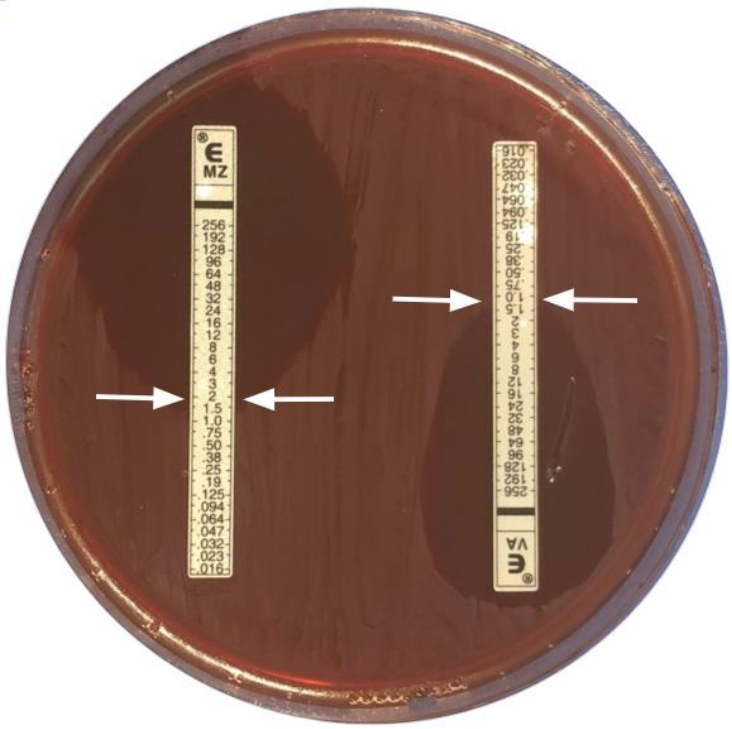

Figure 25: Antibiotic susceptibility test results of MZ and VA

A: MZ and VA plated on a lawn of *E. faecalis* ATCC 92912 and was a negative control strain. E-tests were performed as described in section 2.4. MIC values (μg/mL) are indicated by the red arrows.

B: MZ and VA plated on a lawn of *C. difficile* ATCC 9689 and was used as a positive control strain. E-tests were performed as described in section 2.4. MIC values (μg/mL) are indicated by the white arrows.

Breakpoint data used to determine the antibiotic susceptibility of Vancomycin and Metronidazole were determined from the CLSI and EUCAST guidelines. Both susceptibility for these agents were relatively low, being ≤ 2 μg/mL as the epidemiological cutoffs (ECOFF). These values are previously determined by EUCAST and CLSI respectively. Of note, two types of breakpoints are defined, wild-type breakpoints and clinical breakpoints. Wild-type organisms are classified as species with the absence of phenotypically detectable acquired resistance mechanisms to a specific agent. The wild-type MIC is the diameter of inhibition zone or MIC determined in liquid culture for a collection of organisms devoid of phenotypically detectable acquired resistance. The range within the MIC of wild-type species is largely attributable to technical variations within and between laboratories. Wild-type *C. difficile* is easily identified, as there is no appearance of a clearance zone during antibiotic testing. This can be seen with fluoroquinolone antibiotics, as *C. difficile* has acquired the resistance gene to fluoroquinolones, leading to no observable clearance zones during testing with this particular agent.

Clinical breakpoints, on the other hand, are determined for everyday use in a clinical laboratory setting in order to appropriately advise patients on their therapy. They are generally harder to determine, as they require a larger subset of patient data to accurately determine the appropriate MIC value. Clinical breakpoints will separate strains according to the probability of the strains being killed by a specific bacterial agent; therefore collected data also relies on the success and failure of antimicrobial therapy in order to determine the values [217]. EUCAST uses three categories to define a species interaction with an agent; susceptible (S), resistant (R) and susceptible with increased exposure (I). The (S) category strains are susceptible to standard dosing

regimens and therefore, there is a high likelihood of therapeutic success using a standard dosing regimen of the agent. (I) strains are microorganisms with a high likelihood of therapeutic success as a result of increased exposure to an agent, by adjusting the dosing regimen or by modifying its concentration at the site of action. (R) strains are microorganisms with the high likelihood of therapeutic failure despite increased exposure. Thus, the EUCAST and CLSI breakpoints accurately allow for the identification of susceptible and resistant strains, which otherwise would be merely recorded as observed trends. Despite the clinical breakpoints available, antibiotic and organism combinations are still lacking clinical data. With this being said, EUCAST is currently still missing data for imipenem and cefotaxime, while amoxicillin and benzyl penicillin do not have determined ECOFF values, as defined by EUCAST. Regardless of the current difficulties in obtaining adequate clinical breakpoint values, the differences between the two groups are critical to the appropriate treatment of patients in a clinical setting.

E. faecalis ATCC 29212 MIC values were within the ranges defined by EUCAST and CLSI, and thus were used as internal controls in this study (bioMérieux 2014; Clinical and Laboratory Safety Standards Institute, 2015; EUCAST, 2016). Standard antibiotic susceptibility breakpoints for *C. difficile* have been defined by EUCAST and CLSI as 4 μg/mL [217].

3.12 Activity of Metronidazole against clinical C. difficile isolates

For metronidazole activity against *C. difficile*, sensitivity has been defined as follows: < 2 μg/mL as sensitive, and > 2 μg/mL as resistant. Based on these proposed breakpoint values, the population distribution value of Metronidazole resistance was more or less agreed with that of EUCAST. 12 isolates (6%) from the collection were found to be resistant and 188 (94%) were susceptible. The population distribution of metronidazole is comparable to that of EUCAST, with EUCAST MIC90

being 2 μg/mL (Figure 26). We noted that there was a narrow distribution range for metronidazole MIC values within the small collection of samples. The majority of *C. difficile* isolates were determined to be susceptible to the clinically relevant drug metronidazole, since the MIC values were below or equivalent to 2 μg/mL (Figure 26).

3.13 Activity of Vancomycin against clinical C. difficile isolates

The vancomycin antibiotic susceptibility profile showed unimodal distribution and the data was fairly consistent with previously recorded data from EUCAST. The MIC90 was found to be 2 μg/mL, which is agreed with the EUCAST MIC90 of 2 μg/mL. Six isolates from the collection (3.0%) were resistant to vancomycin, while 194 (97.0%) were susceptible to the ECOFF guidelines. Five isolates were completely resistant to vancomycin E-test strip treatment with a maximum MIC value of 256 μg/mL and did not show any zone of inhibition (Figure 26).

A

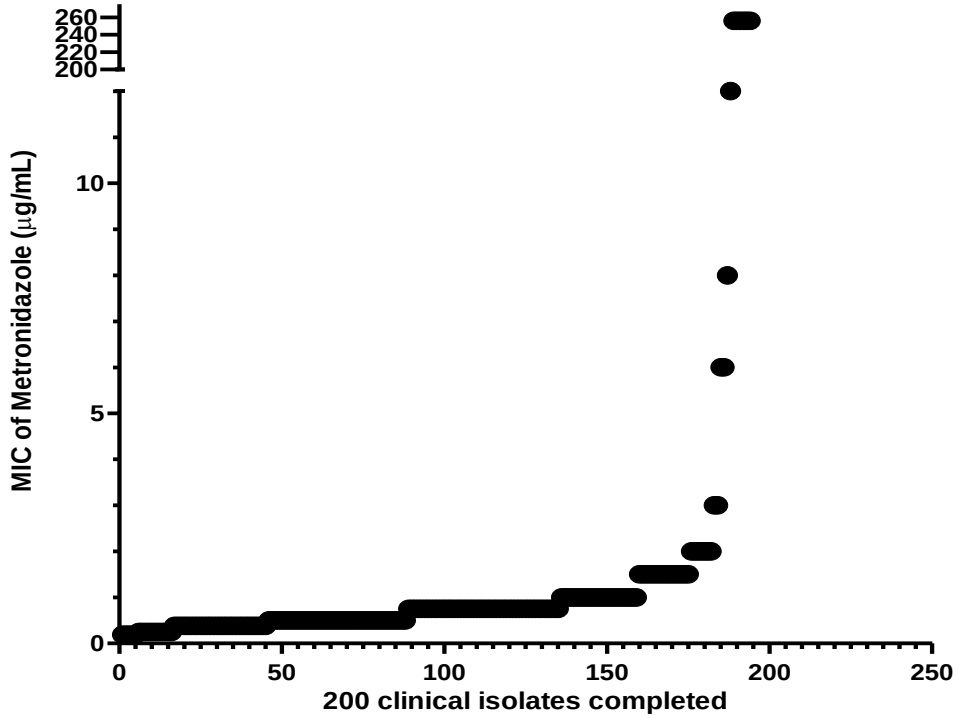
260
240
220
200
10
5
0
MIC of Metronidazole (μg/mL)
0
50
100
150
200
250
200 clinical isolates completed

B

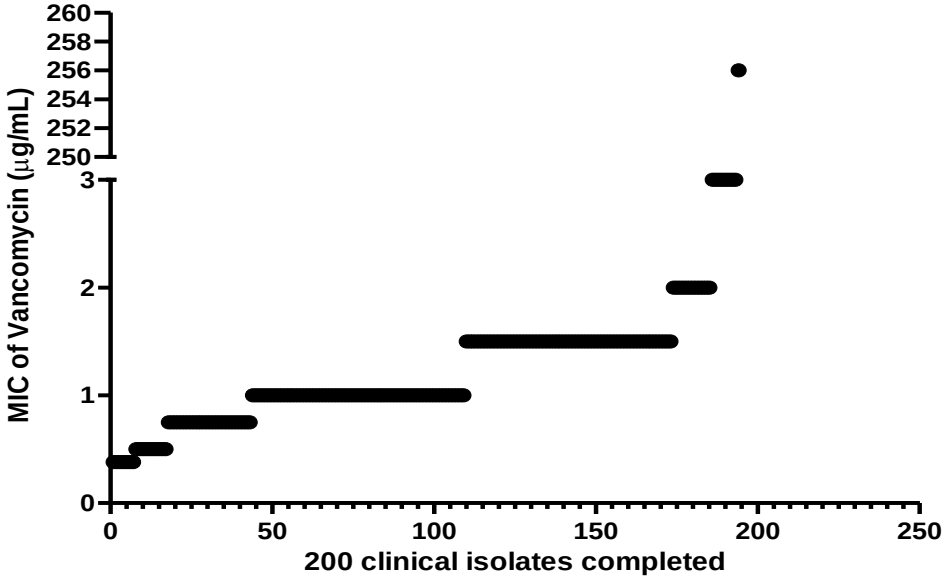
260
258
256
254
252
250
3
2
1
0
MIC of Vancomycin (μg/mL)
0
50
100
150
200
250
200 clinical isolates completed

C

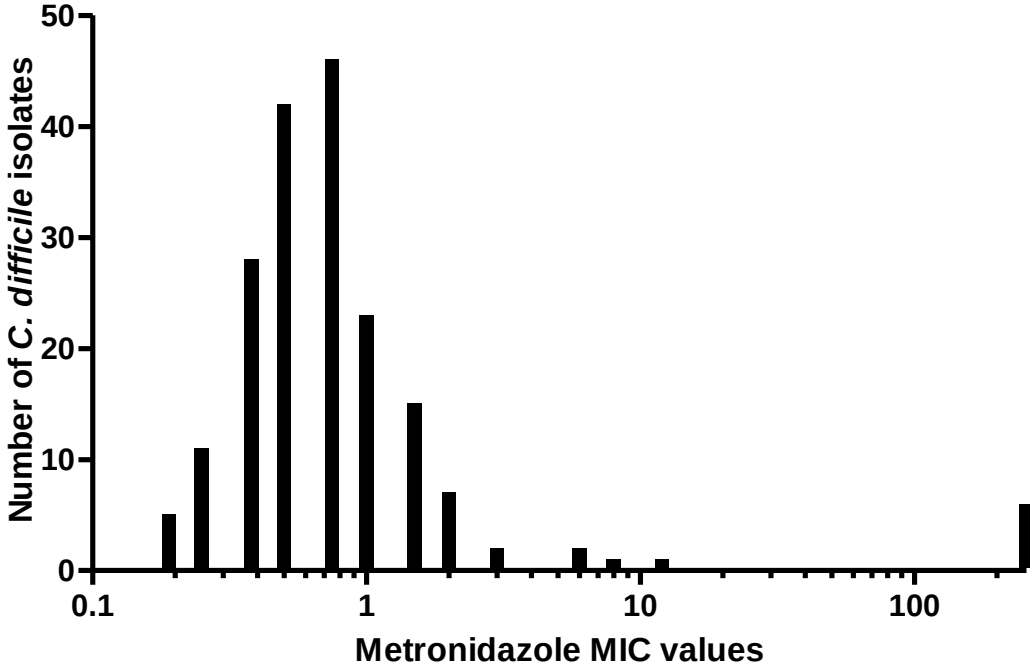
Number of C. difficile isolates
50
40
30
20
10
0
0.1
1
10
100
Metronidazole MIC values

D

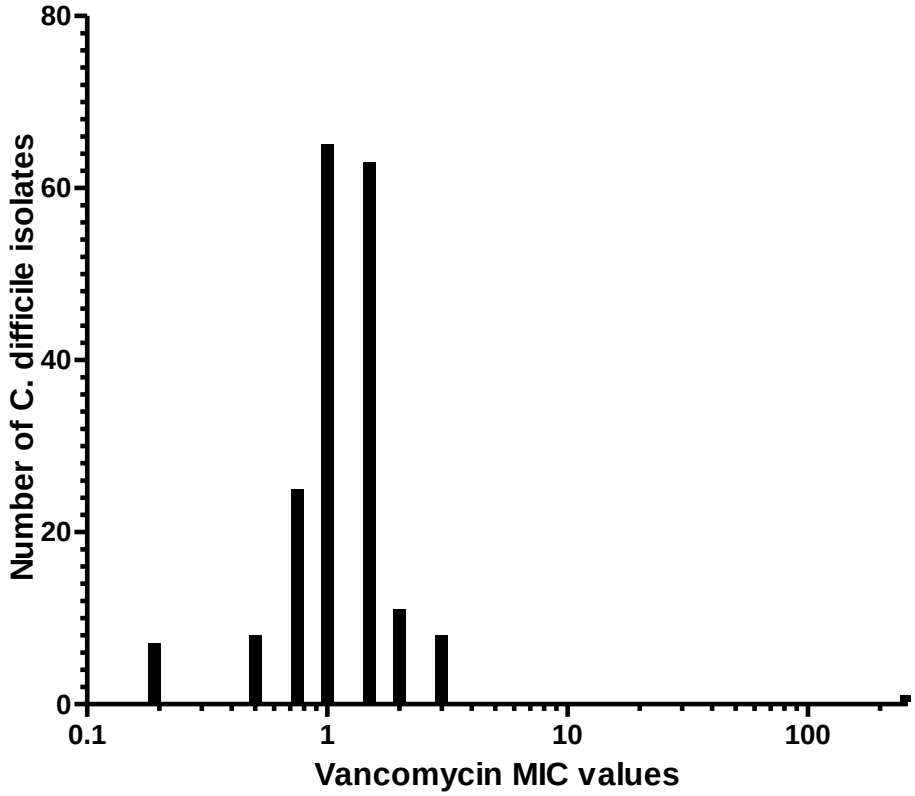
Number of C. difficile isolates
80
60
40
20
0
0.1
1
10
100
Vancomycin MIC values

Figure 26: Distribution of Metronidazole and Vancomycin MIC against 200 clinical *C. difficile* isolates

Metronidazole and Vancomycin MIC was determined for the collection of *C. difficile* isolates. MIC values were compared using EUCAST and CLSI guidelines for *C. difficile*. Isolates were classified as susceptible or resistant for each strain.

A: Metronidazole MIC against *C. difficile*, as determined by EUCAST is 2 μg/mL and 12 clinical isolates demonstrated resistance to this antibacterial agent.

B: Vancomycin MIC against *C. difficile*, as determined by EUCAST is 2 μg/mL, and 9 clinical isolates demonstrated resistance to this antibacterial agent.

C: Metronidazole MIC against 200 *C. difficile* isolates reveals 12 isolates with a MIC value greater then 2 μg/mL.

D: Vancomycin MIC against 200 clinical *C. difficile* isolates reveals 9 isolates with a MIC value greater than 2 μg/mL.

3.14 Raja 42 exhibits great potency towards C. difficile

MIC of Raja 42 against reference strain *C. difficile* ATCC 9689 was determined using a 96-well plate-based testing format, as described in section 2.4 (Figure 27). Positive inhibition by Raja 42 against *C. difficile* ATCC 9689 was determined by the absence of bacterial growth, confirmed visually and via optical density using a plate reader. Using an arbitrary MIC spectrum with values ranging from 1.1 μg/mL to 600 μg/mL, the MIC for Raja 42 was determined as 4.6 μg/mL. This concentration is superior to the MIC needed for *E. coli* cell death. To correlate the MIC values to diameters of inhibition zones, the same MIC spectrum was used and plated against a lawn of *C. difficile* ATCC 9689 (Table 2, in the Appendix section). Ultimately, in order to compare the efficacy of Raja 42 to that of current antibacterial agents, a therapeutic index was generated (Table 1). A therapeutic index (TI) value is the ratio between the toxic dose (TD_{50}) and the therapeutic dose of a drug (ED_{50}), used as the measure of relative safety of the drug for a particular treatment. Drugs can be classified as having a narrow therapeutic index, such as Vancomycin, where the therapeutic index value falls below 10. Drugs with narrow therapeutic indexes have small differences in dose or blood-concentration and may lead to serious therapeutic failures or adverse drug reactions. Most antibiotics, such as β-lactams, macrolides and quinolones have a wide therapeutic index and therefore do not require therapeutic drug monitoring. Therapeutic index values are dependent on the completion of human drug trials or at the least, obtaining the LD_{50} data from animal models. Jiang and colleagues suggests that the calculated TI is a predictor of specificity and the higher the TI value, the higher the specificity for bacteria [218]. The paper alludes to the TI as a widely accepted parameter to represent the specificity of an antimicrobial agent in prokaryotes *versus* eukaryotic cells [218]. In these circumstances, the TI can be calculated

as a ratio of the IC_{50} values and the MIC_{50}, thus a larger value is indicative of greater specificity for prokaryotic cells.

A

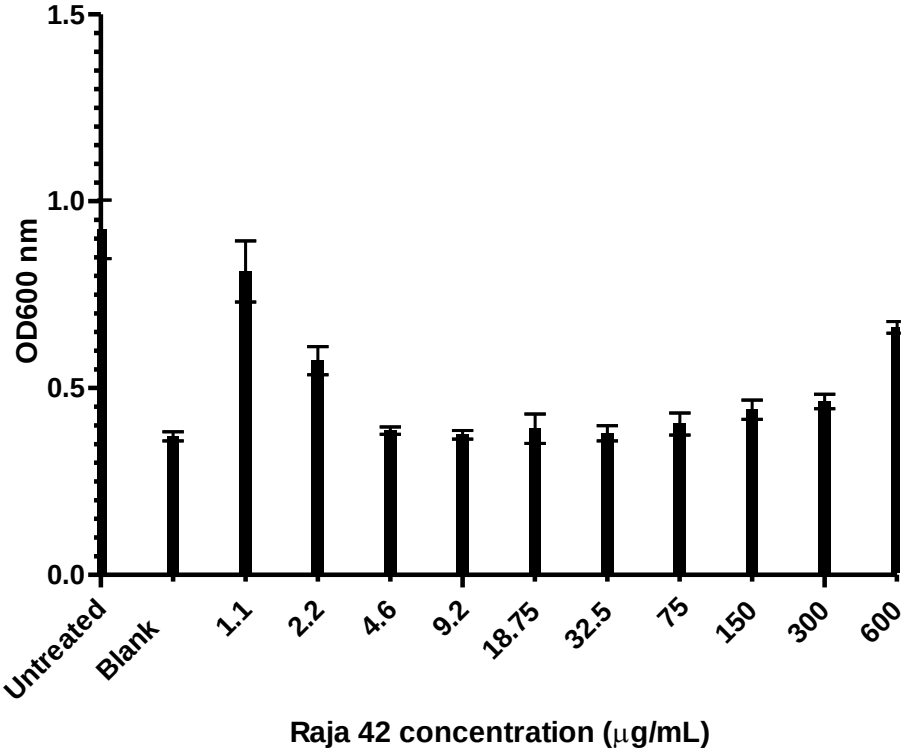
1.5
1.0
0.5
0.0
OD600 nm
Untreated
Blank
1.1
2.2
4.6
9.2
18.75
32.5
75
150
300
600
Raja 42 concentration (µg/mL)

B

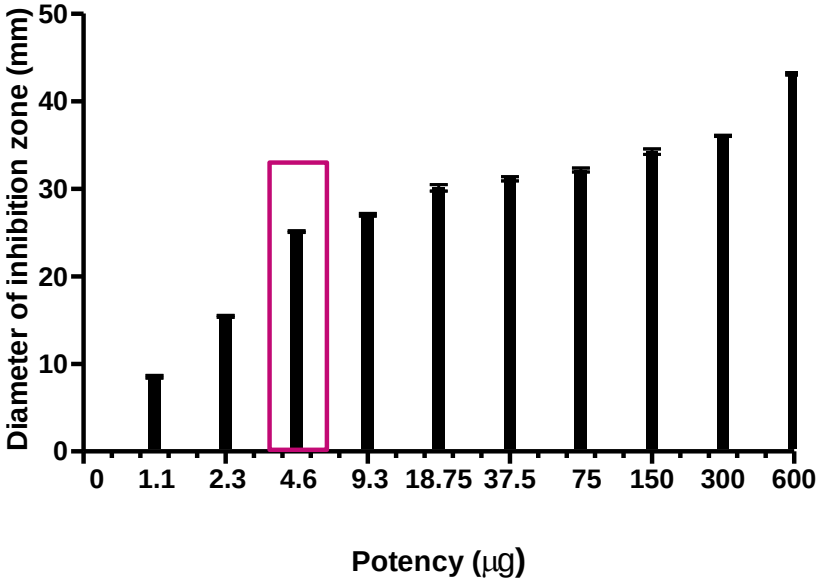
50
40
30
20
10
0
Diameter of inhibition zone (mm)
0
1.1
2.3
4.6
9.3
18.75
37.5
75
150
300
600
Potency (µg)

Figure 27: Raja 42 MIC value against *C. difficile* is superior to that of *E. coli* K12

A: Average diameters of inhibition zones plotted for Raja 42 against *C. difficile* ATCC 9689. Triplicates were performed for each compound and the diameters were expressed by average ± standard deviation. The values presented are mean ± SEM (n = 3). The "n = 3" shown above denotes three independent experiments with samples from three different bacterial populations.

B: *C. difficile* ATCC 9689 tube broth MIC correlation to diameters of inhibition zones.

Table 1: Therapeutic index of clinically relevant antibiotics

The therapeutic index of five clinically relevant antibiotics provides insight into the efficacy of Raja 42. MIC breakpoints can be correlated to therapeutic index. Clinically relevant antibiotics include Clindamycin, Vancomycin and Metronidazole.

Antibacterial agent	TD_{50}	ED_{50}	Therapeutic Index	Index value
Clindamycin	100 mg/kg/day	7.10 mg/kg	14.28	moderate
Metronidazole	524.0 mg/kg/day	19.5 mg/kg	26.8	high
Vancomycin	130.4 mg/kg/day	17.5 mg/kg	7.45	low

Antibacterial agent	GI_{50}	MIC_{50}	*Therapeutic Index	Index value
Raja 42	93.72 µM	7.71 µM	12.15	moderate

The sensitivity of the *C. difficile* clinical isolates to Raja 42 was also determined using a high throughput screening assay (Figure 28). Sixty isolates from the initial collection were selected according to specific inclusion criteria. Isolates were selected on the absence or presence of select toxins (toxin A, toxin B, binary toxin), the collection date and their previously identified antibiotic susceptibility profiles. MIC was determined using a 96-well plate, as described in section 2.4, and included a dilution range corresponding to the highest and lowest values identified against *C. difficile* ATCC 9689 strain. Breakpoints were predicted using the ECOFF MIC breakpoints software generated by EUCAST. The 95.0% and 97.5% subset ECOFF values for Raja 42 corresponded to18.75 µg/mL. Thus the epidemiological (S) cutoff corresponded to ≤ 18.75 µg/mL, while anything greater than 18.75 µg/mL was considered (R). Among the *C. difficile* collection, 81.7% were sensitive to Raja 42 and 18% displayed resistance to Raja 42. Of the resistant strains, 5.0% displayed complete resistance, determined at the highest MIC value tested of 600 µg/mL. Of the isolates that were resistant to Metronidazole and Vancomycin, 90.3% were susceptible to Raja 42 treatment.

A

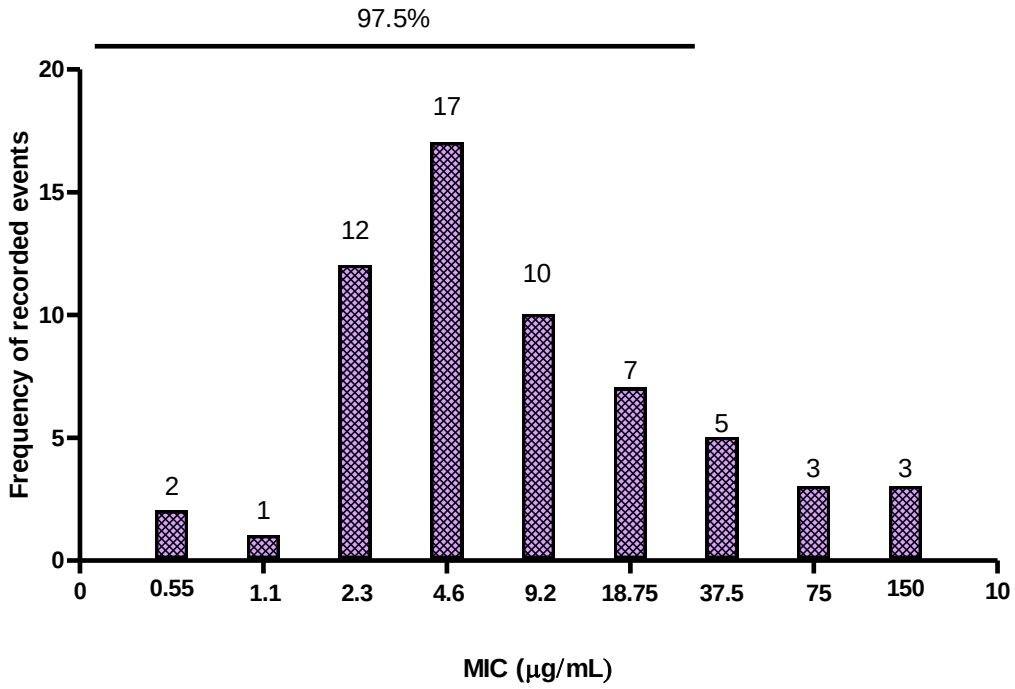

B

Frequency	Rate of resistance
11	18.3%

Figure 28: Distribution of 60 *C. difficile* isolates against Raja 42 MIC range reveals MIC cutoff to be <18.75 μg/mL

A: 60 *C. difficile* clinical isolates were selected based on a variety of criteria including toxin presence or absence, collection date and antimicrobial susceptibility profile. Isolates were treated with serial dilutions of Raja 42 ranging from 150 μg/mL 0.55 μg/mL using a 96-well plate. All assays were carried out in triplicate to ensure accuracy.

Using the EUCAST Epidemiological Cut-Off Finder (ECOFFinder), the 95.0% and 97.5% subset ECOF values corresponded to a MIC value of 18.75 μg/mL.

B: The frequency and rate of resistance to Raja 42 was determined according to the predicted ECOF values.

4.0 Discussion

4.1 Raja 42, a promising novel antibacterial agent

Twenty-seven active compounds were identified from the screening of a library of 211 novel compounds (Table 2, in the Appendix section). The 27 active compounds showed antibacterial activity against gram-positive and gram-negative strains, antibiotic-resistant strains as well as anaerobic and aerobic species. Through further examination, the novel Raja 42 compound was found to have better killing properties than certain known antibiotics such as Kanamycin (as confirmed through flow cytometry) (Figure 13). In order to determine a putative mechanism of action, microscopy and membrane depolarization assays were carried out and revealed that Raja 42 works at the membrane level (Figure 15 and Figure 17). In order to further elucidate the potential MOA, data from bacterial genomic sequencing and bacterial transformations have shown the MOA of Raja 42 to potentially utilize the Fenton reaction to generate ROS and to exhibit its antibacterial activity (Figure 5). As broad-spectrum activity is a desirable property of novel antibacterial compounds, extensive characterization and mechanistic studies were carried out as part of my Ph.D. research project.

Multiple governing bodies including the World Health Organization (WHO) express the need for novel antibacterial therapies in order to help combat the growing prevalence of antibiotic resistant bacterial strains [219]. They go on to mention that a decline in private investments and lack of innovation are undermining the efforts to combat drug-resistant bacterial infections. The report highlights a worrying gap in activity against the highly resistant NDM-1 *E.* coli, with only three novel antibiotics in the pipeline [219]. The NDM-1 cassette makes bacteria resistant to a multitude of antibiotics, including the carbapenams, the last line of defence against antimicrobial resistant

infections. While γ-lactam compounds have yet to be described for their antibacterial properties, the similar molecular backbone of β-lactams have allowed γ-lactams to be recognized as potential antibacterial agents. Previous work has unravelled the mechanism of β-lactam antibiotics, which act primarily through the interaction of the drug with the necessary enzymes (transpeptidases, carboxypeptidases) required for peptidoglycan synthesis [220]. Although the MOA of γ-lactams has yet to be determined, Caruano and colleagues discuss the recently discovered importance of a suitable activated amide bond within the γ-lactam structure, which is essential for its antibacterial activity [220].

The most striking feature of Raja 42 is its ability to preferentially kill a wide range of bacterial species, with no toxicity to very low-toxicity levels in both cancer and non-cancer breast cell line [213]. As previously described by Solomon, Hu and Lee, compound Raja 42 exhibited GI_{50} values, which represents the concentration that results in a 50% growth inhibition for cytotoxic compounds compared to untreated cells, ranging from 70.67 μM±1.24 to 93.72 μM±1.89 for the noncancer MCF10A and 1845B5 cell lines, respectively. Raja 42 exhibited lower GI_{50} values on the MDA-MB231, MDA-MB468 and MCF7 cancer cell lines with values of 26.48 μM±0.65, 82.84 μM±1.68 and 51.24 μM±1.44, respectively [221]. As the GI_{50} values are greater then 10 μM, the compounds can be considered inactive, as described by Lefranc and colleagues [222]. The low toxicity levels towards mammalian cell lines, especially for noncancer cells, make Raja 42 a very promising candidate to be used in future studies. Recent developments of novel antibacterial compounds have been met with very limited success, partly due to the lack of mechanistic data available for these developed compounds [220]. Although several γ-lactam antibacterial agents have been synthesized, none has been described the spectrum of antibacterial activity, as most work has just

focused on the chemical synthesis of the compounds [220]. The most important property of Raja 42 that distinguishes it from other compounds is its ability to target both aerobic and anaerobic species, but strikingly also target both antibiotic-resistant and non-resistant gram-positive and negative bacteria. An important property common to all bacterial species is the presence of a cell wall. Compromising bacterial cell wall integrity could be an efficient antimicrobial mechanism in order to target a variety of species, as it is a structural component common to most bacterial species. When considering broad-spectrum antibacterial therapy, β-lactam agents including penicillin and amoxicillin are recognized as the most successful antibacterial drugs, partly due to their specific interference of the bacterial cell wall with minimal side-effects.

The induction of ROS may also increase the potency of bacterial killing; however, it may lead to undesirable side effects in host cells [223]. The hypothesis that ROS producing antibiotics may lead to mitochondrial dysfunctions in mammalian cells has recently been proposed. However, despite measuring oxidative damage markers in blood and mammary glands of mice, Kalghatgi and colleagues found no evidence of tissue damage or dysfunction [224]. Other ROS generating compounds, such as fluoroquinolones (nofloxacin, ciprofloxacin, moxifloxacin) and aminoglycosides (kanamycin, neomycin, tobramycin) have been extensively studied [225]. However, data from clinical trials has focused on toxicity and adverse side effects with less focus on secondary mechanisms, which may be contributing to cellular damage [226], [227]. Besides traditional strategies to develop novel antibiotics, exploring the lethal activity of antibiotics is currently a feasible approach. Recent studies have shown ROS to play an important role in regulating both antibiotic resistance and antimicrobial lethality [228]. Therefore, the success of drugs like Vancomycin and Kanamycin is partly attributable to their adverse effects on the

bacterial cell wall synthesis and incorporation of mistranslated proteins into the cell wall respecticely. Hence, an ideal drug would be: (1) bacterial cell specific by differential permeability or specific target of action (eg: cell wall receptor binding); and (2) active against a unique aspect of bacterial respiration (eg: bacterial metabolism) in order to avoid the dysfunction and toxicities to the normal tissues.

The compound, Raja 42, has broad spectrum activity, and high potency against a variety of bacterial species, as compared to other clinically used antibiotics and, hence, satisfies one of the requirements for a desirable drug. Secondly, Raja 42 displays low GI_{50} values against noncancer breast cell lines; hence it may potentially be safe and effective. When comparing Raja 42 to clinically used antibiotics, the potential therapeutic index calculated appears to suggest that Raja 42 may be advantageous over Vancomycin which shows a low TI value.

The data presented in this thesis demonstrates that the mechanism of action by which Raja 42 exhibits antibacterial activity is through its activity at the membrane and through the induction of ROS via metabolic pathways.

4.2 Raja 42 displays potency towards a diverse collection of bacterial species

Overuse and misuse of antibiotics are a major cause of multidrug resistance development and, ultimately, often the failure of antibiotic therapies. With the misuse of clinical antibiotics, prolonged exposure to the drugs leads to the microbes' resistance, requiring the use of multiple combination therapies and further increasing the risk of developing multidrug-resistant microorganisms. The use of broad spectrum antibiotics is invaluable in controlling hospital-

acquired infections in a clinical setting. Therefore, a common approach is to treat patients with a broad spectrum compound, as the initial empiric therapy, in order to cover multiple sometimes unknown pathogens associated with clinical manifestations [229]. Although this approach may lead to downstream antibiotic resistance, it is often used to treat patients with infection of multidrug-resistant organisms, or to treat patients when the test results could not be done or when the results are not clear. Despite this, Williams and colleagues found no significant difference in the clinical outcomes of paediatric patients treated with broad-spectrum therapy compared to narrow spectrum therapy in the treatment of community acquired pneumonia [230]. The median length of hospital stay, admission to the intensive care unit and readmission was analyzed and no significant differences were found thus solidifying the use of broad-spectrum therapy.

To determine the activity of Raja 42, an initial dose of 50 µg/mL, 100 µg/mL and 200 µg/mL were plated against *E. coli* K12. The resultant data demonstrated that Raja 42 MIC is 50 µg/mL. Further studies to determine the spectrum of activity of Raja 42 were accomplished by screening a variety of different bacterial strains, including gram-positive, gram-negative, aerobic, anaerobic and antibiotic resistant strains (Figure 10). Raja 42 displayed preferential activity towards *C. difficile* and was 1.5 fold more effective towards *C. difficile* in comparison to NDM-1 *E. coli*. In comparison, Raja 42 exhibited greater potency than several antibiotics being used at clinics, including kanamycin, ampicillin and vancomycin when tested against *E. coli* or *C. difficile* (Table 2 found in the Appendix section). A technical problem faced was that compound Raja 47, initially selected for mechanistic studies, exhibited superior potency to Raja 42; however NMR screening revealed it to be the parent compound (isatin) with added impurities and not the initially proposed structure. To overcome this problem, compound Raja 42 was accurately identified through NMR

and a large quantity of the compound was produced in order to keep potency consistent throughout the work carried out in this thesis. It is evident that compound Raja 42 overcomes MDR strains, suggesting that it may not be a substrate for drug efflux proteins.

4.3 Raja 42 impacts the outer membrane of bacterial species

To gain better insights into the mechanism of action (MOA) of Raja 42, it was necessary to confirm whether this compound acted in a bacteriostatic or bactericidal manner. A time-kill curve monitors bacterial killing by specific antibacterial agents over a specified length of time [231]. The resultant curves may be interpreted using mathematical models to determine kinetics. Alternatively, a pharmacodynamics model can be used to determine the bactericidal or static effect of a drug [232].

There was a significant reduction of cell viability by 30 min post treatment with Raja 42, of which the pattern was similar to that of Kanamycin, a bactericidal aminoglycoside. In contrast the bacterial cell number in the sample treated with Clindamycin, a bacteriostatic drug, slowly increased following an initial decrease at around 30 min post treatment. This data clearly indicate that Raja 42 is a bactericidal agent.

To gain better insight into Raja 42's MOA, a membrane depolarization assay was performed in order to assess bacterial membrane integrity following drug treatment. Cells were assessed via a fluorometric assay using the membrane permeable $DiSC_3$ dye. *E. coli* K12 was incubated for 60 min with the fluorescent dye to allow cellular uptake; this followed by treatment with Raja 42. There was a significant increase in fluorescence emitted over a 10-minute time point, indicative of $DiSC_3$ presence in the environmental supernatant. This confirmed that the bacterial membrane

integrity was compromised in the presence of Raja 42 within a short time frame, which is consistent with the notion that Raja 42 function point is at the level of bacterial cell membrane. Compounds acting at the level of the cell envelope, such as β-lactams and glycopeptides, interfere with specific steps in homeostatic cell wall synthesis [221]. They are typically lipophilic compounds which can bind to cell wall proteins (involved in redox balancing reactions of NAD+/NADH) and affect cell morphology, by changing cell shape and size, inducing cellular stress responses and ultimately leading to cell lysis [233]. Time-lapse microscopy was carried out in order to observe any morphological differences (Figure 18), while fluorescence microscopy was conducted in order to determine the rapidity of Raja 42 killing, indicative of bactericidal action at the level of the cell membrane (Figure 19).

Evaluating the relative potency of Raja 42 as a novel antibacterial compound requires comparison of its activity with that of other antibacterial agents. In order to determine the percentage of cell death in the cell populations, flow cytometry was used, which showed that *E. coli* K12 were killed at a higher percentage of the population in the presence of Raja 42 than in Kanamycin (Figure 13). Cell treatment with Kanamycin displayed a greater proportion of injured (cells which were starting to become compromised and became dead at a later time point) and live cells compared to the samples treated with Raja 42, alluding to this novel compound's encouraging efficacy. All of the injured cells eventually died. In the untreated *E. coli* K12 sample, 1% of bacteria underwent cell death, and the remaining cell population progressed a normal cell cycle. In the Raja 42-treated sample, 79.3% of cells underwent cell death, whilst 66.8% underwent cell death in kanamycin-treated cells. While aminoglycosides, such as kanamycin, target the 30S subunit of ribosomes, Davis *et al* have concluded the lethal mode of aminoglycosides requires the insertion of misread

proteins into the membrane of *E. coli* [234]. Additional studies revealed that aminoglycoside generation of ROS is dependent on a redox-responsive Arc two-component system involved in the crosstalk between the Cpx-Arc systems [223]. The authors observed that ROS formation was the result of altered proteins at the membrane level, causing the cells to shift their oxygen consumption levels, making it readily available for cellular respiration. The same authors also demonstrated that bacterial envelope stress is broadly-related to ROS generation with the use of bactericidal compounds, alluding to a common mechanism for clinically used antibiotics [235]. Each of these networks is governed by a threshold regulation. If sub-lethal doses of antibiotic are administered, cells may become resistant to the compound; however, if a lethal dose is administered, cell death will occur rapidly. Raja 42 is similar to aminoglycosides and β-lactams in their ability to disrupt the bacterial cell envelope (either directly or through incorporation of mistranslated proteins), leading to rapid cell death.

4.4 Raja 42 promotes the generation of reactive oxygen species (ROS)

The mechanism of action of γ-lactam antibacterials has not been described in the literature. The notion that the induction of ROS is a major mechanism of antibacterial agents in killing bacteria has recently come to light [236]. γ-lactams, specifically Raja 42, make use of ROS as part of their killing mechanism. ROS is a natural side effect of aerobic respiration (Figure 5) and is generated through successive single-electron reductions ultimately generating superoxide (O^{2-}), hydrogen peroxide (H_2O_2) and the hydroxyl radical (OH^-). As originally proposed by Kohanski and colleagues, NADH produced in the citric acid cycle is further oxidized by the electron transport chain (ETC), leading to hyperactivation (excitation) of the ETC and downstream production of

superoxide and hydrogen peroxide [237]. Consequently, the hydrogen peroxide generated by this reaction will bind iron sulphur clusters and thus destabilize ferrous iron (Fe^{2+}). This iron is therefore free to react with neighbouring hydrogen peroxide and actively participate in the Fenton reaction to generate hydroxyl radicals, as described in section 1.4.1.6.3. As a result of radical formation, damage to DNA, RNA, lipid and protein can occur [238].

In order to determine changes in expression of proteins following treatment of Raja 42, 2D gel analysis was performed. Bacterial proteins have an average size of 300 aa with the bulk of them exhibiting a low acidic-neutral pI (5.5-7.0) [239]. *E. coli* proteins in particular are relatively neutral but also contain a variety of mildly acidic and basic proteins, in order to withstand the range of different pH within the body. While 2D gel is an ideal tool for discovery-phase research, not all expressed proteins can be displayed in a single gel. Using a commercially available IPG strip of pH 3-6, 2D gel analysis was carried out on *E. coli* K12 cells following treatment with Raja 42 in order to determine changes in the bacterial protein profile. Figure 16 shows a 2D gel for proteins extracted from ½ of the MIC of Raja 42 treated *E. coli* K12. Mass Spectrometry analysis revealed upregulations of 16 different proteins, 2 of which were notably involved in bacterial metabolism. SodA and $AhpC_1$ were identified and their role in bacterial metabolism was determined by previous literature [240]. SodA plays an active role in the dismutation of hydrogen peroxide and elevated levels are indicative of ROS generation. Similarly, $AhpC_1$ is also responsible for the scavenging of hydrogen peroxide with the goal of reducing the intracellular levels of ROS in the cell. These findings are consistent with those of Bollenbach and Kishony who observed the transcriptional responses of key metabolic genes in response to various combinational antibiotic therapies [241]. They observed differences in the transcriptional levels of SodA, which was

noticeably upregulated in response to combination therapies of bactericidal antibiotics when compared to normalized expression levels. Data from the 2D PAGE appear that Raja 42 treatment caused cells to upregulate these ROS associated proteins in response to cellular stress.

To gain further insights into whether Raja 42 may kill bacteria by inducing ROS, *E. coli* K12 cells were treated with ½ MIC of Raja 42, ampicillin (β-lactam antibiotic) or a combination of Raja 42 and thiourea (an ROS scavenger). The concentration of hydrogen peroxide released in the supernatant was then measured. By 60-minute post-treatment with Raja 42, 2×10^6 bacterial cells generated substantial amount of hydrogen peroxide, a level similar to that of ampicillin, both generating 0.3 nmol of H_2O_2. In contrast, treatment of cells with the combination of Raja 42 and thiourea depleted H_2O_2 concentrations by half to 0.14 nmol when compared to treatment of Raja 42 alone (Figure 15). This result was corroborated with that of Western blot assay carried out with NDM-1 *E. coli* as treatment with ½ MIC of Raja 42 showed substantial upregulation of sodA (Figure 18). When compared to 100 ng of purified protein, Raja 42 was capable of upregulating sodA to comparable levels. This was quantified through QPCR, which demonstrated a 5,600-fold increase in the level of sodA mRNA in response to Raja 42 (Figure 21). SodA encodes MnSOD, an important ROS scavenger, and increase in sodA levels have been associated with increased ROS generation within the cell [242]. Raja 42 not only increases SodA production within the cell but also increases it to significant levels. These findings strongly agree with previous reports of cellular damage within the cell due to internal ROS production [242].

Through the Fenton reaction, generation of ROS species such as hydroxyl radicals relies heavily on the availability of intracellular iron as well as a reducing agent, most commonly NADH. In

addition to DNA damage, these ROS species will also target lipids in the cell wall, as well as RNA, and protein synthesis machinery. Oxidation of sulfhydryl groups and oxidative adduction of amino acid residues are just some of the ways RNA integrity may be compromised through ROS [243]. In order to assess further downstream damage, as a result of ROS generation, an RNA electropherogram was generated, to determine the level of RNA damage. To address this question, the integrity of the total RNA present in the ribosomal fraction of *E. coli* K12 cells was assessed using the Agilent 2100 bioanalyzer. Data in Figure 19 demonstrate the effect of an 18-hour Raja 42 (25 µg/mL) treatment on the integrity of total RNA in cellular fractions obtained during *E. coli* K12 RNA extraction. As expected, there were degradation bands present in the sample treated with positive control, rifamycin. Rifamycin is a reversible RNA binding agent and is known to cause downstream RNA degradation and decay following inhibition of RNA synthesis [244]. All samples displayed two sharp bands at the positions of the 23S and 16S RNA with addition of a third band appearing above the 23S RNA. The most likely explanation for the slightly larger band above the 23S RNA is likely pre-translational modification of 23S rRNA. Typical in eukaryotic cells, the RNA undergoes post-transcriptional modifications (eg: splicing, capping and polyadenylation) allowing it to be processed into rRNA. As previously reported by Tolmecki and colleagues, the presence of Y pre-processed RNA bands is often seen slightly above the sharp 28S RNA bands during RNA electrophoresis [245]. Here I speculate that possibility of a pre-processed RNA band appearing slightly above the 23S bacterial rRNA, as the band does not appear to be the result of plasmid or gDNA contamination, which would display bands greatly above the RNA bands. Cells treated with Raja 42 displayed a similar smeared nucleotide banding pattern to that of rifamycin, confirming the presence of RNA damage from Raja 42 treatment. This data added

evidence that Raja 42 treatment causes damage to rRNA, which may possibly have occurred due to generation of abundant ROS.

In order to circumvent bacterial stress, the glyoxylate shunt is used as an adaptive mechanism often linked to stress adaptation [246]. The glyoxylate shunt serves as a bypass mechanism in the TCA cycle, allowing the circumvention of the decarboxylation steps in which NADH is produced. By upregulating this shunt, bacteria may lower NADH production and thus avoid antibiotic-induced ROS production. It has been previously reported that this shunt is induced in *Pseudomonas aeruginosa* during oxidative stress [247]. It has also been shown that isocitrate lyase plays an important role in avoiding ROS induction. In the *Mycobacterium tuberculosis* species, specific isocitrate lyase deletion mutant was found to be more susceptible than the wild-type to various antibiotics and it was found that the addition of an antioxidant restored susceptibility to the levels of the wild-type [248]. It has been previously shown that the treatment of bacteria with sub-lethal concentration of certain antibiotics, such as the β-lactams ticarcillin and carbenicillin, increases mutation rates, resulting in the emergence of multidrug-resistant strains [249]. Kohanski and colleagues observed a strong correlation between ROS formation and mutation rate following treatment with sub-lethal concentrations of bactericidal agents. Sub-lethal concentrations of Raja 42 were used to generate Raja 42-resistant *E. coli* K12. In the experiment, bacteria were initially treated with ¼ MIC Raja 42, and the surviving population was subcultured for five times. This process was repeated incrementally with increasing concentrations of Raja 42. *E. coli* population survived at 1.0 MIC of Raja 42 and this defined Raja 42-resistant *E.coli*. Several Raja 42-resistant mutantsclones were used for determining their genomic DNA sequences with the aim of further confirming the mechanism of action of Raja 42. In order to have maximum genome coverage,

Illumina sequencing was performed. Microscopy and ChromoSelect agar were used to confirm the identity of the *E. coli* species prior to sending out for sequencing. ChromoSelect agar contains X-salmon and X-glucuronidase (two chromogenic substrates) that when cleaved by β-D-galactosidase, result in a salmon-red colony in the presence of coliform bacteria or a dark blue colony when cleaved by the β-D-glucuronidase enzyme of *E. coli* species. Parental genomes and 5 mutant genomes were sequenced for both *E. coli* K12 DH5α and NDM-1 *E. coli*.

Genomes were assembled into multiple contigs and further annotated. It was not felt that closing the genomes completely using the MinION was necessary at this time since the draft genome provided sufficient coverage. The assembled sequencing data provided useful information to proceed with taxonomic identification and further analysis to detect sequence alterations, and mutation sites. Through the alignment of the parental genome with those of the five Raja 42-resistant clones, it was identified that a 27 bp deletion was present in all Raja 42 resistant isolates. The parental sequence was initially aligned to the NCBI sequence and revealed small variations confirming the need to sequence the parental strain when completing genome comparisons.

Using the EcoCyc platform (a subset of the BioCyc database specific for *E. coli*) and the Snapgene software (v5.1), the comparative genome analysis function was used to determine the gene neighbourhood for which the 27 bp deletion occurred. It was revealed that the deletion was located at nucleotide position 954,547 relative to *serX* and 317 bp upstream of *ghrA*, which is located at nucleotide position 954,841 (Figure 20).

Confirmation of the *E. coli* K12 DH5α was completed using the Snapgene (v5.1) software in order to identify and confirm the genotypic characteristics associated with this strain. This strain contains a characteristic *recA* gene mutation (*recA1*) in which a nucleotide substitution, at nucleotide 482 of the recA gene, from G to A, causes a missense amino acid change at position 160 of the gene[250]. *recA* is responsible for repairing and maintaining *E. coli* DNA. *recA* is required for homologous recombination as well as bypass of mutagenic DNA lesions by the SOS response, in addition to lacking recombinase activity [251]. RecA-SSB-ssDNA nucleo-filament catalyzes homologous strand exchange of the broken ends allowing for double strand break repair [241]. To repair double-strand breaks without loss of sequence information, the presence of two repeats is often necessary [252]. As a result of the *recA* mutation, the RecA protein loses its functions including its recombination role. Consequently, this leads to the lack of formation of multimeric forms of plasmids through recombination. Thus, this strain is suitable for carrying plasmids with monomeric size and the resoning for its increased popularity for plasmid production and purification.

In addition to the recA modification, the DH5α *E. coli* K12 also contains an F-, endA1, and relA1 genotype. The F plasmid, a DNA plasmid called Fertility Factor, is responsible for bacterial conjugation, in which this feature is absent from the DH5α [253]. The endA1, coding for the endonuclease 1, is responsible for non-specific digestion. A base-pair substitutation mutation in this gene, leading to an amino acid changes, inactivates the endonuclease activity in this strain, allowing for improved quality of plasmid DNA isolation [254]. However, the relA1 mutation causes the strain to develop a lipid structure which radically differs from the wild-type and is

characterized by an accumulation of neutral phospholipids and saturated fatty acids. Consequently, the membrane is more fragile in regards to osmotic shock and sonication while having lower likelihood of protein leakage and cell lysis due to the increased amounts of saturated fatty acids [255].

Insertion and deletion mutations can affect all parts of the genome and are most prevalent when the DNA contains sections of short or medium repeat, specifically interspersed repeats [256]. This largely occurs since repeat sequences can cause strand slippage with the resulting polynucleotide having a larger or smaller number of repeats respectively. When scenarios of strand slippage surface, recombinational mechanisms are employed in a *recA*-dependent reaction. Bacterial strains with the *recA1* mutation will undergo a bypass mechanism as there is no pairing of homologous regions and thus the rates of large deletion mutations remain low. During recombination of DSBs or strand slippage (as a result of deletions or additions), the first repeat sequence is removed and subsequent repeat sequences are preserved, allowing for resumption of accurate DNA replication [257].

Our analysis of the gene neighbourhood surrounding the 27 bp deletion revealed a series of both repeat sequences, flanked by spacer regions, both of which contained sequence similarity from one spacer to the next. Analysis of the Raja 42-resistant genome revealed that the 27 bp deletion occurred in 1 of the 2 initially present repeat sequences found in the Raja 42-susceptible strain. Comparatively to the MG1655 strain, the DH5α strain contained 1 less repeat and spacer sequence, at nucleotide position 954,545 in the genome. The Raja 42-susceptible DH5α strain, also contained 1 less repeat and spacer than the MG1655 however, discrepancy occurred at the first

repeat and spacer sequence (Figure 20). The deletion observed in the Raja 42-resistant strain occurred in the last interspersed repeat sequence suggesting that recombinational bypass is not the mechanism by which Raja 42 is promoting bactericidal activity. Through this analysis, one could speculate on the possibility that the Raja 42 compound is causing a form of mutagenesis, although further evidence is required. A likely possibility, which required further elucidation, is that Raja 42 aided in the selection of the deletion mutant as it would ensure a means of survival to the bacterial cells. In line with observation made by Byzmek and Lovett, the authors noted that deletions occurring in short repeats of the genome impacted the functions of neighbouring genes as a result [258]. The authors also noted that deletions of medium-interspersed repeats shows weak or no RecA-dependent DNA-pairing or strand exchange protein [259]. Based on the presented evidence and previous work of these authors, the deletion of a medium-interspersed repeats following Raja 42 treatment is independent from recombinational events led by RecA protein as the DH5α strain lacks the necessary recombination machinery. Although further evidence is required and one may only speculate a mechanism at this time, it can be concluded that the expression from the upstream promoter region associated with the repeat sequences is important for GhrA expression.

In the extensively studied lac-operon model requires two enzymes: a permease to transport the lactose and a β-galactosidase to cleave the lactose molecule into glucose and galactose [260]. These enzymes are encoded by two contiguous genes, Y and Z, which belong to the same operon. A third gene, A (encoding for a transaacetylase not required for lactose metabolism) and a fourth gene, I, also belongs to the operon and encodes for the lac repressor which blocks the expression

of both Z and Y. The lac promoter site, P, is upstream of the operon, while the lac operator site, O, is located between the promoter and Z gene [260].

Previous work has suggested that transcription of the lac operon is up-regulated through the binding of CRP to the promoter, which is activated by the binding of cAMP [261]. The CRP-cAMP complex was shown to activate transcription initiation of the lac promoter via an indirect component of the activation resulted from an enhancement of the fraction of promoters productively bound by RNA polymerase [261]. In addition, direct enhancement of RNA polymerase binding at the principal lac promoter (lac P1) was previously identified suggesting that a combination of indirect and direct activation by CRP-cAMP is responsible for the large activation observed [261]. CRP-cAMP binds to a specific sequence called the CAP site, which is located upstream of the promoter region and is necessary expression of the lac operon. Mutations in the CAP site have been shown to prevent CRP-cAMP binding consequently decreasing the expression levels of the lac operon [262]. A partial nucleotide sequence, ATGTG, common to the CAP binding site has also been identified at nucleotide position 954,764 of the Raja 42-resistant genome. This sequence is located adjacently to the Fis dual transcriptional regulator, upstream of *ghrA.* As previously described, it could be postulated that the 27 bp deletion identified in the Raja 42-resistant genomes, located upstream of the promoter region, may follow a similar mechanism to that of the CRP-cAMP, as bacterial expression of *ghrA* is greatly reduced when treated with Raja 42. Therefore, it can be concluded that this repeat region upstream of the *ghrA* promoter, which suffered a deletion event is important for *ghrA* expression.

In regard to the conclusions of the above noted authors, I decided to investigate wheather the deletion observed in the Raja 42-resistant genome had an impact on surrounding genes in the

neighbourhood. Having previously identified the impact of Raja 42 on *sodA*, I sought to identify genes in the neighbourhood, which may play a role in the metabolism and respiration pathways, ultimately impacting ROS generation. It was observed that a neighbouring gene, 317 bp downstream of the deletion, was *ghrA*. Upon computational analysis of the *ghrA* genome, it was noted that both *ghrA* and serX share a common promoter element, the δ-70 factor which has the TAAATT sequence. The δ-70 factor is an additional promoter element to the conventional TATA (Pribnow box) element, common to prokaryotes. The DNA located upstream and surrounding the transcription initiation sites typically confers promoter activity for a gene. Specifically, the 27 bp deletion is located 197 bp upstream of the *ghrA* promoter region.

Interestingly, both promoter recognition sequences for *serX* and *ghrA* share a common recognition sequence for binding the transcriptional regulator: Fis. The Fis dual transcriptional regulator regulates the genes involved in translation (tRNA and rRNA) as well as genes involved in metabolism, stress response, biofilm formation, virulence, motility and chemotaxis [246, 247]. Fis will autoregulate its own expression as well as that of *serX* and *ghrA*. The remote transcription initiation involving the cis-acting elements displayed in our analysis could act similarly to the CRP-lac operon model in the sense that a deletion in this critical region, in turn has impacted the expression of downstream genes, specifically *ghrA*. Of poignance, the deletion in the upstream repeat section observed in the Raja 42-resistant mutants has abolished the transcription initiation leading to decreased promoter activity in the resistant mutants compared to the wild-type.

The 27 bp nucleotide deletion observed in Raja 42-resistant cells has an important impact on the function of ghrA, in the gene neighbourhood. Genomic neighbourhood influences the transcriptional activity of genes within it, and genetic manipulation, natural or induced mutations alter the neighbourhood of genes, and have been shown to affect its expression [265]. In the model described by Oliver and colleagues, the similarity of gene expression within neighbourhoods is likely the result of co-regulation within an expression neighbourhood [266]. In turn this may be due to incidental interactions between promoters and transcriptional enhancers. In this model, transcription of one or more genes in a genomic cluster is regulated by transcription factors binding at the appropriate sites and activating nearby genes as well as the target genes. As a result, inappropriate transcription of select genes, highly impact the expression of neighbouring genes within the cluster[266]. Consequently, alterations to the gene neighbourhood, such as deletion events, can impact multiple adjacent genes in the cluster. Very similar to the 27 bp deletion observed in the Raja 42-resistant bacteria, the immediate downstream gene in the neighbourhood, *ghrA* was noticeably impacted as a result of this deletion. Although *ghrA* was the only gene investigated at this time, further evidence is necessary to determine the impact of the deletion on additional genes from the neighbourhood, such as those upstream of the deletion site, and those downstream of *ghrA*. Understanding the roles and regulations of neighbour genes are necessary to guide our understanding of the underlying mechanisms which may be affecting transcriptional regulation.

Of note, the 27 bp deletion identified during my analysis may possibly directly affect the termination of *serX*, which encoded for tRNA-serine, as the deletion removes a nucleotide from the coding region of this gene. Consequently, this is likely to cancel the termination, which

normally occurs at a strong GC rich stem, which could result in the continuous transcription of *serX*. Although in a yeast model, with *S. cerevisciae,* Bloom-Ackermann and colleagues observed that tRNAs and proximal genes carrying identical anti-codons are important for the genomic surrounding to tRNA expression [286]. Importantly, the authors concluded that deletions occurring in regulatory regions of low-copy tRNA family genes illicited a stress response[267]. From these conclusions, one could postulate the deletion occurring in *serX*, may in turn impact the stress-response, through a decrease in the adjacent ghrA. As a result, the treated *E. coli* cells would be able to circumvent the delirious effects of Raja 42 treatment, ultimately allowing them to survive.

GhrA plays an active role in the glyoxylate shunt and is responsible for the NADPH-dependent bidirectional conversion of glyoxylate to glycolate. With a decreased conversion of glyoxylate to glycolate, glyoxylate levels are increased in the cell and the glyoxylate shunt is upregulated. Consequently, the decarboxylation steps generating NADH in the TCA cycle are bypassed, allowing bacteria to survive and resist ROS generation, hence making them resistant to Raja 42 activity. Analysis of the genomic neighbourhood sequence identified the upstream tRNA-serine at position 954,658 and a downstream zinc-binding phosphatase, coded by *YcdX* at position 955,884 within the genome. Both *YcdW, X, Y* and *Z* belong to the same operon.

To probe the mechanism of resistance to Raja 42, a “rescue experiment” was carried out on Raja 42-resistant clones. The resultant data confirmed the need of *ghrA* for the Raja 42-mediated bacterial killing as an ectopic expression of *ghrA* restored their sensitivity to Raja 42. Since the

Raja 42-resistant clones harboured a deletion upstream of *ghrA*, if reintroducing *ghrA* conferred susceptibility to the cells, this could greatly strengthen the hypothesis that Raja 42 generates ROS as mechanism of action. These results from this work are consistent with previous reports indicating the necessity of ghrA in the production of glycolate for the glyoxylate shunt [268]. In summary, Alkim *et al* reported that knockout constructs of the ghrA gene in *E. coli* resulted in decreased production of glycolate and glycolic acid. The authors noted an upregulation in detectable glyoxylate levels within the cell. However, increases of glycolate and glycolic acid were observed when ghrA gene expression had been restored in the cells. To further probe the possibility of the importance of *ghrA* in Raja 42's mechanism of action, Western blot analysis was carried out (Figure 24). The resultant data demonstrated the presence of detectable levels of GhrA in the Raja 42 rescued cells, which had previously undergone transformation with a *ghrA* containing plasmid. These levels were similar to those detected in parental DH5α cells.This data would indicate the necessity for ghrA in regulating levels of glyoxylate within the cell, therefore helping mitigate circumvention to ROS generation.

4.5 What is the connection between loss of membrane integrity and ROS generation?

To better understand if there was a relationship between damaged bacterial cell membrane and ROS generation, various assays were carried out including time-kill assay, membrane depolarization assay, immunobloting and genomic sequencing. The resultant data showed that Raja 42 rapidly inhibits bacterial growth within the first 30 min of treatment. I also found that Raja 42 impacts the bacterial membrane with cells becoming non-motile immediately after treatment.

Additionally, data also showed that Raja 42 induced ROS to the nanomolar level-within 30 min of the treatment.

Yu and colleagues have demonstrated a time dependent relationship between bacterial ROS generation and rapid bacterial killing [269]. The authors concluded that polymixin E (a non-ribosomal antibiotic) was able to rapidly generate ROS, within a few min, reaching lethal levels at 60 min in a time dependent manner in the *Paenibacillus polymyxa* species. Polymixin E, also known as colistin, is an antibiotic used for the treatment of gram-negative species. This antibiotic works by binding to the bacterial membrane and causes alterations to membrane proteins and increasing permeability and causing death of the bacteria. In previous work completed by Sampson and colleagues, the treatment of the gram-negative bacillus, *Acinetobacter baumannii,* with polymyxin antibiotics was described [270]. They observed rapid killing, within the first 30 min of treatment with a notable decrease in CFUs following treatment of cells with polymyxin. They also noted elevated levels of H_2O_2, with lethal levels accumulating in the cell within 30 min post-treatment. Their work highlights new findings of polymyxin causing mis-translation of membrane proteins and causing the downstream activation of the CpxAR envelope stress-sensing two-component system. Activation of the CpxAR envelope stress-sensing system may be involved in the cross-talk with the ArcA system, leading to changes in expression of genes involved in cellular metabolism and cellular respiration, as described by Kohanski *et al.* [235]. As described above, Raja 42 causes loss of cell membrane integrity. This raises the possibility that Raja 42 may activate the Cpx-ArcA two-component system through its membrane damaging activity. The activation of the two-component system by Raja 42 could in turn lead to the upregulation of respiration, rapidly causing lethal accumulation of ROS. To further discuss this point, Hong *et al,* proposed a model

in which a primary change was necessary for the elevated and continued production of ROS species within the cell, which in turn caused a secondary lesion, leading to cell death [271]. My data would be consistent with this proposed model, as Raja 42 may cause the formation of a primary change through its disruption of the cell membrane and a subsequent increase in the level of ROS. The authors noted that ROS mediated damage likely triggers subsequent rounds of ROS formation and notable accumulation of ROS within the cell [271]. This may attribute to the lethal accumulated ROS in the cell, eventually leading to cell death. Following the induction of a primary change, Raja 42 may activate pathways leading to increased ROS formation and cause secondary damage such as membrane depolarization and internal damage to RNA. As these secondary changes are too great to be repaired, thus cell death may occur. ROS may also contribute to killing by overwhelming repair of primary stress damage.

Bacteria produce a variety of enzymes to mitigate ROS-mediated cellular damage. SODs and AhpC are two of the most well-known enzymes involved in the reduction of ROS formation, and help dismutate those species once they have been formed. Recent studies have demonstrated the importance of ROS scavenging enzymes and the role they play during ROS upregulation within the cell [272]. Oh and colleagues observed a significant upregulation of SodA, AhpC and KatA in *Campylobacter jejuni* cells following treatment with kanamycin or chloramphenicol [295]. They measured internal cellular H_2O_2 levels and concluded that, despite increases in ROS scavenger enzymes, lethal levels of ROS production at later time points overwhelmed the activity of scavengers, leading to cell death [272]. My data demonstrates that Raja 42 treatment of *E. coli* K12 did lead to an increased cellular production of the ROS scavengers SodA and

AhpC. However, Raja 42 did rapidly produce the lethal level of H_2O_2, leading to cell death within 30 min of the treatment even when the level of scavenger enzymes was also increased.

Although gram-positive and gram-negative species differ in their cell wall composition, Raja 42 is effective on both groups. Gram-positive species have a thick layer of peptidoglycan with an absence of an outer lipid layer whereas gram-negative species have a thin peptidoglycan layer and the presence of an outer lipid membrane. The gram-negative cell envelope also contains an outer membrane and layer of lipopolysaccharide (LPS). Antibiotics such as β-lactams or glycopeptides, which bind to the bacterial cell wall, will anchor directly to the peptidoglycan layer of the cell. Specifically**,** β-lactams inhibit the last step in peptidoglycan synthesis by acylating the transpeptidase involved in cross-linking peptides to form peptidoglycan. β-lactams specifically target PBPs and consequently interrupt the terminal transpeptidation process. β-lactams affect membrane integrity directly causing alterations in cell wall protein expression levels, ultimately altering cell wall metabolism. Since both gram positive and gram-negative species contain a peptidoglycan layer, the antibiotics are able to bind various bacterial species due to this common attribute in the cell wall. Raja 42 may initially bind both gram positive and negative species causing alterations to the cell membrane, as was observed during the membrane depolarization assay. In aerobic bacteria, the downstream production of lethal ROS levels is a contributing factor to the bactericidal activity of Raja 42. In anaerobic bacteria that lack ROS producing capabilities, it is postulated that downstream damage may occur from dysregulation of Stickland-type fermentation, leading to internal damage as is discussed further herein.

4.6 The combination of Raja 42 and other antibiotics can effectively kill Raja 42-resistant bacteria, although either one alone is not effective

The emergence of multidrug resistant (MDR) bacterial strains is the primary reason of antibiotic therapy failure. Prolonged exposure to a single antibiotic can increase the probability of developing simultaneous resistance to many different classes of antibiotics, leading to the problem of multidrug resistance. Despite the negative clinical impact of MDR microorganisms, they can provide insight into the mechanism of action of antibiotic agents. While the development of Raja 42-resistant *E. coli* K12 helped to establish a MOA model of Raja 42, this posed a new challenge, neededing to be addressed. Therefore, combination therapies were explored to control Raja 42-resistant strains if they eventually emerge in future. The MIC of Raja 42 was used in combination with either the MIC of Clindamycin, Neomycin, Kanamycin, Ampicillin, or Vancomycin against Raja 42-resistant clones (Figure 22). The combinational therapies showed a marked improvement. Neomycin and Kanamycin showed synergistic effects when used in combination with Raja 42, while Clindamycin, Ampicillin and Vancomycin displayed an additive effect under the same conditions. Although in a different setting, Ye and colleagues revealed a novel metabolic mechanism in which the presence of exogenous alanine, glucose and fructose contributed to bacterial cell death through upregulation of ROS generation [273]. They concluded that exogenous alanine was able to reprogram the necessary metabolic pathways in order to upregulate the TCA when used in combination with the aminoglycoside, Kanamycin. They noted dramatic quantifiable increases in ROS production as a result of the combination therapy in the treatment of multidrug resistant *E. tarda*. The potency of the combination therapy may have been due to an increase in specific amino acids or a sugar moiety upon interaction with Raja 42. It is tempted to speculate

that the combination of Raja 42 treatment with the aminoglycosides Kanamycin and Neomycin (which demonstrated synergistic activity) could potentially be the result of proteomic modifications (such as specific redox modifications) to key proteins necessary for metabolic adaptation for the generation of ROS. Combination treatment with Raja 42 may have resulted in increased proteomic changes, such as leading to increased bioavailability of various metabolites which could further be used to enhance the aminoglycoside ROS generation in the cell. This notion may be relevant to previous reports that showed synergistic effects of aminoglycoside when combined with β-lactam antibiotics, in which case the latter mediated the disturbance of the cell wall of gram negative species, facilitating the passage of aminoglycosides into the periplasmic space [267–269]. Antibiotics with structural similarities to β-lactam-and γ-lactam compounds such as Raja 42 may play a beneficial role for causing the synergistic effects.

4.7 Genetic diversity amongst *C. difficile* isolates collected at HSN

Multiplex PCR based methods were used to rapidly identify the genetic phylotype of a collection of *C. difficile* isolates, as previously identified by the Nokhbeh group. The *C. difficile* isolates were grouped into multiple categories according to (i) the presence of various toxins (tcdA, tcdB, tcdT), (ii) the susceptibility profiles to commonly used antibiotics (vancomycin, metronidazole, clindamycin, azithromycin, etc.), and (iii) the dates of collection. The characterization of bacterial strains is an important aspect when treating patients in a clinical setting as they can help identify a proper course of the treatment. The presence or absence of the PaLoc is an important indicator of symptomatic and asymptomatic patients. Identification of PaLoc could avoid putting patients at risk of developing CDI that might happen when broad-spectrum antibiotics are used.-Thus, through

specific selection criteria, the collection of *C. difficile* isolates used in this study represented a phylogenetic composition from patients treated at HSN and varying trends can be accounted for by considering the collection dates. Therefore, the collection was deemed suitable for the testing of Raja 42 efficacy against clinical strains in the community setting.

4.8 Antibiotic susceptibility of *C. difficile* isolates

Antibiotic susceptibility of the *C. difficile* isolates observed by this study may be dependent upon the frequency of prescription of the selected antibiotics at HSN. At HSN, Metronidazole is predominantly the first line of therapy for *C. difficile* and can be found under the commercial name "Flagyl." Flagyl is often administered in the respiratory, oncology and palliative care units. Among the 200 *C. difficile* isolates, 12 (6%) were found to be resistant to metronidazole, six of which were resistant to the maximal dose of 256 µg/mL of Metronidazole. As Metronidazole is the current first line of therapy at HSN, this finding is striking given the implications of the severity of a *C. difficile* infection, as 6% resistant rate is quite high. This result predicts that 6% of patients with *C. difficle* entering into HSN would fail their initial therapy unless there is a preclinical measurement is implemented, thus persistence of the disease in the community. Similarly, from the strains tested against Vancomycin, 9 of 200 isolates (4.5%) were found to be resistant. These findings lead to the conclusion that ≤ 5% of patients treated with Vancomycin for *C. difficile* infection at HSN would result in treatment failure and persistence in the community. These kinds of treatment failures may be preventable, if the genomic or plasmid DNA of *C. difficile* isolated from patients is analyzed to determine appropriate drug prior to treatment.

Although the levels of Metronidazole and Vancomycin resistance in patients with *C. difficile* at HSN are somewhat similar, metronidazole does harbour increased levels of resistance. In line with the Provincial Infectious Diseases Advisory Committee (PIDAC), Metronidazole therapy should be the first line therapy for mild *C. difficile* cases while Vancomycin should be the first line therapy for moderate to severe cases as it is a more potent compound which displays lower levels of acquired resistance. While Metronidazole and Vancomyin resistance rates at HSN are on the lower spectrum, those same resistance rates can greatly vary according to geographic location. According to a pan-European survey, resistance rates to Metronidazole therapy was 5.3% in Iran, while it was 15.6% resistance in China and 18.3% in Israel [270–272]. Metronidazole resistance rates have also seen a steady increase in the United States rising from 3.6% to 13.3% between 2011 and 2017 respectively [280]. Very similarly, *C. difficile* resistance rates to Vancomycin is 8%-17.9% in the United States, suggesting a serious problem for Vancomycin therapy in the future [281]. With the global resistance rate of *C. difficile* to Metronidazole and Vancomycin being so elevated, our data suggest that resistance rates at HSN are significantly less.

In a study conducted by Zar *et al*, they found that the treatment outcomes with Metronidazole treatment was 84%, while the overall rate of cure for CDI patients using Vancomycin was 97% [133]. They attributed the rate of resistance to these therapies as primary determinants for their use in treating mild or severe cases of CDI. It is particularly concerning that both mild case therapy and severe case therapy display similar levels of resistance in patients at HSN. In hospitals with fewer resources (which include hospitals in remoter and under-serviced areas), rather than treating a few individuals with the best care possible targeting the broader population is often a key approach. Through personalized identification of their isolate susceptibility, patients could benefit

from Vancomycin treatment instead of initially receiving Metronidazole and further prolonging their illness and treatment regimen. Unfortunately, this would require rapid isolate susceptibility testing, either in the form of costly E-testing or through specialized Flow-cytometry Assisted Susceptibility Testing (FAST).

4.9 Raja 42 efficacy against *C. difficile*

Of the 200 clinical *C. difficile* isolates tested against Vancomycin and Metronidazole, a collection of 60 representative isolates were curated in order to test Raja 42 efficacy. Isolates with various susceptibility profiles and collection dates were chosen to determine the MIC of Raja 42. Initially using the ATCC 9689 *C. difficile* strain, the MIC of Raja 42 was determined as 4.6 µg/mL within serial dilutions ranging from 600 µg/mL to 1.1 µg/mL. Satellite colonies that appeared were isolated, grown and their new MIC values determined. Using these newly determined MIC values, a serial dilution range from 150 µg/mL to 0.55 µg/mL was selected for the MIC concentration of Raja 42 against 60 representative isolates. The ECOFFinder program developed by EUCAST, is a program, which allows researchers to estimate the appropriate cut-off values using nonlinear regression of expanding subsets. This is the software currently used by EUCAST to establish ECOFF values and is a useful tool for examining pattern distributions. The 95.0% and 97.5% subset ECOFF values for Raja 42 corresponded to 18.75 µg/mL. Thus the epidemiological (S) cutoff corresponded to ≤ 18.75 µg/mL, while anything greater than 18.75 µg/mL was considered (R). From the strains tested with Raja 42, 49 of the 60 isolates (81%) were susceptible to Raja 42. The 11 isolates that showed resistance to Raja 42 may be due to inherent resistance to γ-lactam antibiotics as the clinical isolates have not been previously exposed to Raja 42. As Raja 42 is not

yet being used in the clinical setting, specific strain resistance to this compound could be the result of drug efflux pumps. In previously described studies, the presence of novel efflux pumps, such as CD2068 in *C. difficile*, are key mediators in the inherent resistance mechanism of MDR organisms [282]. The authors show that CD2068, although novel in *C. difficile*, is also found in *E. coli*. It is possible that the efflux pump was acquired through horizontal gene transfer *via* bacterial conjugation allowing it to be expressed in a different bacterial species. This could be a possible mechanism by which certain clinical *C. difficile* isolates, originating from different patients, could have developed an inherent resistance to Raja 42.

In order to determine the efficacy of Raja 42 compared to Metronidazole and Vancomycin, analysis of the clinical isolates susceptibility profiles was carried out. Of the collection of 200 clinical isolates, 21 isolates were resistant to Metronidazole or Vancomycin therapy. 20 of those isolates were found in the collection tested against Raja 42 and 95% of isolates were susceptible to Raja 42 treatment. From a clinical perspective, Raja 42 could prove to be an invaluable resource in the treatment of mild and severe *C. difficile* infections when first line therapies are no longer successful. Raja could be used as an individual therapy or possibly a combination therapy in order to support the efficacy of Vancomycin treatment. If used as a combination therapy in order to treat severe CDI, Raja 42 could help decrease the length of the antibiotic treatment administered to patients, alleviating the potential for MDR organisms to develop. The use of certain antibiotics can cause adverse reactions and side effects with prolonged use; such is the case with Vancomycin. In order to evaluate the overall safety of a drug, a therapeutic index makes use of pharmacokinetics in order to determine whether a drug requires therapeutic monitoring. The TI values are calculated as a ratio of the toxic dose 50 and the effective dose 50. The TI values are calculated from data

collected during patient clinical trials and are dependent on multiple factors and may vary according to patient age, mode of administration, sex and comorbidities. Most antibiotics have a moderate to elevated TI value and therefore do not require therapeutic monitoring. Some antibiotics such as aminoglycosides and Vancomycin have a low therapeutic index value and have been associated with nephrotoxicity (usually reversible) and ototoxicity (often reversible) [283]. Table 1 highlights the calculated TI values for some common antibacterial agents, such as Metronidazole and Vancomycin. In order to determine the potential efficacy of Raja 42 use in a clinical setting, a TI value needs to be calculated. As previously described by Jiang *et al*, in the absence of ED_{50} and TD_{50} values, one can use the toxic concentration of an antimicrobial to use as a surrogate predictor of the TI value [218]. Therefore, the MIC_{50} value of Raja 42 against *C. difficile* was used as well as the GI_{50} value for Raja 42 against the MCF10-A non-tumorigenic breast cells. Since the toxic concentration is usually higher than the IC_{50} value, the TI calculation for Raja 42 represents a speculative value, which may be conservative. The TI value calculated for Raja 42 was of 12.15, falling under the moderate TI category. This would make Raja 42 a competitive compound, as its TI value is greater than Vancomycin (7.45) and relatively similar to that of Clindamycin (14.28).

Based on the data collected, less than 20% of patients treated with Raja 42 at HSN would result in therapy failure. In comparison to both Metronidazole and Vancomycin, Raja 42 could be a competitive novel compound in the treatment of clinical *C. difficile* infections at HSN. With low levels of resistance, and increased sensitivity at the 97.5% ECOFF subset, Raja 42 could be used as an effective novel agent or used as a combinational therapy in treating patients with CDI. Although Raja 42 efficacy was tested on 60 clinical isolates selected for their specific attributes,

Raja 42 would also need to be tested in a non-biased manner. Screening for the susceptibility of *C. difficile* isolates against Raja 42 in clinical practice could easily be performed in 96 well plate serial microdilutions, as there is no E-test available for Raja 42 at this time. Overall data presented here suggest that Raja 42 has the potential to be an effective antimicrobial therapy with limited adverse reactions, making it a competitive novel agent.

4.10 Shedding light on the Raja 42 functional mechanism against *C. difficile* and *H. pylori*

The potential molecular mechanism of Raja 42 has been elucidated in aerobic species, however it remains to be determined for anaerobic bacteria. As Raja 42 is equally effective on both aerobic and anaerobic bacteria, it is possible that Raja 42 does not have a single dominating mechanism. Rather, the effects of Raja 42 could be the result of multiple mechanisms. For example, Raja 42 may dysregulate bacterial metabolism under both aerobic and anaerobic conditions, perhaps in slightly different molecular mechanisms. Raja 42 works at the metabolic level by increasing the generation of ROS, but also acts at the membrane level, as demonstrated by its rapid killing kinetics and membrane depolarization. Raja 42's activity at the membrane level could explain its ability to inhibit anaerobic species, such as *C.* difficile who lack an electron transport chain and do not utilize oxygen in their metabolic processes. While anaerobic species don't make use of the electron transport chain, they do use the citric acid cycle (TCA) and follow Stickland-type amino acid fermentation [284]. Stickland-type metabolism allows the fermentation of amino acids, with the first step yielding the production of NAD+ in order to allow the oxidation and reduction of amino acids to ultimately generate ATP [285]. For *C. difficile* in particular, the Stickland reaction

generates NAD+ in order to prevent the unnecessary formation of NADH and is modulated by Rex, a global redox-sensing regulator that responds to the NAD+/NADH ratio [286]. It has been previously shown that Rex is a key regulator in coordinating the expression of *C. difficile* metabolism and virulence genes [287]. The binding of Rex to its target site is completely inhibited by NADH and so Rex is only an active repressor when NAD+/NADH ratios indicate adequate NAD+ [288].

As Raja 42 has been shown to increase NADH production through the TCA in aerobic species, resulting in generation of ROS, a possible mechanism in anaerobic species may involve a dysregulation in the NAD+/NADH. Based on published literature [284], it is apparent that *C. difficile* goes to various lengths in order to avoid production of NADH, therefore, if the mechanism of Raja 42 in aerobic species involves the upregulation of NADH, this could negatively impact *C. difficile* metabolic functions. As demonstrated in Figure 10, 50 µg/mL Raja 42 exhibited moderate antibacterial activity against *H. pylori*, with an average diameter of inhibition zone of 10 mm. Compared to the diameters in the inhibition of *C. difficile, S. aureus* and *E. coli, H. pylori* has the smallest clearance zone in the presence of Raja 42. It would be of interest to examine the antibacterial activity of Raja 42 in combination with PPI and or with clarithromycin and amoxicillin as most therapies used for the eradication of *H. pylori* rely heavily on those additional compounds.

As a microaerophilic anaerobe, *H. pylori*, requires the presence of oxygen to grow, but requires lower levels of oxygen (typically 2-10% O_2) in order to thrive. As the mechanism of Raja 42 in aerobic bacteria has been identified as taking hold of the metabolic TCA pathway in order to generate ROS, it is possible that the metabolism of *H. pylori* overcompensates, rendering it less

susceptible to Raja 42 compared to *C. difficile*. With the metabolism of *H. pylori* following in part aerobic and anaerobic traits, its bidirectional metabolism can possibly reduce its susceptibility, to some extent, to Raja 42, when compared to organisms that adhere to a strictly aerobic or anaerobic metabolism. Of note, *H. pylori* predominantly reside in the stomach, a highly acidic environment with elevated pH, whereas both *E. coli* and *C. difficile* are characteristic of the intestinal area with a neutral pH. Differences in environmental pH may have an effect on bacterial species physiology and response to ROS metabolism. This could potentially explain Raja 42 increased efficacy towards the *C. difficile* and *E. coli* species.

The findings described in this thesis put forth an elaborated elucidation of the mechanism of Raja 42 as an antibacterial agent. Future studies, specifically looking at anaerobic Stickland reactions and the importance of the Rex modulator of NAD+/NADH in *C. difficile* may give a better understanding of the mechanism of Raja 42 in *C. difficile* and other anaerobic species.

4.11 Concluding remarks and Future directions

The general direction of this thesis was to identify the scope of activity of Raja 42 and to determine its mechanism of action in killing bacteria. The findings from this work helped deduce that Raja 42 is a broad-spectrum antibacterial agent, a highly desirable property in the development of novel antibacterial agents. In addition, Raja 42 is capable of killing multidrug resistant strains when used alone, or in combination with clinically used antibacterial agents. Both synergistic and additive effects have also been seen when Raja 42 is used in combination with aminoglycosides, such as neomycin and kanamycin, or other antibiotics. Therefore, Raja 42 would potentially be an appropriate compound to use when clinically resistant strains need to be dealt with. Raja 42 acts

very rapidly as a bactericidal agent and has been shown to rapidly work at the membrane level. Antibiotics acting at the membrane level most commonly include the β-lactams, glycopeptides and bacitracin classes. These different classes of antibiotics contain compounds capable of acting against gram-positive, gram-negative and a few anaerobic species, working in independent fashions. Despite the broad-spectrum nature of these classes, there are several limitations, which include their suboptimal capability at fighting infection when used as a monotherapy [289]. β-lactams are often incapable of treating severe infections resulting from gram-positive species such as streptococcal as single agents, often necessitating the use of combinational therapy to target both gram-positive and gram-negative bacteria simultaneously.

Raja 42 is a single compound capable of acting against both the gram-positive, gram-negative, aerobic and anaerobic MDR species. The data described in this thesis suggest that Raja 42 is superior to certain clinically used monotherapies that are acting at bacterial membrane, as demonstrated by its ability to kill Vancomycin resistant strains. The estimated TI value of Raja 42 is strong encouragement to warrant further investigation of this novel compound in a clinical model.

The data presented in this thesis also highlight the mechanism by which Raja 42 has a bactericidal effect in gram-negative species. I have also shown the importance of the citric acid cycle and superoxide dismutase in the generation of ROS *via* increased activity in the Fenton reaction. This adds to the previous reports that lethal concentrations of β-lactam antibiotics contribute to antibiotic killing mechanisms, while sub-lethal concentrations confer mutation development and further resistance [290]. By taking hold of the bacteriums metabolic pathways in order to manipulate ROS production, Raja 42 induces RNA damage and membrane depolarization,

ultimately leading to cell death. Given Raja 42's mechanism of lethality utilizing reactive oxygen species, it is important to investigate the impact of ROS release following cellular apoptosis. Kalghatgi and colleagues demonstrated exogenously produced ROS circulating in mice, following bactericidal therapy, to cause mitochondrial dysfunction and damage to mammalian cell membranes [291]. ROS, exogenous to mammalian cells (produced by bacterial lysis) has been reported in certain conditions such as neurodegenerative diseases, diabetes mellitus, cardiovascular and respiratory diseases to name a few [24].

Although it has been demonstrated that Raja 42 impacts the expression levels of TCA element ghrA, the 27 bp deletion identified in the Raja 42-resistant genome occurs slightly upstream to the promoter region of this gene. While the analysis conducted alludes to the possibility that Raja 42 is potentially causing a form of mutagenisis, further experiments to probe the impact of neighbouring genes would be worthwhile. In order to determine the impact on the gene neighbourhood, this system could be modelled in a plasmid and further used to carry out a gel mobility shift assay. By performing this type of experiment, this would allow for the identification of the proteins involved in the regulation of this gene neighbourhood following treatment with Raja 42.

While the mechanism of Raja 42 has been described in aerobic species, it would be desirable to identify its mechanism in anaerobic species. Strictly anaerobic species require the complete absence of oxygen for growth and sporulation, as their internal metabolism lacks the necessary machinery to convert oxygen and exposure to exogenous O_2 levels can lead to bacterial cell death. The identification of Raja 42's mechanism in anaerobic species could greatly increase

our understanding of this novel compound allowing for downstream improvements with specific target sites in mind.

Various assays can be carried out in order to determine the potential mechanism in anaerobic species. Firstly, a biased screening approach can be used, during which the efficacy of Raja 42 treatment on randomized *C. difficile* isolates can be explored. Evaluating the anaerobic metabolism and the ratios of NAD+/NADH could determine alterations in cellular fermentation, which could be causative of downstream cellular functioning. Comparative genomics analysis could allow the determination of a ghrA analogue or sodA protein present in *C. difficile* clinical isolates, which may help elucidate the mechanism in anaerobic species. Work completed by Permpoonpattana and colleagues [90], functionally characterized a set of proteins found on the spore coat of *C. difficile* and identified the presence of the sodA protein. Although the rationale for the presence of a sodA protein on an anaerobic species has yet to be determined, it is postulated that sodA may play an integral role in protecting *C. difficile* against exogenous oxidative stress. As evidenced by previous work, it is possible that sodA plays a role in polymerizing spore coat proteins in the presence of H_2O_2 [292]. Since the mode of action of Raja 42 in aerobic species induces lethal ROS production, the mechanism in anaerobic species could be further elucidated through bacterial genomic sequencing. Determining the induction and inhibition of transcriptional and translational activities in the presence or absence of Raja 42 in an anaerobic bacterial model could also help identify the mechanism in this group.

Secondly, the combination therapy of Raja 42 with Metronidazole and Vancomycin can be explored in order to help determine the mechanism in an anaerobic population. When used in combination, Raja 42 and aminoglycoside antibiotics produce a synergistic effect (

Figure **22**), illustrating the role of combination therapy at overcoming antibiotic resistance. Evaluation of combinational therapy against generated Raja 42-resistant *C. difficile* could prove to be valuable in determining the mechanism in anaerobic species. Although combination therapy of Metronidazole and Vancomycin is less effective than oral Vancomycin alone [293], treatment with Raja 42 has shown to be effective against Vancomycin and Metronidazole resistant *C. difficile* strains. Combination of first line therapies with Raja 42 could prove to be very effective against resistant strains and also narrow down the mechanism against clinical *C. difficile*.

Although data from this work demonstrate the potential mechanism of the novel Raja 42 antibacterial agent, further research, in a clinical model is needed to evaluate Raja 42 as a novel therapy.

Future directions in order to use Raja 42 in a clinical setting would warrant further investigation into the specific mechanism in anaerobic species following Raja 42. Also, determining the therapeutic index values, using the ED50 and TD50 in an animal model would be necessary in order for Raja 42 to be used as a novel therapeutic compound. The knowledge provided by my current work is very useful in the clinical development of a novel broad-spectrum therapy or combination therapy to support existing and failing treatments.

5.0 References

[1] "THE TREASURE CALLED ANTIBIOTICS.," *Ann. Ib. Postgrad. Med.*, vol. 14, no. 56, 2016.

[2] D. Lyddiard, Jones GL, and Greatrex BW, "Keeping it simple: lessons from the golden era of antibiotic discovery," *FEMS Microbiol Lett*, vol. 363, 2016, doi: doi:10.1093/femsle/fnw084.

[3] Lee Ventola C., "The Antibiotic Resistance Crisis: Part 1: Causes and Threats. Pharmacy and Therapeutics," *Pharm. Ther.*, vol. 40, no. 277, 2015.

[4] Julian Davies DD, "Origins and Evolution of Antibiotic Resistance," *Microbiol Mol Biol Rev*, vol. 74, no. 417, 2010.

[5] Ball P, "Quinolone generations: natural history or natural selection?," *J Antimicrob Chemother*, vol. 46, pp. 17–24, 2000.

[6] Coates ARM, Halls G, Hu Y., "Novel classes of antibiotics or more of the same?," *Br J Pharmacol*, vol. 163, pp. 184–194, 2011.

[7] Kmietowicz Z, "Few novel antibiotics in the pipeline, WHO warns.," *BMJ*, vol. 358, 2017.

[8] "Understanding Emerging and Re-emerging Infectious Diseases." NIH Curriculum Supplement Series. National Institutes of Health (US);, 2007.

[9] Petersen MH, Holm MO, Pedersen SS, Lassen AT, Pedersen C., "Incidence and prevalence of hospital-acquired infections in a cohort of patients admitted to medical departments," *Dan Med Bull*, vol. 57, no. 11, p. A4210, 2010.

[10] M. Behnke, S. J. Aghdassi, S. Hansen, L. A. P. Diaz, P. Gastmeier, and B. Piening, "The Prevalence of Nosocomial Infection and Antibiotic Use in German Hospitals," *Dtsch. Aerzteblatt Online*, Dec. 2017, doi: 10.3238/arztebl.2017.0851.

[11] R. Danasekaran, G. Mani, and K. Annadurai, "Prevention of healthcare-associated infections: protecting patients, saving lives," *Int. J. Community Med. Public Health*, vol. 1, no. 1, p. 67, 2014, doi: 10.5455/2394-6040.ijcmph20141114.

[12] M. Haque, M. Sartelli, J. McKimm, and M. B. Abu Bakar, "Health care-associated infections – an overview," *Infect. Drug Resist.*, vol. Volume 11, pp. 2321–2333, Nov. 2018, doi: 10.2147/IDR.S177247.

[13] L. Valiquette, C. N. A. Chakra, and K. B. Laupland, "Financial Impact of Health Care-associated Infections: When Money Talks," *Can. J. Infect. Dis. Med. Microbiol.*, vol. 25, no. 2, pp. 71–74, 2014, doi: 10.1155/2014/279794.

[14] H. A. Khan, F. K. Baig, and R. Mehboob, "Nosocomial infections: Epidemiology, prevention, control and surveillance," *Asian Pac. J. Trop. Biomed.*, vol. 7, no. 5, pp. 478–482, May 2017, doi: 10.1016/j.apjtb.2017.01.019.

[15] J. W. Warren, “Catheter-associated urinary tract infections,” *Int. J. Antimicrob. Agents*, vol. 17, no. 4, pp. 299–303, Apr. 2001, doi: 10.1016/S0924-8579(00)00359-9.

[16] Centers for Disease Control and Prevention (CDC), “Vital signs: central line-associated blood stream infections--United States, 2001, 2008, and 2009.” 2011.

[17] D. J. Anderson, “Surgical Site Infections,” *Infect. Dis. Clin. North Am.*, vol. 25, no. 1, pp. 135–153, Mar. 2011, doi: 10.1016/j.idc.2010.11.004.

[18] D. A. Hufnagel, W. H. Depas, and M. R. Chapman, “The Biology of the Escherichia coli Extracellular Matrix,” *Microbiol. Spectr.*, vol. 3, no. 3, Jun. 2015, doi: 10.1128/microbiolspec.MB-0014-2014.

[19] J. J. Farmer, M. A. Asbury, F. W. Hickman, D. J. Brenner, and THE ENTEROBACTERIACEAE STUDY GROUP, “Enterobacter sakazakii: A New Species of ‘Enterobacteriaceae’ Isolated from Clinical Specimens,” *Int. J. Syst. Bacteriol.*, vol. 31, no. 1, pp. 109–109, Jan. 1981, doi: 10.1099/00207713-31-1-109.

[20] Z. D. Blount, “The unexhausted potential of E. coli,” *eLife*, vol. 4, p. e05826, Mar. 2015, doi: 10.7554/eLife.05826.

[21] T. Conway and P. S. Cohen, “Commensal and Pathogenic Escherichia coli Metabolism in the Gut,” in *Metabolism and Bacterial Pathogenesis*, Conway and Cohen, Eds. American Society of Microbiology, 2015, pp. 343–362.

[22] H. Nikaido and M. Vaara, “Molecular basis of bacterial outer membrane permeability.,” *Microbiol. Rev.*, vol. 49, no. 1, pp. 1–32, 1985, doi: 10.1128/MMBR.49.1.1-32.1985.

[23] P. Plésiat and H. Nikaido, “Outer membranes of Gram-negative bacteria are permeable to steroid probes,” *Mol. Microbiol.*, vol. 6, no. 10, pp. 1323–1333, May 1992, doi: 10.1111/j.1365-2958.1992.tb00853.x.

[24] E. Kessler and M. Safrin, “Synthesis, processing, and transport of Pseudomonas aeruginosa elastase.,” *J. Bacteriol.*, vol. 170, no. 11, pp. 5241–5247, 1988, doi: 10.1128/JB.170.11.5241-5247.1988.

[25] A. J. Dijkstra and W. Keck, “Peptidoglycan as a barrier to transenvelope transport.,” *J. Bacteriol.*, vol. 178, no. 19, pp. 5555–5562, 1996, doi: 10.1128/JB.178.19.5555-5562.1996.

[26] W. Dowhan, “Role of phospholipids in Escherichia coli cell function,” in *Advances in Cellular and Molecular Biology of Membranes and Organelles*, vol. 4, Elsevier, 1995, pp. 189–217.

[27] R. M. Macnab and M. K. Ornston, “Normal-to-curly flagellar transitions and their role in bacterial tumbling. Stabilization of an alternative quaternary structure by mechanical force,” *J. Mol. Biol.*, vol. 112, no. 1, pp. 1–30, May 1977, doi: 10.1016/S0022-2836(77)80153-8.

[28] J. M. Rand, G. C. Gordon, C. R. Mehrer, and B. F. Pfleger, “Genome sequence and analysis of Escherichia coli production strain LS5218,” *Metab. Eng. Commun.*, vol. 5, pp. 78–83, Dec. 2017, doi: 10.1016/j.meteno.2017.10.001.

[29] N. T. Perna, J. D. Glasner, V. Burland, and G. Plunkett, “The Genomes of Escherichia coli K-12 and Pathogenic E. coli,” in *Escherichia Coli*, Elsevier, 2002, pp. 3–53.

[30] H. F. Wertheim *et al.*, “The role of nasal carriage in Staphylococcus aureus infections,” *Lancet Infect. Dis.*, vol. 5, no. 12, pp. 751–762, Dec. 2005, doi: 10.1016/S1473-3099(05)70295-4.

[31] K. B. Laupland *et al.*, “The changing epidemiology of Staphylococcus aureus bloodstream infection: a multinational population-based surveillance study,” *Clin. Microbiol. Infect.*, vol. 19, no. 5, pp. 465–471, May 2013, doi: 10.1111/j.1469-0691.2012.03903.x.

[32] C. Allard *et al.*, “Secular changes in incidence and mortality associated with Staphylococcus aureus bacteraemia in Quebec, Canada, 1991–2005.,” *Clin. Microbiol. Infect.*, vol. 14, no. 5, pp. 421–428, May 2008, doi: 10.1111/j.1469-0691.2008.01965.x.

[33] K. C. Carroll, “Rapid Diagnostics for Methicillin-Resistant Staphylococcus aureus: Current Status,” *Mol. Diagn. Ther.*, vol. 12, no. 1, pp. 15–24, Jan. 2008, doi: 10.1007/BF03256265.

[34] D. E. Voth and J. D. Ballard, “Clostridium difficile Toxins: Mechanism of Action and Role in Disease,” *Clin. Microbiol. Rev.*, vol. 18, no. 2, pp. 247–263, Apr. 2005, doi: 10.1128/CMR.18.2.247-263.2005.

[35] C. Karen C. and B. John G., “Biology of *Clostridium difficile* : Implications for Epidemiology and Diagnosis,” *Annu. Rev. Microbiol.*, vol. 65, no. 1, pp. 501–521, Oct. 2011, doi: 10.1146/annurev-micro-090110-102824.

[36] N. M. Khardori, “Health Care–Associated Clostridium difficile Infection in Adults Admitted to Acute Care Hospitals in Canada: A Canadian Nosocomial Infection Surveillance Program Study,” *Yearb. Med.*, vol. 2009, pp. 137–138, Jan. 2009, doi: 10.1016/S0084-3873(09)79629-4.

[37] L. Heinlen and J. D. Ballard, “Clostridium difficile Infection,” *Am. J. Med. Sci.*, vol. 340, no. 3, pp. 247–252, Sep. 2010, doi: 10.1097/MAJ.0b013e3181e939d8.

[38] E. J. Kuijper, B. Coignard, and P. Tüll, “Emergence of Clostridium difficile-associated disease in North America and Europe,” *Clin. Microbiol. Infect.*, vol. 12, pp. 2–18, 2006, doi: 10.1111/j.1469-0691.2006.01580.x.

[39] J. G. Bartlett, “Clostridium difficile: History of Its Role as an Enteric Pathogen and the Current State of Knowledge About the Organism,” *Clin. Infect. Dis.*, vol. 18, no. Supplement_4, pp. S265–S272, May 1994, doi: 10.1093/clinids/18.Supplement_4.S265.

[40] C. Rodriguez, J. Van Broeck, B. Taminiau, M. Delmée, and G. Daube, “Clostridium difficile infection: Early history, diagnosis and molecular strain typing methods,” *Microb. Pathog.*, vol. 97, pp. 59–78, Aug. 2016, doi: 10.1016/j.micpath.2016.05.018.

[41] J. G. Fox, “The non-H pylori helicobacters: their expanding role in gastrointestinal and systemic diseases,” *Gut*, vol. 50, no. 2, pp. 273–283, Feb. 2002, doi: 10.1136/gut.50.2.273.

[42] International Agency for Research on Cancer., *Schistosomes, Liver Flukes and Helicobacter Pylori.* 1994.

[43] F.-B. Xue, “Association of *H. pylori* infection with gastric carcinoma: A meta analysis,” *World J. Gastroenterol.*, vol. 7, no. 6, p. 801, 2001, doi: 10.3748/wjg.v7.i6.801.

[44] F. Jacob and J. Monod, “Genetic Regulatory Mechanisms in the Synthesis of Proteins,” in *Molecular Biology*, Elsevier, 1989, pp. 82–120.

[45] C. Beloin, A. Roux, and J.-M. Ghigo, “Escherichia coli Biofilms,” in *Bacterial Biofilms*, vol. 322, T. Romeo, Ed. Berlin, Heidelberg: Springer Berlin Heidelberg, 2008, pp. 249–289.

[46] M. A. Savageau, “Escherichia coli Habitats, Cell Types, and Molecular Mechanisms of Gene Control,” *Am. Nat.*, vol. 122, no. 6, pp. 732–744, Dec. 1983, doi: 10.1086/284168.

[47] L. R. Hoffman *et al.*, “Escherichia coli Dysbiosis Correlates With Gastrointestinal Dysfunction in Children With Cystic Fibrosis,” *Clin. Infect. Dis.*, vol. 58, no. 3, pp. 396–399, Feb. 2014, doi: 10.1093/cid/cit715.

[48] P. M. Griffin and R. V. Tauxe, “The Epidemiology of Infections Caused by Escherichia coli O157: H7, Other Enterohemorrhagic E. coli, and the Associated Hemolytic Uremic Syndrome,” *Epidemiol. Rev.*, vol. 13, no. 1, pp. 60–98, 1991, doi: 10.1093/oxfordjournals.epirev.a036079.

[49] E. Scallan *et al.*, “Foodborne Illness Acquired in the United States—Major Pathogens,” *Emerg. Infect. Dis.*, vol. 17, no. 1, pp. 7–15, Jan. 2011, doi: 10.3201/eid1701.P11101.

[50] J. W. Foster, “Escherichia coli acid resistance: tales of an amateur acidophile,” *Nat. Rev. Microbiol.*, vol. 2, no. 11, pp. 898–907, Nov. 2004, doi: 10.1038/nrmicro1021.

[51] Torres AG, Kaper JB, “Pathogenicity islands of intestinal E. coli.,” *Curr Top Microbiol Immunol*, vol. 265, no. 1, pp. 31–48, 2002.

[52] J. C. Paton and A. W. Paton, “Pathogenesis and diagnosis of Shiga toxin-producing Escherichia coli infections,” *Clin. Microbiol. Rev.*, vol. 11, no. 3, pp. 450–479, Jul. 1998.

[53] J. P. Nataro and J. B. Kaper, “Diarrheagenic Escherichia coli,” *Clin. Microbiol. Rev.*, vol. 11, no. 1, pp. 142–201, Jan. 1998, doi: 10.1128/CMR.11.1.142.

[54] K. G. Campellone, “Cytoskeleton-modulating effectors of enteropathogenic and enterohaemorrhagic Escherichia coli: Tir, EspFU and actin pedestal assembly: Regulation of

actin assembly by Tir and EspFU," *FEBS J.*, vol. 277, no. 11, pp. 2390–2402, Jun. 2010, doi: 10.1111/j.1742-4658.2010.07653.x.

[55] A. G. Torres *et al.*, "Identification and Characterization of lpfABCC'DE, a Fimbrial Operon of Enterohemorrhagic Escherichia coli O157:H7," *Infect. Immun.*, vol. 70, no. 10, pp. 5416–5427, Oct. 2002, doi: 10.1128/IAI.70.10.5416-5427.2002.

[56] J. Xicohtencatl-Cortes *et al.*, "Intestinal adherence associated with type IV pili of enterohemorrhagic Escherichia coli O157:H7," *J. Clin. Invest.*, vol. 117, no. 11, pp. 3519–3529, Nov. 2007, doi: 10.1172/JCI30727.

[57] S. Cooper and C. E. Helmstetter, "Chromosome replication and the division cycle of Escherichia coli," *J. Mol. Biol.*, vol. 31, no. 3, pp. 519–540, Feb. 1968, doi: 10.1016/0022-2836(68)90425-7.

[58] W. D. Donachie, "Relationship between Cell Size and Time of Initiation of DNA Replication," *Nature*, vol. 219, no. 5158, pp. 1077–1079, Sep. 1968, doi: 10.1038/2191077a0.

[59] S. Poston, "Methicillin-Resistant Staphylococcus aureus. Clinical Management and Laboratory Aspects: Edited by MARY T. CAFFERKEY. 1992. Marcel Dekker, New York. Pp. 202. 89.75.," *J. Med. Microbiol.*, vol. 38, no. 6, pp. 459–459, Jun. 1993, doi: 10.1099/00222615-38-6-459.

[60] R. J. Stenstrom, "The Risk of Methicillin-resistant Staphylococcus aureus (MRSA) Infection Based on Previous MRSA Colonization in Emergency Department Patients," *Acad. Emerg. Med.*, vol. 13, no. 5Supplement 1, pp. S144–S144, May 2006, doi: 10.1197/j.aem.2006.03.309.

[61] S. H. Cohen *et al.*, "Clinical Practice Guidelines for Clostridium difficile Infection in Adults: 2010 Update by the Society for Healthcare Epidemiology of America (SHEA) and the Infectious Diseases Society of America (IDSA)," *Infect. Control Hosp. Epidemiol.*, vol. 31, no. 05, pp. 431–455, May 2010, doi: 10.1086/651706.

[62] E. G. Semenyuk *et al.*, "Analysis of Bacterial Communities during Clostridium difficile Infection in the Mouse," *Infect. Immun.*, vol. 83, no. 11, pp. 4383–4391, Nov. 2015, doi: 10.1128/IAI.00145-15.

[63] V. C. Antharam *et al.*, "Intestinal Dysbiosis and Depletion of Butyrogenic Bacteria in Clostridium difficile Infection and Nosocomial Diarrhea," *J. Clin. Microbiol.*, vol. 51, no. 9, pp. 2884–2892, Sep. 2013, doi: 10.1128/JCM.00845-13.

[64] M. B. Francis, C. A. Allen, R. Shrestha, and J. A. Sorg, "Bile Acid Recognition by the Clostridium difficile Germinant Receptor, CspC, Is Important for Establishing Infection," *PLoS Pathog.*, vol. 9, no. 5, p. e1003356, May 2013, doi: 10.1371/journal.ppat.1003356.

[65] S. P. Sambol, M. M. Merrigan, J. K. Tang, S. Johnson, and D. N. Gerding, “Colonization for the Prevention of *Clostridium difficile* Disease in Hamsters,” *J. Infect. Dis.*, vol. 186, no. 12, pp. 1781–1789, Dec. 2002, doi: 10.1086/345676.

[66] S. Pechine, C. Janoir, and A. Collignon, “Variability of Clostridium difficile Surface Proteins and Specific Serum Antibody Response in Patients with Clostridium difficile-Associated Disease,” *J. Clin. Microbiol.*, vol. 43, no. 10, pp. 5018–5025, Oct. 2005, doi: 10.1128/JCM.43.10.5018-5025.2005.

[67] S. Di Bella, P. Ascenzi, S. Siarakas, N. Petrosillo, and A. di Masi, “Clostridium difficile Toxins A and B: Insights into Pathogenic Properties and Extraintestinal Effects,” *Toxins*, vol. 8, no. 5, p. 134, May 2016, doi: 10.3390/toxins8050134.

[68] R. J. Carman, A. L. Stevens, M. W. Lyerly, M. F. Hiltonsmith, B. G. Stiles, and T. D. Wilkins, “Clostridium difficile binary toxin (CDT) and diarrhea,” *Anaerobe*, vol. 17, no. 4, pp. 161–165, Aug. 2011, doi: 10.1016/j.anaerobe.2011.02.005.

[69] K. Aktories, C. Schwan, and T. Jank, “*Clostridium difficile* Toxin Biology,” *Annu. Rev. Microbiol.*, vol. 71, no. 1, pp. 281–307, Sep. 2017, doi: 10.1146/annurev-micro-090816-093458.

[70] M. Rupnik and S. Janezic, “An Update on Clostridium difficile Toxinotyping,” *J. Clin. Microbiol.*, vol. 54, no. 1, pp. 13–18, Jan. 2016, doi: 10.1128/JCM.02083-15.

[71] G. Triadafilopoulos, C. Pothoulakis, M. J. O’Brien, and J. T. LaMont, “Differential effects of Clostridium difficile toxins A and B on rabbit ileum,” *Gastroenterology*, vol. 93, no. 2, pp. 273–279, Aug. 1987, doi: 10.1016/0016-5085(87)91014-6.

[72] M. Riegler *et al.*, “Clostridium difficile toxin B is more potent than toxin A in damaging human colonic epithelium in vitro.,” *J. Clin. Invest.*, vol. 95, no. 5, pp. 2004–2011, May 1995, doi: 10.1172/JCI117885.

[73] G. A. Hammond and J. L. Johnson, “The toxigenic element of Clostridium difficile strain VPI 10463,” *Microb. Pathog.*, vol. 19, no. 4, pp. 203–213, Oct. 1995, doi: 10.1016/S0882-4010(95)90263-5.

[74] S. Matamouros, P. England, and B. Dupuy, “Clostridium difficile toxin expression is inhibited by the novel regulator TcdC: TcdC inhibits C. difficile toxin expression,” *Mol. Microbiol.*, vol. 64, no. 5, pp. 1274–1288, May 2007, doi: 10.1111/j.1365-2958.2007.05739.x.

[75] N. Mani and B. Dupuy, “Regulation of toxin synthesis in Clostridium difficile by an alternative RNA polymerase sigma factor,” *Proc. Natl. Acad. Sci.*, vol. 98, no. 10, pp. 5844–5849, May 2001, doi: 10.1073/pnas.101126598.

[76] R. Govind and B. Dupuy, “Secretion of Clostridium difficile Toxins A and B Requires the Holin-like Protein TcdE,” *PLoS Pathog.*, vol. 8, no. 6, p. e1002727, Jun. 2012, doi: 10.1371/journal.ppat.1002727.

[77] L. Bouillaut, T. Dubois, A. L. Sonenshein, and B. Dupuy, “Integration of metabolism and virulence in Clostridium difficile,” *Res. Microbiol.*, vol. 166, no. 4, pp. 375–383, May 2015, doi: 10.1016/j.resmic.2014.10.002.

[78] M. Monot *et al.*, “Clostridium difficile: New Insights into the Evolution of the Pathogenicity Locus,” *Sci. Rep.*, vol. 5, no. 1, p. 15023, Dec. 2015, doi: 10.1038/srep15023.

[79] R. A. Stabler *et al.*, “Comparative Phylogenomics of Clostridium difficile Reveals Clade Specificity and Microevolution of Hypervirulent Strains,” *J. Bacteriol.*, vol. 188, no. 20, pp. 7297–7305, Oct. 2006, doi: 10.1128/JB.00664-06.

[80] K. E. Dingle *et al.*, “Evolutionary History of the Clostridium difficile Pathogenicity Locus,” *Genome Biol. Evol.*, vol. 6, no. 1, pp. 36–52, Jan. 2014, doi: 10.1093/gbe/evt204.

[81] J. G. S. Ho, A. Greco, M. Rupnik, and K. K.-S. Ng, “Crystal structure of receptor-binding C-terminal repeats from Clostridium difficile toxin A,” *Proc. Natl. Acad. Sci.*, vol. 102, no. 51, pp. 18373–18378, Dec. 2005, doi: 10.1073/pnas.0506391102.

[82] D. J. Reinert, T. Jank, K. Aktories, and G. E. Schulz, “Structural Basis for the Function of Clostridium difficile Toxin B,” *J. Mol. Biol.*, vol. 351, no. 5, pp. 973–981, Sep. 2005, doi: 10.1016/j.jmb.2005.06.071.

[83] M. O. P. Ziegler, T. Jank, K. Aktories, and G. E. Schulz, “Conformational Changes and Reaction of Clostridial Glycosylating Toxins,” *J. Mol. Biol.*, vol. 377, no. 5, pp. 1346–1356, Apr. 2008, doi: 10.1016/j.jmb.2007.12.065.

[84] D. Higgins and J. Dworkin, “Recent progress in *Bacillus subtilis* sporulation,” *FEMS Microbiol. Rev.*, vol. 36, no. 1, pp. 131–148, Jan. 2012, doi: 10.1111/j.1574-6976.2011.00310.x.

[85] E. Steiner *et al.*, “Multiple orphan histidine kinases interact directly with Spo0A to control the initiation of endospore formation in Clostridium acetobutylicum: Sporulation initiation in clostridia,” *Mol. Microbiol.*, vol. 80, no. 3, pp. 641–654, May 2011, doi: 10.1111/j.1365-2958.2011.07608.x.

[86] M. J. L. de Hoon, P. Eichenberger, and D. Vitkup, “Hierarchical Evolution of the Bacterial Sporulation Network,” *Curr. Biol.*, vol. 20, no. 17, pp. R735–R745, Sep. 2010, doi: 10.1016/j.cub.2010.06.031.

[87] F. C. Pereira *et al.*, “The Spore Differentiation Pathway in the Enteric Pathogen Clostridium difficile,” *PLoS Genet.*, vol. 9, no. 10, p. e1003782, Oct. 2013, doi: 10.1371/journal.pgen.1003782.

[88] J. D. Haraldsen and A. L. Sonenshein, “Efficient sporulation in Clostridium difficile requires disruption of the σK gene: Gene disruption essential for sporulation,” *Mol. Microbiol.*, vol. 48, no. 3, pp. 811–821, Apr. 2003, doi: 10.1046/j.1365-2958.2003.03471.x.

[89] L. Saujet *et al.*, “Genome-Wide Analysis of Cell Type-Specific Gene Transcription during Spore Formation in Clostridium difficile,” *PLoS Genet.*, vol. 9, no. 10, p. e1003756, Oct. 2013, doi: 10.1371/journal.pgen.1003756.

[90] P. Permpoonpattana, E. H. Tolls, R. Nadem, S. Tan, A. Brisson, and S. M. Cutting, “Surface Layers of Clostridium difficile Endospores,” *J. Bacteriol.*, vol. 193, no. 23, pp. 6461–6470, Dec. 2011, doi: 10.1128/JB.05182-11.

[91] P. Setlow, “I will survive: DNA protection in bacterial spores,” *Trends Microbiol.*, vol. 15, no. 4, pp. 172–180, Apr. 2007, doi: 10.1016/j.tim.2007.02.004.

[92] A. E. Cowan, E. M. Olivastro, D. E. Koppel, C. A. Loshon, B. Setlow, and P. Setlow, “Lipids in the inner membrane of dormant spores of Bacillus species are largely immobile,” *Proc. Natl. Acad. Sci.*, vol. 101, no. 20, pp. 7733–7738, May 2004, doi: 10.1073/pnas.0306859101.

[93] D. Paredes-Sabja and M. R. Sarker, “Germination response of spores of the pathogenic bacterium Clostridium perfringens and Clostridium difficile to cultured human epithelial cells,” *Anaerobe*, vol. 17, no. 2, pp. 78–84, Apr. 2011, doi: 10.1016/j.anaerobe.2011.02.001.

[94] A. O. Henriques and C. P. Moran, Jr., “Structure, Assembly, and Function of the Spore Surface Layers,” *Annu. Rev. Microbiol.*, vol. 61, no. 1, pp. 555–588, Oct. 2007, doi: 10.1146/annurev.micro.61.080706.093224.

[95] A. Howerton, M. Patra, and E. Abel-Santos, “A New Strategy for the Prevention of Clostridium difficile Infection,” *J. Infect. Dis.*, vol. 207, no. 10, pp. 1498–1504, May 2013, doi: 10.1093/infdis/jit068.

[96] D. Paredes-Sabja, P. Setlow, and M. R. Sarker, “Germination of spores of Bacillales and Clostridiales species: mechanisms and proteins involved,” *Trends Microbiol.*, vol. 19, no. 2, pp. 85–94, Feb. 2011, doi: 10.1016/j.tim.2010.10.004.

[97] J. A. Sorg and A. L. Sonenshein, “Bile Salts and Glycine as Cogerminants for Clostridium difficile Spores,” *J. Bacteriol.*, vol. 190, no. 7, pp. 2505–2512, Apr. 2008, doi: 10.1128/JB.01765-07.

[98] L. V. McFarland, M. E. Mulligan, R. Y. Y. Kwok, and W. E. Stamm, “Nosocomial Acquisition of *Clostridium difficile* Infection,” *N. Engl. J. Med.*, vol. 320, no. 4, pp. 204–210, Jan. 1989, doi: 10.1056/NEJM198901263200402.

[99] S. S. Johal, “Clostridium difficile associated diarrhoea in hospitalised patients: onset in the community and hospital and role of flexible sigmoidoscopy,” *Gut*, vol. 53, no. 5, pp. 673–677, May 2004, doi: 10.1136/gut.2003.028803.

[100] C. A. Muto *et al.*, “A Large Outbreak of *Clostridium difficile* –Associated Disease with an Unexpected Proportion of Deaths and Colectomies at a Teaching Hospital Following Increased Fluoroquinolone Use,” *Infect. Control Hosp. Epidemiol.*, vol. 26, no. 3, pp. 273–280, Mar. 2005, doi: 10.1086/502539.

[101] L. C. McDonald *et al.*, “Clinical Practice Guidelines for Clostridium difficile Infection in Adults and Children: 2017 Update by the Infectious Diseases Society of America (IDSA) and Society for Healthcare Epidemiology of America (SHEA),” *Clin. Infect. Dis.*, vol. 66, no. 7, pp. e1–e48, Mar. 2018, doi: 10.1093/cid/cix1085.

[102] M. M. Riggs, A. K. Sethi, T. F. Zabarsky, E. C. Eckstein, R. L. P. Jump, and C. J. Donskey, “Asymptomatic Carriers Are a Potential Source for Transmission of Epidemic and Nonepidemic Clostridium difficile Strains among Long-Term Care Facility Residents,” *Clin. Infect. Dis.*, vol. 45, no. 8, pp. 992–998, Oct. 2007, doi: 10.1086/521854.

[103] N. Bagdasarian, K. Rao, and P. N. Malani, “Diagnosis and Treatment of *Clostridium difficile* in Adults: A Systematic Review,” *JAMA*, vol. 313, no. 4, p. 398, Jan. 2015, doi: 10.1001/jama.2014.17103.

[104] D. M. Dumford, M. M. Nerandzic, B. C. Eckstein, and C. J. Donskey, “What is on that keyboard? Detecting hidden environmental reservoirs of Clostridium difficile during an outbreak associated with North American pulsed-field gel electrophoresis type 1 strains,” *Am. J. Infect. Control*, vol. 37, no. 1, pp. 15–19, Feb. 2009, doi: 10.1016/j.ajic.2008.07.009.

[105] Katsuhiko. Amimoto, Taichi. Noro, Eiji. Oishi, and Mitsugu. Shimizu, “A novel toxin homologous to large clostridial cytotoxins found in culture supernatant of Clostridium perfringens type C,” *Microbiology*, vol. 153, no. 4, pp. 1198–1206, Apr. 2007, doi: 10.1099/mic.0.2006/002287-0.

[106] J. G. Bartlett and D. N. Gerding, “Clinical Recognition and Diagnosis of *Clostridium difficile* Infection,” *Clin. Infect. Dis.*, vol. 46, no. s1, pp. S12–S18, Jan. 2008, doi: 10.1086/521863.

[107] B. E. Dunn, G. P. Campbell, G. I. Perez-Perez, and M. J. Blaser, “Purification and characterization of urease from Helicobacter pylori,” *J. Biol. Chem.*, vol. 265, no. 16, pp. 9464–9469, Jun. 1990.

[108] G. Geis, S. Suerbaum, B. Forsthoff, H. Leying, and W. Opferkuch, “Ultrastructure and biochemical studies of the flagellar sheath of Helicobacter pylori,” *J. Med. Microbiol.*, vol. 38, no. 5, pp. 371–377, May 1993, doi: 10.1099/00222615-38-5-371.

[109] B. A. Rader, S. R. Campagna, M. F. Semmelhack, B. L. Bassler, and K. Guillemin, “The Quorum-Sensing Molecule Autoinducer 2 Regulates Motility and Flagellar Morphogenesis in Helicobacter pylori,” *J. Bacteriol.*, vol. 189, no. 17, pp. 6109–6117, Sep. 2007, doi: 10.1128/JB.00246-07.

[110] J. P. Celli *et al.*, “Rheology of Gastric Mucin Exhibits a pH-Dependent Sol−Gel Transition,” *Biomacromolecules*, vol. 8, no. 5, pp. 1580–1586, May 2007, doi: 10.1021/bm0609691.

[111] G. R. Van den Brink, “H pylori colocalises with MUC5AC in the human stomach,” *Gut*, vol. 46, no. 5, pp. 601–607, May 2000, doi: 10.1136/gut.46.5.601.

[112] S. K. Lindén *et al.*, “MUC1 Limits Helicobacter pylori Infection both by Steric Hindrance and by Acting as a Releasable Decoy,” *PLoS Pathog.*, vol. 5, no. 10, p. e1000617, Oct. 2009, doi: 10.1371/journal.ppat.1000617.

[113] M. Aspholm *et al.*, “SabA Is the H. pylori Hemagglutinin and Is Polymorphic in Binding to Sialylated Glycans,” *PLoS Pathog.*, vol. 2, no. 10, p. e110, Oct. 2006, doi: 10.1371/journal.ppat.0020110.

[114] M. Unemo *et al.*, “The Sialic Acid Binding SabA Adhesin of *Helicobacter pylori* Is Essential for Nonopsonic Activation of Human Neutrophils,” *J. Biol. Chem.*, vol. 280, no. 15, pp. 15390–15397, Apr. 2005, doi: 10.1074/jbc.M412725200.

[115] H. Von Döhren, “Antibiotics: Actions, origins, resistance, by C. Walsh. 2003. Washington, DC: ASM Press. 345 pp. $99.95 (hardcover).,” *Protein Sci.*, vol. 13, no. 11, pp. 3059–3060, Jan. 2009, doi: 10.1110/ps.041032204.

[116] A. J. Long, I. J. Clifton, P. L. Roach, J. E. Baldwin, P. J. Rutledge, and C. J. Schofield, “Structural Studies on the Reaction of Isopenicillin N Synthase with the Truncated Substrate Analogues δ-(L -α-aminoadipoyl)- L -cysteinyl-glycine and δ-(L -α-aminoadipoyl)- L -cysteinyl- D -alanine † , ‡,” *Biochemistry*, vol. 44, no. 17, pp. 6619–6628, May 2005, doi: 10.1021/bi047478q.

[117] J. C. Sheehan, “THE CHEMISTRY OF SYNTHETIC AND SEMISYNTHETIC PENICILLINS,” *Ann. N. Y. Acad. Sci.*, vol. 145, no. 2 Comparative A, pp. 216–223, Sep. 1967, doi: 10.1111/j.1749-6632.1967.tb50220.x.

[118] S. N. Maiti, O. A. Phillips, R. G. Micetich, and D. M. Livermore, “ChemInform Abstract: β-Lactamase Inhibitors: Agents to Overcome Bacterial Resistance,” *ChemInform*, vol. 30, no. 11, p. no-no, Jun. 2010, doi: 10.1002/chin.199911343.

[119] P. N. Bennett and M. J. Brown, “Clinical pharmacology,” in *Clinical Pharmacology*, Elsevier, 2008, pp. 3–4.

[120] J. Velasco, J. Luis Adrio, M. Ángel Moreno, B. Díez, G. Soler, and J. Luis Barredo, “Environmentally safe production of 7-aminodeacetoxycephalosporanic acid (7-ADCA) using recombinant strains of Acremonium chrysogenum,” *Nat. Biotechnol.*, vol. 18, no. 8, pp. 857–861, Aug. 2000, doi: 10.1038/78467.

[121] M. G. Page, “Emerging cephalosporins,” *Expert Opin. Emerg. Drugs*, vol. 12, no. 4, pp. 511–524, Nov. 2007, doi: 10.1517/14728214.12.4.511.

[122] J. A. Paladino, J. L. Sunderlin, M. E. Singer, M. H. Adelman, and J. J. Schentag, “Influence of extended-spectrum β-lactams on gram-negative bacterial resistance,” *Am. J. Health. Syst. Pharm.*, vol. 65, no. 12, pp. 1154–1159, Jun. 2008, doi: 10.2146/ajhp070435.

[123] W. A. Parker, “Book Review: Gaddum’s Pharmacology, 9th Ed,” *Drug Intell. Clin. Pharm.*, vol. 20, no. 12, pp. 993–993, Dec. 1986, doi: 10.1177/106002808602001226.

[124] G. S. Singh, “β-Lactams in the New Millennium. Part 1. Monobactams and Carbapenems,” *ChemInform*, vol. 35, no. 29, Jul. 2004, doi: 10.1002/chin.200429275.

[125] R. L. Charnas, J. Fisher, and J. R. Knowles, “Chemical studies on the inactivation of Escherichia coli RTEM β-lactamase by clavulanic acid,” *Biochemistry*, vol. 17, no. 11, pp. 2185–2189, May 1978, doi: 10.1021/bi00604a025.

[126] I. Rizwi, A. K. Tan, A. L. Fink, and R. Virden, “Clavulanate inactivation of Staphylococcus aureus β-lactamase,” *Biochem. J.*, vol. 258, no. 1, pp. 205–209, Feb. 1989, doi: 10.1042/bj2580205.

[127] A. R. English, J. A. Retsema, A. E. Girard, J. E. Lynch, and W. E. Barth, “CP-45,899, a Beta-Lactamase Inhibitor That Extends the Antibacterial Spectrum of Beta-Lactams: Initial Bacteriological Characterization,” *Antimicrob. Agents Chemother.*, vol. 14, no. 3, pp. 414–419, Sep. 1978, doi: 10.1128/AAC.14.3.414.

[128] C. Liu *et al.*, “Clinical Practice Guidelines by the Infectious Diseases Society of America for the Treatment of Methicillin-Resistant Staphylococcus aureus Infections in Adults and Children: Executive Summary,” *Clin. Infect. Dis.*, vol. 52, no. 3, pp. 285–292, Feb. 2011, doi: 10.1093/cid/cir034.

[129] T. L. Holland, C. Arnold, and V. G. Fowler, “Clinical Management of *Staphylococcus aureus* Bacteremia: A Review,” *JAMA*, vol. 312, no. 13, p. 1330, Oct. 2014, doi: 10.1001/jama.2014.9743.

[130] A. F. Brown, J. M. Leech, T. R. Rogers, and R. M. McLoughlin, “Staphylococcus aureus Colonization: Modulation of Host Immune Response and Impact on Human Vaccine Design,” *Front. Immunol.*, vol. 4, 2014, doi: 10.3389/fimmu.2013.00507.

[131] D. A. Leffler and J. T. Lamont, “Treatment of Clostridium difficile-Associated Disease,” *Gastroenterology*, vol. 136, no. 6, pp. 1899–1912, May 2009, doi: 10.1053/j.gastro.2008.12.070.

[132] D. M. Musher *et al.*, “Relatively Poor Outcome after Treatment of Clostridium difficile Colitis with Metronidazole,” *Clin. Infect. Dis.*, vol. 40, no. 11, pp. 1586–1590, Jun. 2005, doi: 10.1086/430311.

[133] F. A. Zar, S. R. Bakkanagari, K. M. L. S. T. Moorthi, and M. B. Davis, “A Comparison of Vancomycin and Metronidazole for the Treatment of Clostridium difficile-Associated Diarrhea, Stratified by Disease Severity,” *Clin. Infect. Dis.*, vol. 45, no. 3, pp. 302–307, Aug. 2007, doi: 10.1086/519265.

[134] D. N. Gerding, C. A. Muto, and R. C. Owens, Jr., “Treatment of *Clostridium difficile* Infection,” *Clin. Infect. Dis.*, vol. 46, no. s1, pp. S32–S42, Jan. 2008, doi: 10.1086/521860.

[135] C. M. Surawicz *et al.*, “Guidelines for Diagnosis, Treatment, and Prevention of Clostridium difficile Infections:,” *Am. J. Gastroenterol.*, vol. 108, no. 4, pp. 478–498, Apr. 2013, doi: 10.1038/ajg.2013.4.

[136] O. Rotimi, “Histological identification of Helicobacter pylori: comparison of staining methods,” *J. Clin. Pathol.*, vol. 53, no. 10, pp. 756–759, Oct. 2000, doi: 10.1136/jcp.53.10.756.

[137] A. Ruzsovics, B. Molnar, and Z. Tulassay, “Deoxyribonucleic acid-based diagnostic techniques to detect Helicobacter pylori,” *Aliment. Pharmacol. Ther.*, vol. 19, no. 11, pp. 1137–1146, Jun. 2004, doi: 10.1111/j.1365-2036.2004.01934.x.

[138] L. Gatta *et al.*, “Effect of Proton Pump Inhibitors and Antacid Therapy on 13C Urea Breath Tests and Stool Test for Helicobacter Pylori Infection,” *Am. J. Gastroenterol.*, vol. 99, no. 5, pp. 823–829, May 2004, doi: 10.1111/j.1572-0241.2004.30162.x.

[139] W. D. Chey, G. I. Leontiadis, C. W. Howden, and S. F. Moss, “ACG Clinical Guideline: Treatment of Helicobacter pylori Infection:,” *Am. J. Gastroenterol.*, vol. 112, no. 2, pp. 212–239, Feb. 2017, doi: 10.1038/ajg.2016.563.

[140] H.-J. Ma, “Quadruple therapy for eradication of *Helicobacter pylori*,” *World J. Gastroenterol.*, vol. 19, no. 6, p. 931, 2013, doi: 10.3748/wjg.v19.i6.931.

[141] J. A. Salcedo and F. Al-Kawas, “Treatment of Helicobacter pylori Infection,” *Arch. Intern. Med.*, vol. 158, no. 8, p. 842, Apr. 1998, doi: 10.1001/archinte.158.8.842.

[142] C. C. Winterbourn, “The Biological Chemistry of Hydrogen Peroxide,” in *Methods in Enzymology*, vol. 528, Elsevier, 2013, pp. 3–25.

[143] J. Cadet and J. R. Wagner, “DNA Base Damage by Reactive Oxygen Species, Oxidizing Agents, and UV Radiation,” *Cold Spring Harb. Perspect. Biol.*, vol. 5, no. 2, pp. a012559–a012559, Feb. 2013, doi: 10.1101/cshperspect.a012559.

[144] R. Whittenbury, “Hydrogen Peroxide Formation and Catalase Activity in the Lactic Acid Bacteria,” *J. Gen. Microbiol.*, vol. 35, no. 1, pp. 13–26, Apr. 1964, doi: 10.1099/00221287-35-1-13.

[145] L. C. Seaver and J. A. Imlay, “Are Respiratory Enzymes the Primary Sources of Intracellular Hydrogen Peroxide?,” *J. Biol. Chem.*, vol. 279, no. 47, pp. 48742–48750, Nov. 2004, doi: 10.1074/jbc.M408754200.

[146] J. A. Imlay, “Transcription Factors That Defend Bacteria Against Reactive Oxygen Species,” *Annu. Rev. Microbiol.*, vol. 69, no. 1, pp. 93–108, Oct. 2015, doi: 10.1146/annurev-micro-091014-104322.

[147] M. Gu and J. A. Imlay, “The SoxRS response of Escherichia coli is directly activated by redox-cycling drugs rather than by superoxide: Redox-cycling drugs directly activate SoxR,” *Mol. Microbiol.*, vol. 79, no. 5, pp. 1136–1150, Mar. 2011, doi: 10.1111/j.1365-2958.2010.07520.x.

[148] J. A. Imlay, “Cellular Defenses against Superoxide and Hydrogen Peroxide,” *Annu. Rev. Biochem.*, vol. 77, no. 1, pp. 755–776, Jun. 2008, doi: 10.1146/annurev.biochem.77.061606.161055.

[149] M. Gu and J. A. Imlay, “Superoxide poisons mononuclear iron enzymes by causing mismetallation: Superoxide poisons mononuclear iron enzymes,” *Mol. Microbiol.*, vol. 89, no. 1, pp. 123–134, Jul. 2013, doi: 10.1111/mmi.12263.

[150] K. Keyer and J. A. Imlay, “Superoxide accelerates DNA damage by elevating free-iron levels,” *Proc. Natl. Acad. Sci.*, vol. 93, no. 24, pp. 13635–13640, Nov. 1996, doi: 10.1073/pnas.93.24.13635.

[151] J. M. McCord, B. B. Keele, and I. Fridovich, “An Enzyme-Based Theory of Obligate Anaerobiosis: The Physiological Function of Superoxide Dismutase,” *Proc. Natl. Acad. Sci.*, vol. 68, no. 5, pp. 1024–1027, May 1971, doi: 10.1073/pnas.68.5.1024.

[152] C. C. Winterbourn, “Reconciling the chemistry and biology of reactive oxygen species,” *Nat. Chem. Biol.*, vol. 4, no. 5, pp. 278–286, May 2008, doi: 10.1038/nchembio.85.

[153] A. Hall, K. Nelson, L. B. Poole, and P. A. Karplus, “Structure-based Insights into the Catalytic Power and Conformational Dexterity of Peroxiredoxins,” *Antioxid. Redox Signal.*, vol. 15, no. 3, pp. 795–815, Aug. 2011, doi: 10.1089/ars.2010.3624.

[154] Z. A. Wood, “Peroxiredoxin Evolution and the Regulation of Hydrogen Peroxide Signaling,” *Science*, vol. 300, no. 5619, pp. 650–653, Apr. 2003, doi: 10.1126/science.1080405.

[155] H. Sies, “Oxidative stress: oxidants and antioxidants,” *Exp. Physiol.*, vol. 82, no. 2, pp. 291–295, Mar. 1997, doi: 10.1113/expphysiol.1997.sp004024.

[156] E. Hidalgo and B. Demple, “Adaptive responses to Oxidative Stress: The soxRS and oxyR Regulons,” in *Regulation of Gene Expression in Escherichia coli*, Boston, MA: Springer US, 1996, pp. 435–452.

[157] D. A. Leffler and J. T. Lamont, “*Clostridium difficile* Infection,” *N. Engl. J. Med.*, vol. 372, no. 16, pp. 1539–1548, Apr. 2015, doi: 10.1056/NEJMra1403772.

[158] P. Johanesen *et al.*, “Disruption of the Gut Microbiome: Clostridium difficile Infection and the Threat of Antibiotic Resistance,” *Genes*, vol. 6, no. 4, pp. 1347–1360, Dec. 2015, doi: 10.3390/genes6041347.

[159] P. Spigaglia, “Recent advances in the understanding of antibiotic resistance in *Clostridium difficile* infection,” *Ther. Adv. Infect. Dis.*, vol. 3, no. 1, pp. 23–42, Feb. 2016, doi: 10.1177/2049936115622891.

[160] C. Slimings and T. V. Riley, “Antibiotics and hospital-acquired Clostridium difficile infection: update of systematic review and meta-analysis,” *J. Antimicrob. Chemother.*, vol. 69, no. 4, pp. 881–891, Apr. 2014, doi: 10.1093/jac/dkt477.

[161] E. Sawabe *et al.*, "Molecular analysis of Clostridium difficile at a university teaching hospital in Japan: a shift in the predominant type over a five-year period," *Eur. J. Clin. Microbiol. Infect. Dis.*, vol. 26, no. 10, pp. 695–703, Sep. 2007, doi: 10.1007/s10096-007-0355-8.

[162] N. S. Ambrose, M. Johnson, D. W. Burdon, and M. R. B. Keighley, "The influence of single dose intravenous antibiotics on faecal flora and emergence of *Clostridium difficile*," *J. Antimicrob. Chemother.*, vol. 15, no. 3, pp. 319–326, 1985, doi: 10.1093/jac/15.3.319.

[163] F. de Lalla *et al.*, "Third generation cephalosporins as a risk factor for *Clostridium difficile* -associated disease: a four-year survey in a general hospital," *J. Antimicrob. Chemother.*, vol. 23, no. 4, pp. 623–631, 1989, doi: 10.1093/jac/23.4.623.

[164] D. C. Hooper, "Mechanisms of fluoroquinolone resistance," *Drug Resist. Updat.*, vol. 2, no. 1, pp. 38–55, Feb. 1999, doi: 10.1054/drup.1998.0068.

[165] J. C. Wang and A. S. Lynch, "Transcription and DNA supercoiling," *Curr. Opin. Genet. Dev.*, vol. 3, no. 5, pp. 764–768, Oct. 1993, doi: 10.1016/S0959-437X(05)80096-6.

[166] E. L. Zechiedrich and N. R. Cozzarelli, "Roles of topoisomerase IV and DNA gyrase in DNA unlinking during replication in Escherichia coli.," *Genes Dev.*, vol. 9, no. 22, pp. 2859–2869, Nov. 1995, doi: 10.1101/gad.9.22.2859.

[167] S. C. Kampranis and A. Maxwell, "Conformational Changes in DNA Gyrase Revealed by Limited Proteolysis," *J. Biol. Chem.*, vol. 273, no. 35, pp. 22606–22614, Aug. 1998, doi: 10.1074/jbc.273.35.22606.

[168] H. Oh and C. Edlund, "Mechanism of quinolone resistance in anaerobic bacteria," *Clin. Microbiol. Infect.*, vol. 9, no. 6, pp. 512–517, Jun. 2003, doi: 10.1046/j.1469-0691.2003.00725.x.

[169] M. He *et al.*, "Emergence and global spread of epidemic healthcare-associated Clostridium difficile," *Nat. Genet.*, vol. 45, no. 1, pp. 109–113, Jan. 2013, doi: 10.1038/ng.2478.

[170] D. Drudy, L. Kyne, R. O'Mahony, and S. Fanning, "*gyrA* Mutations in Fluoroquinolone-resistant *Clostridium difficile* PCR-027," *Emerg. Infect. Dis.*, vol. 13, no. 3, pp. 504–505, Mar. 2007, doi: 10.3201/eid1303.060771.

[171] C. Vuotto, I. Moura, F. Barbanti, G. Donelli, and P. Spigaglia, "Subinhibitory concentrations of metronidazole increase biofilm formation in *Clostridium difficile* strains," *Pathog. Dis.*, vol. 74, no. 2, p. ftv114, Mar. 2016, doi: 10.1093/femspd/ftv114.

[172] T. Thapa *et al.*, "Multiple Factors Modulate Biofilm Formation by the Anaerobic Pathogen Clostridium difficile," *J. Bacteriol.*, vol. 195, no. 3, pp. 545–555, Feb. 2013, doi: 10.1128/JB.01980-12.

[173] J. A. Leeds, M. Sachdeva, S. Mullin, S. W. Barnes, and A. Ruzin, “In vitro selection, via serial passage, of Clostridium difficile mutants with reduced susceptibility to fidaxomicin or vancomycin,” *J. Antimicrob. Chemother.*, vol. 69, no. 1, pp. 41–44, Jan. 2014, doi: 10.1093/jac/dkt302.

[174] L. Tsutsumi, Y. Owusu, J. Hurdle, and D. Sun, “Progress in the Discovery of Treatments for C. difficile Infection: A Clinical and Medicinal Chemistry Review,” *Curr. Top. Med. Chem.*, vol. 14, no. 1, pp. 152–175, Dec. 2013, doi: 10.2174/15680266136666131113154753.

[175] J. A. O’Brien, B. J. Lahue, J. J. Caro, and D. M. Davidson, “The Emerging Infectious Challenge of Clostridium difficile-Associated Disease in Massachusetts Hospitals: Clinical and Economic Consequences,” *Infect. Control Hosp. Epidemiol.*, vol. 28, no. 11, pp. 1219–1227, Nov. 2007, doi: 10.1086/522676.

[176] E. R. Dubberke *et al.*, “Strategies to Prevent *Clostridium difficile* Infections in Acute Care Hospitals: 2014 Update,” *Infect. Control Hosp. Epidemiol.*, vol. 35, no. 6, pp. 628–645, Jun. 2014, doi: 10.1086/676023.

[177] F. H. Decker, “Outcomes and Length of Medicare Nursing Home Stays: The Role of Registered Nurses and Physical Therapists,” *Am. J. Med. Qual.*, vol. 23, no. 6, pp. 465–474, Nov. 2008, doi: 10.1177/1062860608324173.

[178] M. J. Krauss *et al.*, “A case-control study of patient, medication, and care-related risk factors for inpatient falls,” *J. Gen. Intern. Med.*, vol. 20, no. 2, pp. 116–122, Feb. 2005, doi: 10.1111/j.1525-1497.2005.40171.x.

[179] F. K. Majiduddin, I. C. Materon, and T. G. Palzkill, “Molecular analysis of beta-lactamase structure and function,” *Int. J. Med. Microbiol.*, vol. 292, no. 2, pp. 127–137, Jan. 2002, doi: 10.1078/1438-4221-00198.

[180] M. E. Rupp and P. D. Fey, “Extended Spectrum ??-Lactamase (ESBL)-Producing Enterobacteriaceae: Considerations for Diagnosis, Prevention and Drug Treatment,” *Drugs*, vol. 63, no. 4, pp. 353–365, 2003, doi: 10.2165/00003495-200363040-00002.

[181] A. Chanawong, “SHV-12, SHV-5, SHV-2a and VEB-1 extended-spectrum beta-lactamases in Gram-negative bacteria isolated in a university hospital in Thailand,” *J. Antimicrob. Chemother.*, vol. 48, no. 6, pp. 839–852, Dec. 2001, doi: 10.1093/jac/48.6.839.

[182] M. C. Orencia, J. S. Yoon, J. E. Ness, W. P. C. Stemmer, and R. C. Stevens, “[No title found],” *Nat. Struct. Biol.*, vol. 8, no. 3, pp. 238–242, Mar. 2001, doi: 10.1038/84981.

[183] M. Nukaga, K. Mayama, G. V. Crichlow, and J. R. Knox, “Structure of an extended-spectrum class A β-lactamase from Proteus vulgaris K1,” *J. Mol. Biol.*, vol. 317, no. 1, pp. 109–117, Mar. 2002, doi: 10.1006/jmbi.2002.5420.

[184] F. Bert, “Identification of PSE and OXA beta-lactamase genes in Pseudomonas aeruginosa using PCR-restriction fragment length polymorphism,” *J. Antimicrob. Chemother.*, vol. 50, no. 1, pp. 11–18, Jul. 2002, doi: 10.1093/jac/dkf069.

[185] M. Sanguinetti *et al.*, “Characterization of Clinical Isolates of Enterobacteriaceae from Italy by the BD Phoenix Extended-Spectrum -Lactamase Detection Method,” *J. Clin. Microbiol.*, vol. 41, no. 4, pp. 1463–1468, Apr. 2003, doi: 10.1128/JCM.41.4.1463-1468.2003.

[186] M. Nukaga, S. Kumar, K. Nukaga, R. F. Pratt, and J. R. Knox, “Hydrolysis of Third-generation Cephalosporins by Class C β-Lactamases: STRUCTURES OF A TRANSITION STATE ANALOG OF CEFOTAXIME IN WILD-TYPE AND EXTENDED SPECTRUM ENZYMES,” *J. Biol. Chem.*, vol. 279, no. 10, pp. 9344–9352, Mar. 2004, doi: 10.1074/jbc.M312356200.

[187] N. D. Hanson and C. C. Sanders, “ChemInform Abstract: Regulation of Inducible AmpC β-Lactamase Expression Among Enterobacteriaceae,” *ChemInform*, vol. 31, no. 6, p. no-no, Jun. 2010, doi: 10.1002/chin.200006271.

[188] B. A. Rasmussen *et al.*, “Characterization of IMI-1 beta-lactamase, a class A carbapenem-hydrolyzing enzyme from Enterobacter cloacae.,” *Antimicrob. Agents Chemother.*, vol. 40, no. 9, pp. 2080–2086, Sep. 1996, doi: 10.1128/AAC.40.9.2080.

[189] H. Watanabe *et al.*, “Possible High Rate of Transmission of Nontypeable Haemophilus influenzae, Including -Lactamase-Negative Ampicillin-Resistant Strains, between Children and Their Parents,” *J. Clin. Microbiol.*, vol. 42, no. 1, pp. 362–365, Jan. 2004, doi: 10.1128/JCM.42.1.362-365.2004.

[190] R. Hakenbeck *et al.*, “Penicillin-Binding Proteins in β-Lactam–Resistant *Streptococcus pneumoniae*,” *Microb. Drug Resist.*, vol. 5, no. 2, pp. 91–99, Jan. 1999, doi: 10.1089/mdr.1999.5.91.

[191] K. Hiramatsu, Y. Katayama, H. Yuzawa, and T. Ito, “Molecular genetics of methicillin-resistant Staphylococcus aureus,” *Int. J. Med. Microbiol.*, vol. 292, no. 2, pp. 67–74, Jan. 2002, doi: 10.1078/1438-4221-00192.

[192] X.-Z. Li and H. Nikaido, “Efflux-Mediated Drug Resistance in Bacteria: An Update,” *Drugs*, vol. 69, no. 12, pp. 1555–1623, Aug. 2009, doi: 10.2165/11317030-000000000-00000.

[193] R. M. Williams, B. H. Lee, M. M. Miller, and O. P. Anderson, “Synthesis and x-ray crystal structure determination of 1,3-bridged .beta.-lactams: novel, anti-Bredt .beta.-lactams,” *J. Am. Chem. Soc.*, vol. 111, no. 3, pp. 1073–1081, Feb. 1989, doi: 10.1021/ja00185a043.

[194] J. E. Baldwin, G. P. Lynch, and J. Pitlik, .“GAMMA.-Lactam analogues of .BETA.-lactam antibiotics.,” *J. Antibiot. (Tokyo)*, vol. 44, no. 1, pp. 1–24, 1991, doi: 10.7164/antibiotics.44.1.

[195] V. R. Solomon, C. Hu, and H. Lee, “Hybrid pharmacophore design and synthesis of isatin–benzothiazole analogs for their anti-breast cancer activity,” *Bioorg. Med. Chem.*, vol. 17, no. 21, pp. 7585–7592, Nov. 2009, doi: 10.1016/j.bmc.2009.08.068.

[196] Becton-Dickinson, "LB Agar, Lennox • LB Broth, Lennox." https://legacy.bd.com/europe/regulatory/Assets/IFU/Difco_BBL/244620.pdf.

[197] Jan Hudzicki, "Kirby-Bauer Disk Diffusion Susceptibility Test Protocol," Dec. 08, 2009. https://asm.org/getattachment/2594ce26-bd44-47f6-8287-0657aa9185ad/Kirby-Bauer-Disk-Diffusion-Susceptibility-Test-Protocol-pdf.pdf.

[198] Garcia, Ed., "Broth Microdilution MIC Test for Anaerobic Bacteria," in *Clinical Microbiology Procedures Handbook, 3rd Edition*, American Society of Microbiology, 2010, pp. 61–68.

[199] Life Technologies, "Qubit® dsDNA BR Assay Kits." Feb. 16, 2015, [Online]. Available: https://www.thermofisher.com/document-connect/document-connect.html?url=https%3A%2F%2Fassets.thermofisher.com%2FTFS-Assets%2FLSG%2Fmanuals%2FQubit_dsDNA_BR_Assay_UG.pdf&title=VXNlciBHdWlkZTogUXViaXQgZHNETkEgQlIgQXNzYXkgS2l0cw==.

[200] A. M. Bolger, M. Lohse, and B. Usadel, "Trimmomatic: a flexible trimmer for Illumina sequence data," *Bioinformatics*, vol. 30, no. 15, pp. 2114–2120, Aug. 2014, doi: 10.1093/bioinformatics/btu170.

[201] D. E. Wood, J. Lu, and B. Langmead, "Improved metagenomic analysis with Kraken 2," *Genome Biol.*, vol. 20, no. 1, p. 257, Dec. 2019, doi: 10.1186/s13059-019-1891-0.

[202] A. Bankevich *et al.*, "SPAdes: A New Genome Assembly Algorithm and Its Applications to Single-Cell Sequencing," *J. Comput. Biol.*, vol. 19, no. 5, pp. 455–477, May 2012, doi: 10.1089/cmb.2012.0021.

[203] A. C. E. Darling, "Mauve: Multiple Alignment of Conserved Genomic Sequence With Rearrangements," *Genome Res.*, vol. 14, no. 7, pp. 1394–1403, Jun. 2004, doi: 10.1101/gr.2289704.

[204] T. Carver *et al.*, "Artemis and ACT: viewing, annotating and comparing sequences stored in a relational database," *Bioinformatics*, vol. 24, no. 23, pp. 2672–2676, Dec. 2008, doi: 10.1093/bioinformatics/btn529.

[205] T. Seemann, "Prokka: rapid prokaryotic genome annotation," *Bioinformatics*, vol. 30, no. 14, pp. 2068–2069, Jul. 2014, doi: 10.1093/bioinformatics/btu153.

[206] "Seeman T. Sinippy," *github*. https://github.com/tseemann/snippy (accessed Mar. 08, 2020).

[207] samtools, *bcftools - utilities for variant calling and manipulating VCFs and BCFs*. .

[208] P. D. Karp *et al.*, "The EcoCyc Database," *EcoSal Plus*, vol. 6, no. 1, Jun. 2014, doi: 10.1128/ecosalplus.ESP-0009-2013.

[209] I. M. Keseler *et al.*, “The EcoCyc database: reflecting new knowledge about *Escherichia coli* K-12,” *Nucleic Acids Res.*, vol. 45, no. D1, pp. D543–D550, Jan. 2017, doi: 10.1093/nar/gkw1003.

[210] P. D. Karp *et al.*, “The BioCyc collection of microbial genomes and metabolic pathways,” *Brief. Bioinform.*, vol. 20, no. 4, pp. 1085–1093, Jul. 2019, doi: 10.1093/bib/bbx085.

[211] “Team:TU Darmstadt/Project/Glycolic acid/E coli - 2018.igem.org.” http://2018.igem.org/Team:TU_Darmstadt/Project/Glycolic_acid/E_coli#Cloning (accessed Feb. 02, 2020).

[212] X.-M. Chu *et al.*, “Quinoline and quinolone dimers and their biological activities: An overview,” *Eur. J. Med. Chem.*, vol. 161, pp. 101–117, Jan. 2019, doi: 10.1016/j.ejmech.2018.10.035.

[213] D. J. Dwyer *et al.*, “Antibiotics induce redox-related physiological alterations as part of their lethality,” *Proc. Natl. Acad. Sci.*, vol. 111, no. 20, pp. E2100–E2109, May 2014, doi: 10.1073/pnas.1401876111.

[214] A. Gin, L. Dilay, J. A. Karlowsky, A. Walkty, E. Rubinstein, and G. G. Zhanel, “Piperacillin–tazobactam: a β-lactam/β-lactamase inhibitor combination,” *Expert Rev. Anti Infect. Ther.*, vol. 5, no. 3, pp. 365–383, Jun. 2007, doi: 10.1586/14787210.5.3.365.

[215] C. Cheng *et al.*, “Flagellar Basal Body Structural Proteins FlhB, FliM, and FliY Are Required for Flagellar-Associated Protein Expression in Listeria monocytogenes,” *Front. Microbiol.*, vol. 9, p. 208, Feb. 2018, doi: 10.3389/fmicb.2018.00208.

[216] Insightful Science, *SnapGene*. .

[217] “The European Committee on Antimicrobial Susceptibility Testing. Breakpoint tables for interpretation of MICs and zone diameters. Version 8.0.,” *European Committee on Antimicrobial Susceptibility Testing*. http://www.eucast.org. (accessed Feb. 02, 2020).

[218] Z. Jiang, A. Vasil, M. Vasil, and R. Hodges, “‘Specificity Determinants’ Improve Therapeutic Indices of Two Antimicrobial Peptides Piscidin 1 and Dermaseptin S4 Against the Gram-negative Pathogens Acinetobacter baumannii and Pseudomonas aeruginosa,” *Pharmaceuticals*, vol. 7, no. 4, pp. 366–391, Mar. 2014, doi: 10.3390/ph7040366.

[219] “Lack of new antibiotics threatens global efforts to contain drug-resistant infections,” *World Health Organization*. https://www.who.int/news-room/detail/17-01-2020-lack-of-new-antibiotics-threatens-global-efforts-to-contain-drug-resistant-infections (accessed Apr. 02, 2020).

[220] J. Caruano, G. G. Muccioli, and R. Robiette, “Biologically active γ-lactams: synthesis and natural sources,” *Org. Biomol. Chem.*, vol. 14, no. 43, pp. 10134–10156, 2016, doi: 10.1039/C6OB01349J.

[221] V. R. Solomon, C. Hu, and H. Lee, “Hybrid pharmacophore design and synthesis of isatin–benzothiazole analogs for their anti-breast cancer activity,” *Bioorg. Med. Chem.*, vol. 17, no. 21, pp. 7585–7592, Nov. 2009, doi: 10.1016/j.bmc.2009.08.068.

[222] F. Lefranc *et al.*, “*In Vitro* Pharmacological and Toxicological Effects of Norterpene Peroxides Isolated from the Red Sea Sponge *Diacarnus erythraeanus* on Normal and Cancer Cells,” *J. Nat. Prod.*, vol. 76, no. 9, pp. 1541–1547, Sep. 2013, doi: 10.1021/np400107t.

[223] A. V. Snezhkina *et al.*, “ROS Generation and Antioxidant Defense Systems in Normal and Malignant Cells,” *Oxid. Med. Cell. Longev.*, vol. 2019, pp. 1–17, Aug. 2019, doi: 10.1155/2019/6175804.

[224] S. Kalghatgi *et al.*, “Bactericidal Antibiotics Induce Mitochondrial Dysfunction and Oxidative Damage in Mammalian Cells,” *Sci. Transl. Med.*, vol. 5, no. 192, pp. 192ra85-192ra85, Jul. 2013, doi: 10.1126/scitranslmed.3006055.

[225] M. Goswami, S. H. Mangoli, and N. Jawali, “Involvement of Reactive Oxygen Species in the Action of Ciprofloxacin against Escherichia coli,” *Antimicrob. Agents Chemother.*, vol. 50, no. 3, pp. 949–954, Mar. 2006, doi: 10.1128/AAC.50.3.949-954.2006.

[226] M. P. Mingeot-Leclercq and P. M. Tulkens, “Aminoglycosides: nephrotoxicity,” *Antimicrob. Agents Chemother.*, vol. 43, no. 5, pp. 1003–1012, May 1999, doi: 10.1128/AAC.43.5.1003.

[227] R. E. Brummett and K. E. Fox, “Aminoglycoside-induced hearing loss in humans.,” *Antimicrob. Agents Chemother.*, vol. 33, no. 6, pp. 797–800, Jun. 1989, doi: 10.1128/AAC.33.6.797.

[228] L. Ma, H. Mi, Y. Xue, D. Wang, and X. Zhao, “The mechanism of ROS regulation of antibiotic resistance and antimicrobial lethality,” *Yi Chuan Hered.*, vol. 38, no. 10, pp. 902–909, 20 2016, doi: 10.16288/j.yczz.16-157.

[229] A. R. Tunkel *et al.*, “Practice Guidelines for the Management of Bacterial Meningitis,” *Clin. Infect. Dis.*, vol. 39, no. 9, pp. 1267–1284, Nov. 2004, doi: 10.1086/425368.

[230] D. J. Williams *et al.*, “Narrow Vs Broad-spectrum Antimicrobial Therapy for Children Hospitalized With Pneumonia,” *Pediatrics*, vol. 132, no. 5, pp. e1141–e1148, Nov. 2013, doi: 10.1542/peds.2013-1614.

[231] S. Foerster, M. Unemo, L. J. Hathaway, N. Low, and C. L. Althaus, “Time-kill curve analysis and pharmacodynamic modelling for in vitro evaluation of antimicrobials against Neisseria gonorrhoeae,” *BMC Microbiol.*, vol. 16, no. 1, p. 216, Dec. 2016, doi: 10.1186/s12866-016-0838-9.

[232] R. R. Regoes, C. Wiuff, R. M. Zappala, K. N. Garner, F. Baquero, and B. R. Levin, “Pharmacodynamic Functions: a Multiparameter Approach to the Design of Antibiotic

Treatment Regimens," *Antimicrob. Agents Chemother.*, vol. 48, no. 10, pp. 3670–3676, Oct. 2004, doi: 10.1128/AAC.48.10.3670-3676.2004.

[233] A. Tomasz, "The Mechanism of the Irreversible Antimicrobial Effects of Penicillins: How the Beta-Lactam Antibiotics Kill and Lyse Bacteria," *Annu. Rev. Microbiol.*, vol. 33, no. 1, pp. 113–137, Oct. 1979, doi: 10.1146/annurev.mi.33.100179.000553.

[234] B. D. Davis, L. L. Chen, and P. C. Tai, "Misread protein creates membrane channels: an essential step in the bactericidal action of aminoglycosides.," *Proc. Natl. Acad. Sci.*, vol. 83, no. 16, pp. 6164–6168, Aug. 1986, doi: 10.1073/pnas.83.16.6164.

[235] M. A. Kohanski, D. J. Dwyer, J. Wierzbowski, G. Cottarel, and J. J. Collins, "Mistranslation of Membrane Proteins and Two-Component System Activation Trigger Antibiotic-Mediated Cell Death," *Cell*, vol. 135, no. 4, pp. 679–690, Nov. 2008, doi: 10.1016/j.cell.2008.09.038.

[236] H. Van Acker and T. Coenye, "The Role of Reactive Oxygen Species in Antibiotic-Mediated Killing of Bacteria," *Trends Microbiol.*, vol. 25, no. 6, pp. 456–466, Jun. 2017, doi: 10.1016/j.tim.2016.12.008.

[237] M. A. Kohanski, D. J. Dwyer, B. Hayete, C. A. Lawrence, and J. J. Collins, "A Common Mechanism of Cellular Death Induced by Bactericidal Antibiotics," *Cell*, vol. 130, no. 5, pp. 797–810, Sep. 2007, doi: 10.1016/j.cell.2007.06.049.

[238] P. Belenky *et al.*, "Bactericidal Antibiotics Induce Toxic Metabolic Perturbations that Lead to Cellular Damage," *Cell Rep.*, vol. 13, no. 5, pp. 968–980, Nov. 2015, doi: 10.1016/j.celrep.2015.09.059.

[239] D. L. Tucker, N. Tucker, and T. Conway, "Gene Expression Profiling of the pH Response in Escherichia coli," *J. Bacteriol.*, vol. 184, no. 23, pp. 6551–6558, Dec. 2002, doi: 10.1128/JB.184.23.6551-6558.2002.

[240] L. C. Seaver and J. A. Imlay, "Alkyl Hydroperoxide Reductase Is the Primary Scavenger of Endogenous Hydrogen Peroxide in Escherichia coli," *J. Bacteriol.*, vol. 183, no. 24, pp. 7173–7181, Dec. 2001, doi: 10.1128/JB.183.24.7173-7181.2001.

[241] T. Bollenbach and R. Kishony, "Resolution of Gene Regulatory Conflicts Caused by Combinations of Antibiotics," *Mol. Cell*, vol. 42, no. 4, pp. 413–425, May 2011, doi: 10.1016/j.molcel.2011.04.016.

[242] M. J. Horsburgh, S. J. Wharton, M. Karavolos, and S. J. Foster, "Manganese: elemental defence for a life with oxygen," *Trends Microbiol.*, vol. 10, no. 11, pp. 496–501, Nov. 2002, doi: 10.1016/S0966-842X(02)02462-9.

[243] J. Tamarit, E. Cabiscol, and J. Ros, "Identification of the Major Oxidatively Damaged Proteins in *Escherichia coli* Cells Exposed to Oxidative Stress," *J. Biol. Chem.*, vol. 273, no. 5, pp. 3027–3032, Jan. 1998, doi: 10.1074/jbc.273.5.3027.

[244] A. von Gabain, J. G. Belasco, J. L. Schottel, A. C. Chang, and S. N. Cohen, “Decay of mRNA in Escherichia coli: investigation of the fate of specific segments of transcripts.,” *Proc. Natl. Acad. Sci.*, vol. 80, no. 3, pp. 653–657, Feb. 1983, doi: 10.1073/pnas.80.3.653.

[245] R. Tomecki, P. J. Sikorski, and M. Zakrzewska-Placzek, “Comparison of preribosomal RNA processing pathways in yeast, plant and human cells - focus on coordinated action of endo- and exoribonucleases,” *FEBS Lett.*, vol. 591, no. 13, pp. 1801–1850, Jul. 2017, doi: 10.1002/1873-3468.12682.

[246] L. C. Cerchietti *et al.*, “Abstract 4676: Metabolic reprogramming evoked by nitrosative stress enhances the effect of radiation in brain metastases.,” in *Clinical Trials*, Apr. 2013, pp. 4676–4676, doi: 10.1158/1538-7445.AM2013-4676.

[247] S. Ahn, J. Jung, I.-A. Jang, E. L. Madsen, and W. Park, “Role of Glyoxylate Shunt in Oxidative Stress Response,” *J. Biol. Chem.*, vol. 291, no. 22, pp. 11928–11938, May 2016, doi: 10.1074/jbc.M115.708149.

[248] M. Nandakumar, C. Nathan, and K. Y. Rhee, “Isocitrate lyase mediates broad antibiotic tolerance in Mycobacterium tuberculosis,” *Nat. Commun.*, vol. 5, no. 1, p. 4306, Sep. 2014, doi: 10.1038/ncomms5306.

[249] M. A. Kohanski, M. A. DePristo, and J. J. Collins, “Sublethal Antibiotic Treatment Leads to Multidrug Resistance via Radical-Induced Mutagenesis,” *Mol. Cell*, vol. 37, no. 3, pp. 311–320, Feb. 2010, doi: 10.1016/j.molcel.2010.01.003.

[250] F. R. Bryant, “Construction of a recombinase-deficient mutant recA protein that retains single-stranded DNA-dependent ATPase activity,” *J. Biol. Chem.*, vol. 263, no. 18, pp. 8716–8723, Jun. 1988.

[251] E. A. Kouzminova, E. Rotman, L. Macomber, J. Zhang, and A. Kuzminov, “RecA-dependent mutants in Escherichia coli reveal strategies to avoid chromosomal fragmentation,” *Proc. Natl. Acad. Sci.*, vol. 101, no. 46, pp. 16262–16267, Nov. 2004, doi: 10.1073/pnas.0405943101.

[252] P. Howard-Flanders, “DNA repair and recombination,” *Br. Med. Bull.*, vol. 29, no. 3, pp. 226–235, Sep. 1973, doi: 10.1093/oxfordjournals.bmb.a071012.

[253] B. Hu, P. Khara, and P. J. Christie, “Structural bases for F plasmid conjugation and F pilus biogenesis in *Escherichia coli*,” *Proc. Natl. Acad. Sci.*, vol. 116, no. 28, pp. 14222–14227, Jul. 2019, doi: 10.1073/pnas.1904428116.

[254] B. P. Anton and E. A. Raleigh, “Complete Genome Sequence of NEB 5-alpha, a Derivative of *Escherichia coli* K-12 DH5α,” *Genome Announc.*, vol. 4, no. 6, pp. e01245-16, /ga/4/6/e01245-16.atom, Dec. 2016, doi: 10.1128/genomeA.01245-16.

[255] S. Metzger, G. Schreiber, E. Aizenman, M. Cashel, and G. Glaser, “Characterization of the relA1 mutation and a comparison of relA1 with new relA null alleles in Escherichia coli,” *J. Biol. Chem.*, vol. 264, no. 35, pp. 21146–21152, Dec. 1989.

[256] T. A. Brown, Ed., *Genomes*, 2nd ed. New York: Wiley-Liss, 2002.

[257] O. Kovalchuk and I. Kovalchuk, Eds., *Genome stability: from virus to human application*. Amsterdam: Elsevier/Academic Press, 2016.

[258] M. Bzymek and S. T. Lovett, “Instability of repetitive DNA sequences: The role of replication in multiple mechanisms,” *Proc. Natl. Acad. Sci.*, vol. 98, no. 15, pp. 8319–8325, Jul. 2001, doi: 10.1073/pnas.111008398.

[259] S. T. Lovett, T. J. Gluckman, P. J. Simon, V. A. Sutera, and P. T. Drapkin, “Recombination between repeats in Escherichia coli by a recA-independent, proximity-sensitive mechanism,” *Mol. Gen. Genet. MGG*, vol. 245, no. 3, pp. 294–300, Nov. 1994, doi: 10.1007/BF00290109.

[260] A. J. F. Griffiths, Ed., *Modern genetic analysis*, 2. print. New York: Freeman, 1999.

[261] T. P. Malan, A. Kolb, H. Buc, and W. R. McClure, “Mechanism of CRP-cAMP activation of lac operon transcription initiation activation of the P1 promoter,” *J. Mol. Biol.*, vol. 180, no. 4, pp. 881–909, Dec. 1984, doi: 10.1016/0022-2836(84)90262-6.

[262] N. Irwin and M. Ptashne, “Mutants of the catabolite activator protein of Escherichia coli that are specifically deficient in the gene-activation function.,” *Proc. Natl. Acad. Sci.*, vol. 84, no. 23, pp. 8315–8319, Dec. 1987, doi: 10.1073/pnas.84.23.8315.

[263] S. E. Finkel and R. C. Johnson, “The Fis protein: it’s not just for DNA inversion anymore,” *Mol. Microbiol.*, vol. 6, no. 22, pp. 3257–3265, Nov. 1992, doi: 10.1111/j.1365-2958.1992.tb02193.x.

[264] M. D. Bradley, M. B. Beach, A. P. J. de Koning, T. S. Pratt, and R. Osuna, “Effects of Fis on Escherichia coli gene expression during different growth stages,” *Microbiol. Read. Engl.*, vol. 153, no. Pt 9, pp. 2922–2940, Sep. 2007, doi: 10.1099/mic.0.2007/008565-0.

[265] S. De and M. M. Babu, “Genomic neighbourhood and the regulation of gene expression,” *Curr. Opin. Cell Biol.*, vol. 22, no. 3, pp. 326–333, Jun. 2010, doi: 10.1016/j.ceb.2010.04.004.

[266] B. Oliver, M. Parisi, and D. Clark, “Gene Expression Neighbourhoods,” *J. Biol.*, vol. 1, no. 1, p. 4, 2002, doi: 10.1186/1475-4924-1-4.

[267] Z. Bloom-Ackermann, S. Navon, H. Gingold, R. Towers, Y. Pilpel, and O. Dahan, “A Comprehensive tRNA Deletion Library Unravels the Genetic Architecture of the tRNA Pool,” *PLoS Genet.*, vol. 10, no. 1, p. e1004084, Jan. 2014, doi: 10.1371/journal.pgen.1004084.

[268] C. Alkim, D. Trichez, Y. Cam, L. Spina, J. M. François, and T. Walther, “The synthetic xylulose-1 phosphate pathway increases production of glycolic acid from xylose-rich sugar

mixtures," *Biotechnol. Biofuels*, vol. 9, no. 1, p. 201, Dec. 2016, doi: 10.1186/s13068-016-0610-2.

[269] Z. Yu, Y. Zhu, W. Qin, J. Yin, and J. Qiu, "Oxidative Stress Induced by Polymyxin E Is Involved in Rapid Killing of *Paenibacillus polymyxa*," *BioMed Res. Int.*, vol. 2017, pp. 1–12, 2017, doi: 10.1155/2017/5437139.

[270] T. R. Sampson, X. Liu, M. R. Schroeder, C. S. Kraft, E. M. Burd, and D. S. Weiss, "Rapid Killing of Acinetobacter baumannii by Polymyxins Is Mediated by a Hydroxyl Radical Death Pathway," *Antimicrob. Agents Chemother.*, vol. 56, no. 11, pp. 5642–5649, Nov. 2012, doi: 10.1128/AAC.00756-12.

[271] Y. Hong, J. Zeng, X. Wang, K. Drlica, and X. Zhao, "Post-stress bacterial cell death mediated by reactive oxygen species," *Proc. Natl. Acad. Sci.*, vol. 116, no. 20, pp. 10064–10071, May 2019, doi: 10.1073/pnas.1901730116.

[272] E. Oh, L. McMullen, and B. Jeon, "Impact of oxidative stress defense on bacterial survival and morphological change in Campylobacter jejuni under aerobic conditions," *Front. Microbiol.*, vol. 6, Apr. 2015, doi: 10.3389/fmicb.2015.00295.

[273] J. Ye *et al.*, "Alanine Enhances Aminoglycosides-Induced ROS Production as Revealed by Proteomic Analysis," *Front. Microbiol.*, vol. 9, p. 29, Jan. 2018, doi: 10.3389/fmicb.2018.00029.

[274] M. H. Miller, S. A. Feinstein, and R. T. Chow, "Early effects of beta-lactams on aminoglycoside uptake, bactericidal rates, and turbidimetrically measured growth inhibition in Pseudomonas aeruginosa.," *Antimicrob. Agents Chemother.*, vol. 31, no. 1, pp. 108–110, Jan. 1987, doi: 10.1128/AAC.31.1.108.

[275] R. E. Hancock, V. J. Raffle, and T. I. Nicas, "Involvement of the outer membrane in gentamicin and streptomycin uptake and killing in Pseudomonas aeruginosa.," *Antimicrob. Agents Chemother.*, vol. 19, no. 5, pp. 777–785, May 1981, doi: 10.1128/AAC.19.5.777.

[276] K. Takahashi and H. Kanno, "Synergistic activities of combinations of beta-lactams, fosfomycin, and tobramycin against Pseudomonas aeruginosa.," *Antimicrob. Agents Chemother.*, vol. 26, no. 5, pp. 789–791, Nov. 1984, doi: 10.1128/AAC.26.5.789.

[277] M. Goudarzi *et al.*, "Antimicrobial Susceptibility of Clostridium Difficile Clinical Isolates in Iran," *Iran. Red Crescent Med. J.*, vol. 15, no. 8, pp. 704–711, Aug. 2013, doi: 10.5812/ircmj.5189.

[278] D. Jin *et al.*, "Molecular Epidemiology of Clostridium difficile Infection in Hospitalized Patients in Eastern China," *J. Clin. Microbiol.*, vol. 55, no. 3, pp. 801–810, Mar. 2017, doi: 10.1128/JCM.01898-16.

[279] A. Adler *et al.*, "A national survey of the molecular epidemiology of Clostridium difficile in Israel: the dissemination of the ribotype 027 strain with reduced susceptibility to vancomycin

and metronidazole," *Diagn. Microbiol. Infect. Dis.*, vol. 83, no. 1, pp. 21–24, Sep. 2015, doi: 10.1016/j.diagmicrobio.2015.05.015.

[280] J. Freeman *et al.*, "Pan-European longitudinal surveillance of antibiotic resistance among prevalent Clostridium difficile ribotypes," *Clin. Microbiol. Infect.*, vol. 21, no. 3, pp. 248.e9-248.e16, Mar. 2015, doi: 10.1016/j.cmi.2014.09.017.

[281] D. R. Snydman *et al.*, "U.S.-Based National Sentinel Surveillance Study for the Epidemiology of Clostridium difficile-Associated Diarrheal Isolates and Their Susceptibility to Fidaxomicin," *Antimicrob. Agents Chemother.*, vol. 59, no. 10, pp. 6437–6443, Oct. 2015, doi: 10.1128/AAC.00845-15.

[282] C. Ngernsombat, S. Sreesai, P. Harnvoravongchai, S. Chankhamhaengdecha, and T. Janvilisri, "CD2068 potentially mediates multidrug efflux in Clostridium difficile," *Sci. Rep.*, vol. 7, no. 1, p. 9982, Dec. 2017, doi: 10.1038/s41598-017-10155-x.

[283] M. L. Barclay and E. J. Begg, "Aminoglycoside toxicity and relation to dose regimen," *Adverse Drug React. Toxicol. Rev.*, vol. 13, no. 4, pp. 207–234, 1994.

[284] M. Neumann-Schaal, D. Jahn, and K. Schmidt-Hohagen, "Metabolism the Difficile Way: The Key to the Success of the Pathogen Clostridioides difficile," *Front. Microbiol.*, vol. 10, p. 219, Feb. 2019, doi: 10.3389/fmicb.2019.00219.

[285] L. H. Stickland, "Studies in the metabolism of the strict anaerobes (genus Clostridium)," *Biochem. J.*, vol. 28, no. 5, pp. 1746–1759, Jan. 1934, doi: 10.1042/bj0281746.

[286] L. Bouillaut *et al.*, "Role of the global regulator Rex in control of NAD+ -regeneration in Clostridioides (Clostridium) difficile," *Mol. Microbiol.*, vol. 111, no. 6, pp. 1671–1688, 2019, doi: 10.1111/mmi.14245.

[287] A. R. Richardson †, G. A. Somerville †, and A. L. Sonenshein †, "Regulating the Intersection of Metabolism and Pathogenesis in Gram-positive Bacteria," in *Metabolism and Bacterial Pathogenesis*, Conway and Cohen, Eds. American Society of Microbiology, 2015, pp. 129–165.

[288] D. Brekasis, "A novel sensor of NADH/NAD+ redox poise in Streptomyces coelicolor A3(2)," *EMBO J.*, vol. 22, no. 18, pp. 4856–4865, Sep. 2003, doi: 10.1093/emboj/cdg453.

[289] B. K. English, "Limitations of beta-lactam therapy for infections caused by susceptible Gram-positive bacteria," *J. Infect.*, vol. 69, pp. S5–S9, Nov. 2014, doi: 10.1016/j.jinf.2014.07.010.

[290] R. R. Rosato, R. Fernandez, L. I. Paz, C. R. Singh, and A. E. Rosato, "TCA Cycle-Mediated Generation of ROS Is a Key Mediator for HeR-MRSA Survival under β-Lactam Antibiotic Exposure," *PLoS ONE*, vol. 9, no. 6, p. e99605, Jun. 2014, doi: 10.1371/journal.pone.0099605.

[291] S. Kalghatgi *et al.*, “Bactericidal Antibiotics Induce Mitochondrial Dysfunction and Oxidative Damage in Mammalian Cells,” *Sci. Transl. Med.*, vol. 5, no. 192, pp. 192ra85-192ra85, Jul. 2013, doi: 10.1126/scitranslmed.3006055.

[292] A. O. Henriques, L. R. Melsen, and C. P. Moran, “Involvement of Superoxide Dismutase in Spore Coat Assembly in Bacillus subtilis,” *J. Bacteriol.*, vol. 180, no. 9, pp. 2285–2291, May 1998, doi: 10.1128/JB.180.9.2285-2291.1998.

[293] S. N. Bass, S. R. Bauer, E. A. Neuner, and S. W. Lam, “Comparison of treatment outcomes with vancomycin alone versus combination therapy in severe Clostridium difficile infection,” *J. Hosp. Infect.*, vol. 85, no. 1, pp. 22–27, Sep. 2013, doi: 10.1016/j.jhin.2012.12.019.

6.0 Appendices

6.1 Antibiotic Susceptibilities of C. difficile isolates

Table 2: Antibiotic susceptibility profile for a collection of 200 clinical *C. difficile* isolates collected from patients at HSN

			Metronidazole (MZ)			Vancomycin (VA)		
No. of isolates	C. difficile no.	Sampling Day	Raw	Interpreted	Impact	Raw	Interpreted	Impact
1	ATCC 9689	06/06/2019	1.5	2	S	1.5	2	S
2	ATCC 43596	06/06/2019	1.5	2	S	1.5	2	S
3	ATCC 43598	06/06/2019	1	1	S	1.5	2	S
4	*E. faecalis* ATCC 29212	17/06/2019	256	256	R	3	4	S
5	ATCC 700057	20/06/2019	0.19	0.25	S	8	8	S
6	ATCC 9689 (repeat)	21/06/2019	0.38	0.5	S	1.5	2	S
7	27	41065	0.75	1	S	0.75	1	S

8	31	41066	0.38	0.5	S	2	2	S
9	149	41080	0.75	1	S	0.5	0.5	S
10	151	41079	0.75	1	S	0.75	1	S
11	159	41080	0.75	1	S	1	1	S
12	193	41085	0.25	0.5	S	0.5	1	S
13	203	41086	0.75	1	S	2	2	S
14	227	41090	0.25	0.5	S	0.75	1	S
15	273	41094	0.38	0.5	S	0.5	0.5	S
16	383		0.25	0.5	S	0.38	0.5	S
17	397		0.25	0.5	S	0.38	0.5	S
18	467	41112	1	1	S	0.5	0.5	S
19**	483	41113	1.5	2	S	1	1	S

19	483	41113	1.5	2	S	1.5	2	S
20	503	41115	2	2	S	1.5	2	S
21	567	41125	0.5	1	S	1	1	S

22**	629	41133	0.75	1	S	1	1	S
22	629	41133	0.38	0.5	S	0.75	1	S
23	637	41135	0.75	1	S	0.75	1	S
24**	905**	41161	0.75	1	S	0.75	1	S
24	905	41161	0.5	0.5	S	0.5	0.5	S
25**	911	41162	0.75	1	S	1	1	S
25	911	41162	0.38	0.5	S	3	4	R
26	921	41162	0.19	0.25	S	0.5	0.5	S
27	1017	41168	1	1	S	0.75	1	S
28	1071	41172	0.75	1	S	0.75	1	S
29	1111	41175	0.75	1	S	1	1	S
30	1169	41180	0.19	0.5	S	0.38	0.5	S
31	1229	41187	0.5	0.5	S	0.75	1	S
32**	1243	41188	1.5	2	S	0.5	1	S

32	1243	41188	3	4	R	0.75	1	S
33	1279	41191	0.75	1	S	1.5	2	S
34	1305	41193	0.75	1	S	0.75	1	S
35	1341	41195	0.75	1	S	1	1	S
36	1377	41198	0.5	0.5	S	0.75	1	S
37	1467	41205	0.19	0.5	S	0.38	0.5	S
38	1471	41205	2	2	S	0.5	1	S
39	1625	41215	1	1	S	0.38	0.5	S
40	1891	41236	0.5	1	S	1	1	S
41	1903	41237	0.75	1	S	1	1	S
42	1935	41241	0.75	1	S	1	1	S
43	2029	41247	0.75	1	S	1	1	S
44	2479	41285	0.5	0.5	S	0.38	0.5	S
45	2523	41288	0.38	0.5	S	0.5	0.5	S
46	2903	41318	0.25	0.5	S	0.75	1	S
47** *	2915**	41319	0.38	0.5	S	0.75	1	S

47	2915	41319	0.5	0.5	S	1	1	S
48**	3175	41345	0.75	1	S	0.75	0.75	S
48	3175	41345	0.5	0.5	S	0.5	0.5	S
49	3243	41354	0.5	0.5	S	0.5	0.5	S
50	3501	41376	0.5	0.5	S	0.75	1	S
51	3601	41388	0.5	0.5	S	0.75	1	S
52	3657	41396	0.75	1	S	0.38	0.5	S
53	3861	41422	0.75	1	S	0.75	1	S
54	4031	41439	0.75	1	S	2	2	S
55	4175	41452	1	1	S	3	4	R
56	4257	41461	0.75	1	S	0.5	0.5	S
57	CDR4365	17/07/2013	0.5	0.5	S	1	1	S
58	CDR4373	18/07/2013	0.5	0.5	S	1	1	S
59	CDR4465	29/07/2013	0.5	0.5	S	1	1	S
60	CDR4513	04/08/2013	0.5	0.5	S	1.5	2	S
61	CDR4545	07/08/2013	0.38	0.5	S	1	1	S

62	CDR4587	12/08/2013	1	1	S	1	1	S
63	CDR4653	02/09/2013	0.75	1	S	1.5	2	S
64	CDR4663	13/09/2013	0.38	0.5	S	1	1	S
65	CDR4669	16/09/2013	0.5	1	S	1	1	S
66	CDR4681	27/09/2013	0.25	0.5	S	0.75	1	S
67	CDR4687	06/10/2013	0.75	1	S	1	1	S
68	CDR4703	23/10/2013	0.38	0.5	S	1	1	S
69	CDR4707	26/10/2013	0.38	0.5	S	0.75	1	S
70	CDR4719	03/11/2013	0.38	0.5	S	0.75	1	S
71	CDR4725	13/11/2013	0.5	0.5	S	1	1	S
72	CDR4739	24/11/2013	0.5	0.5	S	0.75	1	S
73	CDR4741	25/11/2013	0.5	0.5	S	1.5	2	S
74	CDR4753	05/12/2013	0.5	0.5	S	1	1	S
75	CDR4761	11/12/2013	0.5	0.5	S	0.75	1	S
76	CDR4765	15/12/2013	0.75	1	S	1.5	2	S
77	CDR4771	20/12/2013	0.5	0.5	S	1	1	S
78	CDR4779	25/12/2013						

79	CDR4795	15/01/2014	0.25	0.5	S	1	1	S
80	CDR4803	24/01/2014	0.38	0.5	S	1	1	S
81	CDR4811	29/01/2014	0.38	0.5	S	1	1	S
82	CDR4813	31/01/2014	0.38	0.5	S	0.75	1	S
83	CDR4819	08/02/2014	0.38	0.5	S	2	2	S
84	CDR4821	09/02/2014	0.19	0.25	S	1	1	S
85	CDR4825	12/02/2014	0.38	0.5	S	2	2	S
86	CDR4829	13/02/2014	2	2	S	1.5	2	S
87	CDR4839	17/02/2014	1	1	S	1	1	S
88	CDR4847	20/02/2014	1	1	S	1.5	2	S
89	CDR4851	28/02/2014	1	1	S	1	1	S
90	CDR4859	04/03/2014	0.5	0.5	S	1	1	S
91	CDR4867	14/03/2014	1	1	S	0.75	1	S
92	CDR4881	21/03/2014	0.75	1	S	1	1	S
93	CDR4897	05/04/2014	1.5	2	S	1.5	2	S
94	CDR4903	09/04/2014	1	1	S	1.5	2	S
95	CDR4909	15/04/2014	0.75	1	S	1	1	S

96	CDR4911	16/04/2014	0.75	1	S	1.5	2	S
97	CDR4917	22/04/2014	0.38	0.5	S	0.75	1	S
98	CDR4921	28/04/2014	0.38	0.5	S	1	1	S
99	CDR4941	12/05/2014	0.75	1	S	1	1	S
100	CDR4949	18/05/2014	0.38	0.5	S	1	1	S
101	CDR4967	30/05/2014	0.5	0.5	S	1	1	S
102	CDR4983	11/06/2014	0.5	0.5	S	0.75	1	S
103	CDR5015	22/06/2014	0.38	0.5	S	1.5	2	S
104	CDR5029	27/06/2014	0.5	0.5	S	1	1	S
105	CDR5041	14/07/2014	0.5	0.5	S	2	2	S
106	CDR5057	25/07/2014	3	4	R	1.5	2	S
107	CDR5059	26/07/2014	1.5	2	S	1.5	2	S
108	CDR5063	01/08/2014	2	2	S	1	1	S
109	CDR5065	02/08/2014	0.75	1	S	1.5	2	S
110	CDR5067	03/08/2014	1	1	S	1	1	S
111	CDR5071	19/08/2014	1.5	2	S	1	1	S
112	CDR5073	25/08/2014	0.75	1	S	1.5	2	S

113	CDR5075	26/08/2014	8	12	R	1.5	2	S
114	CDR5085	08/09/2014	256	256	R	3	4	R
115	CDR5093	14/09/2014	256	256	R	1.5	2	S
116	CDR5099	26/09/2014	0.75	1	S	1	1	S
117	CDR5107	11/10/2014	0.25	0.5	S	2	2	S
118	CDR5111	16/10/2014	256	256	R	256	256	R
119	CDR5117	26/10/2014	0.38	0.5	S	1	1	S
120	CDR5121	10/11/2014	0.19	0.25	S	1	1	S
121	CDR5127	16/11/2014	256	256	R	3	4	R
122	CDR5133	19/11/2014	256	256	R	3	4	R
123	CDR5137	22/11/2014	0.75	1	S	1.5	2	S
124	CDR5139	11/12/2014	256	256	R	3	4	R
125	CDR5141	12/12/2014	6	8	R	1	1	S
126	CDR5145	13/12/2014	0.5	0.5	S	1.5	2	S
127	CDR5153	29/12/2014	0.5	0.5	S	1	1	S
128	CDR5155	27/12/2014	0.5	0.5	S	1	1	S
129	CDR5159	04/01/2015	0.25	0.5	S	1.5	2	S

130	CDR5161	05/01/2015	0.38	0.5	S	1	1	S
131	CDR5163	07/01/2015	0.38	0.5	S	1	1	S
132	CDR5165	14/01/2015	0.38	0.5	S	1.5	2	S
133	CDR5167	15/01/2015	0.5	0.5	S	1	1	S
134	CDR5171	18/01/2015	0.25	0.5	S	1.5	2	S
135	CDR5179	24/01/2015	1	1	S	1.5	2	S
136	CDR5181	26/01/2015	0.75	1	S	1.5	2	S
137	CDR5183	26/01/2015	0.75	1	S	1.5	2	S
138	CDR5185	27/01/2015	0.38	0.5	S	1.5	2	S
139	CDR5189	28/01/2015	0.75	1	S	1.5	2	S
140	CDR5201	01/02/2015	0.75	1	S	1.5	2	S
141	CDR5209	10/02/2015	0.38	0.5	S	1.5	2	S
142	CDR5211	11/02/2015	0.75	1	S	1	1	S
143	CDR5213	12/02/2015	1	1	S	1	1	S
144	CDR5221	02/03/2015	0.5	0.5	S	1.5	2	S
145	CDR5223	06/03/2015	0.38	0.5	S	1.5	2	S
146	CDR5225	08/03/2015	0.38	0.5	S	1	1	S

147	CDR5229	08/03/2015	0.38	0.5	S	1.5	2	S
148	CDR5233	07/03/2015	0.75	1	S	1.5	2	S
149	CDR5235	13/03/2015	0.38	0.5	S	1.5	2	S
150	CDR5237	16/03/2015	0.5	0.5	S	1.5	2	S
151	CDR5239	16/03/2015	0.5	0.5	S	1	1	S
152	CDR5243	20/03/2015	1	1	S	1.5	2	S
153	CDR5245	23/03/2015	0.75	1	S	1.5	2	S
154	CDR5247	26/03/2015	0.75	1	S	1	1	S
155	CDR5249	27/03/2015	0.5	0.5	S	1	1	S
156	CDR5253	02/04/2015	0.25	0.5	S	1.5	2	S
157	CDR5255	02/04/2015	2	2	S	1	1	S
158	CDR5259	07/04/2015	0.75	1	S	1.5	2	S
159	CDR5263	11/04/2015						
160	CDR5267	16/04/2015	0.5	0.5	S	1.5	2	S
161	CDR5269	19/04/2015	1	1	S	1	1	S
162	CDR5273	26/04/2015	0.5	0.5	S	1.5	2	S
163	CDR5277	28/04/2015	0.75	1	S	1.5	2	S

164	CDR5281	30/04/2015	0.5	0.5	S	1.5	2	S
165	CDR5287	08/05/2015	0.5	0.5	S	1	1	S
166	CDR5291	10/05/2015	0.75	1	S	1.5	2	S
167	CDR5293	14/05/2015	0.5	0.5	S	1.5	2	S
168	CDR5297	18/05/2015	0.5	0.5	S	1.5	2	S
169	CDR5299	19/05/2015	0.5	0.5	S	1	1	S
170	CDR5305	21/05/2015	0.38	0.5	S	1.5	2	S
171	CDR5307	21/05/2015	0.5	0.5	S	1	1	S
172	CDR5309	22/05/2015	0.5	0.5	S	1.5	2	S
173	CDR5313	25/05/2015	6	8	R	1.5	2	S
174	CDR5317	26/05/2015	12	16	R	1.5	2	S
175	CDR5319	30/05/2015	1	1	S	2	2	S
176	CDR5321	31/05/2015	1	1	S	3	4	R
177	CDR5329	05/06/2015	1.5	2	S	1.5	2	S
178	CDR5331	06/06/2015	1	1	S	1.5	2	S
179	CDR5335	10/06/2015	1.5	2	S	1	1	S
180	CDR5343	14/07/2015	1	1	S	1.5	2	S

181	CDR5345	16/07/2015	0.5	0.5	S	1	1	S
182	CDR5347	17/07/2015	1	1	S	1.5	2	S
183	CDR5349	17/07/2015	2	2	S	3	4	R
184	CDR5351	22/07/2015	1	1	S	1.5	2	S
185	CDR5429	07/02/2017	0.75	1	S	1.5	2	S
186	CDR5431	11/02/2017	1	1	S	2	2	S
187	CDR5433	13/02/2017	1	1	S	2	2	S
188	CDR5435	13/02/2017	0.5	0.5	S	1	1	S
189	CDR5439	15/02/2017	1.5	2	S	1.5	2	S
190	CDR5441	18/02/2017	1.5	2	S	1.5	2	S
191	CDR5445	21/02/2017	1.5	2	S	1.5	2	S
192	CDR5447	23/02/2017	1.5	2	S	3	4	R
193	CDR5449	24/02/2017	0.75	1	S	2	2	S
194	CDR5451	27/01/2017	1.5	2	S	1.5	2	S
195	CDR5461	30/01/2017	1.5	2	S	1.5	2	S
196	CDR5463	31/01/2017	0.75	1	S	2	2	S
197	CDR5465	27/02/2017	1.5	2	S	1.5	2	S

198	CDR5469	27/02/2017	1.5	2	S	1	1	S
199	CDR5471	28/02/2017	3	4	R	1	1	S
200	CDR5473	26/03/2017	1.5	2	S	1	1	S
201	CDR5475	28/03/2017	2	2	S	1.5	2	S
202	CDR5477	28/03/2017	1	1	S	0.75	1	S

6.2 Antimicrobial activities of 27 active synthetic compounds

Table 3: Antibiotic susceptibility profile for initialy 27 active compounds

Name of compound	**MIC (µg/mL)**	**MIC (µM)**
GOD 12	100 µg/mL	205 µM
GOD 13	150 µg/mL	288 µM
GOD 17	500 µg/mL	113 µM
RAJA 6	500 µg/mL	244 µM
RAJA 11	200 µg/mL	609 µM
RAJA 12	500 µg/mL	105 µM
RAJA 15	500 µg/mL	203 µM
RAJA 17	500 µg/mL	204 µM
RAJA 22	150 µg/mL	560 µM
RAJA 23	150 µg/mL	482 µM
RAJA 24	500 µg/mL	189 µM
RAJA 28	100 µg/mL	245 µM
RAJA 29	100 µg/mL	218 µM

RAJA 30	100 µg/mL	353 µM
RAJA 31	100 µg/mL	307 µM
RAJA 33	100 µg/mL	309 µM
RAJA 36	100 µg/mL	275 µM
RAJA 37	100 µg/mL	180 µM
RAJA 38	200 µg/mL	465 µM
RAJA 41	100 µg/mL	356 µM
RAJA 42	100 µg/mL	358 µM
RAJA 44	150 µg/mL	363 µM
RAJA 45	100 µg/mL	196 µM
RAJA 47	50 µg/mL	117 µM
RAJA 71	500 µg/mL	149 µM
RAJA 73	100 µg/mL	261 µM
RAJA 74	150 µg/mL	449 µM

6.3 List of PCR primers

Table 4: *E. coli* K12 gene specific PCR and QPCR primers used

Primer ID	Direction	Primer sequence (5'-3')	Fragment size (bp)	Reference or Source
soda F	Forward	GCTGAAAGGCGATAAACTGG	80	This study*
soda R	Reverse	AAGCGCCAGAAATAGCTTCA	80	This study*
CysG F	Forward	GAAAGCCTTCTCGACACCTG	106	This study*
CysG R	Reverse	CGTTACAGAAGATGCGACGA	106	This study*
ghrA F	Forward	TCGCACAACGCTTTTCGGGA	965	(1)**
ghrA R	Reverse	TTAGTAGCCGCGTGCGCGGT	965	(1)**

rrsA F	Forward	CTCTTGCCATCGGATGTGC CCA	105	(2)
rrsA R	Reverse	CCAGTGTGGCTGGTCATCC TCTCA	105	(2)

* Designed in house by Dr. James Knockleby and Dr. Hai-Yen Vu.

** Sequence adapted from (1) by Alexis Fong.

(1) Liu, Min et al. "Metabolic engineering of a xylose pathway for biotechnological production of glycolate in Escherichia coli." *Microbial cell factories* vol. 17,1 51. 28 Mar. 2018, doi:10.1186/s12934-018-0900-4

(2) Zhou, Kang et al. "Novel reference genes for quantifying transcriptional responses of Escherichia coli to protein overexpression by quantitative PCR." *BMC molecular biology* vol. 12 18. 23 Apr. 2011, doi:10.1186/1471-2199-12-18

6.4 List of SNP's Analysis

Table 5: *E. coli* K12 genome SNP's detection following Raja 42-resistant alignment to parental strain

Position in genome	Type	Reference sequence	Alteration	Evidence	Effect	Gene
954547	del	CGGTGAGGGGGGGATTGACTCGCTTCG	C	C:28 CGGTGAGGGGGGGATTGACTCGCTTCG:0		
1331518	snp	C	G	G:129 C:0	synonymous_variant c.924G>C p.Thr308Thr	insH-5
3572578	del	CT	C	C:102 CT:0		
4165349	snp	G	A	A:42 G:0	non_coding_transcript_variant	